Prognostics and Maintenance Optimization for Wind Energy Systems

by

Fang Fang Ding

A thesis submitted in partial fulfillment of the requirements for the degree of

Doctor of Philosophy

in

Engineering Management

Department of Mechanical Engineering

University of Alberta

Abstract

Maintenance management in wind energy industry has great impact on overall wind power cost. Optimizing maintenance strategies can substantially reduces the cost and makes wind energy more competitive among the energy resources. Due to the extreme conditions of remote or offshore sites where the wind turbines are installed, corrective maintenance and time-based preventive maintenance are the most adopted strategies in the wind industry in recent years. However, there is need to further reduce wind power cost via maintenance strategy improvement to increase its competitiveness. Industry and research community have been focusing on various maintenance strategies to save the maintenance cost.

This thesis is devoted to developing cost-effective maintenance strategies for wind farms, focusing on conventional time-based maintenance optimization, and prognostics and condition-based maintenance (CBM) optimization within the CBM strategy framework.

Studies are performed on improving corrective maintenance and time-based preventive maintenance strategies, which are currently widely adopted in wind industry. Opportunistic maintenance methods are proposed, which take advantage of economic dependencies existing among the wind turbines, and corrective maintenance chances, to implement preventive maintenance simultaneously. Imperfect preventive maintenance actions are considered as well. The methods demonstrate the immediate benefits of saving the overall maintenance cost for a wind farm.

In the more advanced CBM strategy, the health conditions of components are monitored and predicted, based on which maintenance actions are scheduled to prevent unexpected failures while reducing the maintenance costs. Prognostic techniques are essential in CBM. In particular, the wind direction and speed around wind turbines are changing over time, which leads to instantaneously time-varying load applied to the wind turbines rotors. With focus on gearbox failure due to the gear tooth crack, an integrated prognostics method is developed considering instantaneously varying load condition. The numerical examples demonstrate that the gearbox remaining useful life prediction considering time-varying load is more accurate compared to existing methods under constant-load assumption. In a subsequent extended study, uncertainty in gear tooth crack initiation time is further considered for wind turbine gearbox prognostics method development. The method provides more accurate gearbox remaining useful life prediction compared to the results without considering time-varying load condition.

This thesis also proposes a CBM method considering different turbine types and lead times, as well as the production loss during the shutdown time. The capability to accurately estimate the average maintenance cost for a wind farm with diverse turbines is a key contribution of the proposed method. In addition, this thesis accounts for the inaccuracy in the simulation-based algorithms that most complex problems are solved with. A numerical method for CBM optimization of wind farms is developed to avoid the variations in CBM cost evaluation, which leads to a smooth cost function surface and benefits the optimization process.

The research in this thesis provides innovative methods for maintenance management in the wind power industry. The developed methods will help to significantly reduce the

overall maintenance cost within either conventional maintenance or CBM strategies that the wind farm owners may apply. It will improve the competitive advantage of the wind energy, and promote a clean and sustainable energy future for the society in Canada and worldwide.

Preface

This thesis is an original work by Fang Fang Ding. The following works as part of this thesis have been published. In these works, I was responsible for all major areas of concept formation, data collection and analysis, experiments, as well as manuscript composition. Dr. Zhigang Tian was the supervisory author and assisted with concept formation and manuscript edits.

1. Chapter 3 has been published as F. Ding and Z. Tian, "Opportunistic maintenance for wind farms considering multi-level imperfect maintenance thresholds," *Renew. Energy*, vol. 45, pp. 175–182, 2012 [1].

2. Chapter 4 has been published as F. Ding, Z. Tian, F. Zhao, and H. Xu, "An integrated approach for wind turbine gearbox fatigue life prediction considering instantaneously varying load conditions," *Renew. Energy*, vol. 129, no. Part A, pp. 260–270, Dec. 2018 [2].

3. Chapter 6 has been published as F. Ding, Z. Tian, and A. Amayri, "Condition-based maintenance of wind power generation systems considering different turbine types and lead times," *Int. J. Strateg. Eng. Asset Manag.*, vol. 2, no. 1, pp. 63–79, 2014 [3].

Chapter 5 and 7 are preliminary research and will be continued to be developed for publications.

Acknowledgments

Firstly, I would like to express my sincere gratitude to my supervisor Dr. Zhigang Tian for his continuous support, immense knowledge, encouragement, and incredible patience to my Ph.D study and related research. His guidance helped me in all the time of research, taking courses of my study, doing projects, and writing of the thesis. I could not have imagined finishing my thesis without him. I would also like to thank Dr. Ming J.Zuo for his kindness and wisdom not only in academia but in life that encourages and helps me a lot. I could not wish have better mentors than them for my Ph.D study. I wish them the best in their whole life. My sincere thanks also goes to the rest of my thesis committee: Dr. Amit Kumar, Dr. Yongsheng Ma, Dr. Xiaodong Wang, and Dr. Sharareh Taghipour for their time to review and assessing thesis, insightful comments and questions to incent me to widen my research and improve the thesis.

Secondly, I would like to thank my fellow labmates for unforgettable days and nights we were working together, supporting each other, and for fun we have had during my Ph.D study. Also I thank my friends in Montreal and Edmonton for their always care about me and knowing me of those joys, successes, difficulties, and endless desires of friendship throughout completing my Ph.D program.

Last but not the least, I would like to thank my family: my parents, my husband, my brother, and my two lovely daughters, for their constant and endless love, support, happiness, and pride to me. I feel so wonderful having them in my life and my hard works.

Table of Contents

List of Tables

Table of Figures

List of Acronyms

CBM	Condition based maintenance
SIF	Stress intensity factor
CIT	Crack initiation time
RUL	Remaining useful life
O&M	Operation and maintenance
PHM	Proportional hazard model
ANN	Artificial neural network
SVM	Support vector machine
RFA	Random forest algorithm
BTA	Boosting tree algorithm
CHAID	Chi-square automatic interaction detector
HSMM	Hidden semi-Markov model
DEVS	Discrete event simulation
FE	Finite element
LEC	Levelized energy cost
FMECA	Failure modes effects and criticality analysis
RPN	Risk priority number
SCADA	Supervised control and data acquisition system
PDF	Probability density function

Chapter 1. Introduction

1.1 Background

Renewable energy is playing more and more significant role globally in providing electricity to the world, e.g., solar energy, wind energy, geothermal energy, bioenergy, hydropower, and so on. The traditional energy such as coal, oil, and natural gas are non-renewable and will eventually dwindle, becoming too expensive or environmentally damaging to retrieve. In contrast, many types of renewable energy resources, e.g., wind and solar energy, are constantly replenished and will never run out.

In particular, wind energy grows rapidly as one of the fastest growing renewable energy technologies around the world, and it produces very economical electricity among renewable energy sources [4]. The wind energy is captured by a facility so-called wind turbine. The wind turbines are commonly installed in the remote site or offshore to harvest wind power as much as possible. However, extreme weather conditions that the wind turbines suffer challenge the operation and maintenance (O&M) cost significantly worldwide, and Canadian asset owners are taking environmental challenges seriously. O&M for the turbines installed offshore or on remote locations accounts for about 25% of the levelized energy cost (LEC) [5]. Specifically, O&M costs are two to three times higher than those of land-based wind turbines [6]. Others reported that unscheduled breakdown shares about 70% of total wind turbine maintenance cost [7].

In wind industry, typically there are three categories of maintenance strategies: failure-based maintenance or corrective maintenance, time-based maintenance, and condition-based maintenance (CBM). In failure-based maintenance, the maintenance activities are scheduled by

reacting to failures, which is the most costly strategy since failure may cause catastrophic damage to the whole wind power generation system. Another more recent maintenance strategy is time-based maintenance, which aims at preventing future failures by performing preventive maintenance on a regular basis, e.g., every six months. Age-based maintenance is also a type of time-based maintenance, where maintenance is performed when the component reaches a pre-specified age. Obviously, performing maintenance at shorter intervals or younger age increases the overall maintenance cost while maintenance at longer intervals or older age would miss the chance to prevent the failures. Further to be improved, the time interval between maintenances or the age of the components can be optimized to minimize the total expected maintenance cost in the long term.

Canadian Wind Farm O&M Market Survey Results reported that most of the installed wind farms (about 88%) are less than ten years old in Canada [8]. In this scenario, regular maintenance activities commonly applied in the warranty period, e.g., five years, may combine with corrective maintenance, which is so-called opportunistic maintenance. Opportunistic maintenance has great potential to bring immediate cost savings as it does not need any fault detection and prediction technologies. Opportunistic maintenance has been reported in many industries. It takes advantage of ease of the management for both failure-based maintenance and time-based maintenance. However, the existing studies on opportunistic maintenance for wind power systems are still very few. In this thesis, an opportunistic maintenance method is proposed to demonstrate its outstanding benefits and cost-effectiveness for a wind farm.

CBM has become the most desired missions on maintenance strategies for wind power industry. The principle of CBM is to schedule maintenance activities according to the health condition of the system, which is analyzed based on the information collected from condition monitoring

system. In Canada, condition monitoring system and advanced operation & maintenance strategies contribute to 30% of overall profit increase of wind farms, which are ranked among top 3 opportunities according to the survey results [8]. However, the studies for wind power industry are still relatively new due to the application challenges of condition monitoring techniques regarding the extreme environment harshness.

CBM commonly covers three areas. 1) Diagnostics: to detect, isolate and identify faults when they occur. 2) Prognostics: to predict the future failures to avoid unnecessary maintenance. 3) Maintenance decision making: to schedule maintenance based on detected early faults and predicted remaining useful life. Diagnostic information can help improve prognostics by preparing more accurate event data. A CBM process can involve both diagnostics and prognostics, or either one of them. In this thesis, the research work focuses on prognostics and CBM optimization.

In prognostics, a health condition degradation model is usually applied to predict the critical degradation level representing a failure in the future. One way of modeling degradation process is to learn the relationship between the sensor measurement data and the real health condition, and the degradation process is therefore established, this is a so-called data-driven method. Another way to model the degradation process is to use physics in degradation process to predict the component health condition, which is called a physics-based method. Physics-based methods are significantly challenged when a component is complex to describe its physics and dynamic response, while data-driven methods are also not valid if there are not sufficient data. To benefit from both and exceed their limitations, a combined methodology termed as integrated prognostics method is applied in this thesis, the details are given in the following chapters.

According to the survey [8], gearbox failures cause the most of production loss at Canadian wind farms. Besides, wind turbines work in wind turbulence from time to time, which leads to time-varying torque suffered to the mechanical components of the hub. The torque is changing over time, even during one revolution period. To address this real problem, the study on prognostics in this thesis focuses on gearbox failure prediction under the instantaneously time-varying condition, which has not adequately been considered in the existing literature.

1.2 Research Motivations

The global wind O&M market has been growing at a compound annual rate of 20.6% in the past 10 years, and it is forecasted the market will reach U.S.$27.4 billion by 2025 from U.S.$13.74 billion in 2016 [9]. The huge demand draws the intensive attention of research community to devote on maintenance optimizations for the wind industry.

Y. Sinha and J. A. Steel introduced Failure Modes Effects and Criticality Analysis (FMECA) tool and calculated the Risk Priority Number (RPN) for planning CBM [10]. G. Haddad et al. proposed a wait-to-maintain option maintenance method for wind farms based on prognostic indication value, which is determined using a model that quantifies the benefit from implementing prognostics [11]. [12] and [13] developed data-driven prognostics methods for the wind turbine gearbox using vibration signal data and temperature data respectively, while [14] applied a dynamic Bayesian network as prognostics tool to simulate the degradation of wind turbine gearbox using oil test bed data. [15] utilized statistical techniques and expert system to achieve prognostics and transfer into actionable intelligence. In addition to these most recent studies, reviews of maintenance practice and prognostics techniques for wind turbine systems were provided in [16]–[18]. [16] concluded that three most commonly used data-driven methods,

i.e., Hidden Markov model, Neural Network, and particle filter, are applicable for gearbox prognostics. [17] reviewed the maintenance practices for wind industry including conventional maintenance and CBM strategies. [18] particularly summarized the publications in the order of applied prognostic techniques, e.g., moving average, particle filtering, multivariate statistics, finite element method, etc. Based on the literature review, there are lack of studies of prognostics and CBM specifically considering the time-varying working condition, complex maintenance activities, diversity of wind turbines in a wind farm, and so on. Huge amount of research efforts are still required to solve the problems and reduce the maintenance cost, which can contribute to 30% of overall profit increase of wind farms [8]. The capability of providing accurate failure prediction and considering the actual impact factors in the wind industry needs to improve in the maintenance management process. The conventional maintenance can also be potentially improved to make it more cost-effective.

Failure-based and time-based maintenance are still the primary strategies adopted in the wind power industry nowadays. There is a room for saving cost by implementing preventive maintenance simultaneously when a failure occurs in the farm since the economic dependency exists among components and systems. In this thesis, an opportunistic maintenance approach is proposed to demonstrate its immediate cost benefits to a wind farm. In practice, preventive maintenance does not always return components to the as-good-as new status. Therefore, multi-level maintenance actions are introduced for failure turbines and working turbines respectively, where imperfect preventive maintenance actions are considered. The examples of imperfect preventive maintenance include the addition of a new part, exchange of parts, changes or adjustment to the settings, lubrication or cleaning, etc.

CBM is the most advanced maintenance approach as mentioned in the previous section. In the existing CBM studies for wind farms, many of them did not consider the diversity of wind turbines and their subsystems [19], e.g., they may have different capacity, or they are likely from different suppliers and thus have different lead times, etc. The diversity certainly has impacts on the CBM decisions. In the thesis, an improved CBM method considering various types of wind turbines and maintenance lead times is proposed, in which the power production loss that cannot be ignored is particularly addressed.

In the literature, solving a CBM optimization problem mainly uses simulation method to evaluate the overall maintenance cost for a wind farm due to the complexity, e.g., [19]. The simulation-based method is flexible in modeling the complex problems, but there are variations when it is used for CBM cost evaluation, and the resulting CBM cost function surface is not quite smooth due to its sampling mechanism. This could cause local minima or convergence problems in the optimization process. A numerical method is thus a preference since it is not based on sampling process. In this thesis, a numerical method is developed to solve a CBM optimization problem for a wind farm where multiple turbines are installed.

Prognostics technique dedicates to predict the remaining useful life of a component by utilizing fault degradation model and condition monitoring data. Gearbox failures cause the most of production loss at Canadian wind farms according to Canadian Wind Farm O&M Market Survey Results [8], which is ranked at the highest score of 3.49 followed by blade damage at a score of 3.21. Crack is a dominant fault among various failure modes of the gear. Gearbox in the wind turbine system is under time-varying external load condition because of varying wind speed and direction. This reality is mainly considered in the thesis, and an integrated prognostics approach

considering instantaneously time-varying load condition is developed to predict the gear tooth crack propagation.

Another concern about gearbox prognostics under time-varying external load condition is that the uncertainty of initial crack detection cannot be ignored. In the study, prognostics starts when an initial crack is known. Therefore, prognostics starting at an early point will produce an underestimated remaining useful life (RUL), while prognostics starting at a late point will produce an overestimated RUL. The uncertainty of the crack initiation time certainly affects the prediction of gear remaining useful life. In this thesis, the integrated prognostic approach mentioned above is further improved by introducing the uncertainty of crack initiation time (CIT).

1.3 Research Contributions

In this thesis, we focus on the prognostics and maintenance management study for the wind power systems, the contributions are summarized as follows.

- An opportunistic maintenance approach is developed for wind farms since there is economic dependency existing among components and systems. The preventive maintenance is performed on those components which meet decision-making criteria when there is a chance of failure replacement in the wind farm. Imperfect preventive maintenance actions are considered, which addresses the practical issue that preventive maintenance does not always return components to as-good-as-new status. The proposed opportunistic maintenance policies are defined by the component's age threshold values, and different age thresholds are introduced for failure turbines and working turbines respectively. The comparative study demonstrates that the proposed methods significantly

reduce the maintenance cost. The methods are expected to bring immediate benefits to wind power industry.

- An integrated prognostic approach considering time-varying load condition is developed to predict RUL of wind turbine gearbox. The fatigue crack on the gear tooth is focused on in the study. The method integrates physical gear model and available health condition data. To improve the accuracy of health prediction, the uncertainty of material parameter is improved via Bayesian inference once the new health condition data become available at each inspection interval; thus the crack degradation model is adjusted more and more accurately. An example is provided to demonstrate the effectiveness of the proposed approach. Besides, a comparative study between the proposed varying-load approach and existing constant-load approximation method is conducted, and the results show that the proposed approach can provide a more accurate prediction.

- We investigate the effects of the uncertainty of CIT on gear RUL prediction based on the previous approach. The existing fault detection and diagnostic techniques are limited so that a variation of CIT cannot be ignored. An additional new parameter, the uncertainty of CIT is introduced in the previous integrated prognostic model considering time-varying load condition for the gearbox. A numerical example and comparative study demonstrate the outstanding capability of the developed prognostic method to reflect the CIT uncertainty factor in predicting the RUL.

- We develop a CBM approach considering different types of wind turbines in a wind farm, and various lead times for various turbine components. The method models CBM activities more accurately for wind farms in practice. In the approach, there are two

design variables for each turbine type, i.e., high-level and low-level conditional failure probability for determining a preventive maintenance action. A method for turbine failure probability evaluation considering different lead times is developed, as well as total maintenance cost evaluation method particularly taking production loss into account. Numerical examples are provided to demonstrate the effectiveness of the proposed CBM approach.

- A numerical method to evaluate the overall CBM maintenance cost is developed based on a CBM policy presented in [19], in which the simulation method was applied to estimate the cost. The numerical method developed in this study demonstrates its significance in improving the accuracy, thus better schedule the maintenance activities.

The research in this thesis provides innovative methods for maintenance management in the wind power industry. The developed methods will help to significantly reduce the overall maintenance cost within either conventional maintenance or condition-based maintenance strategies that the wind farm owners may apply. It will improve the competitive advantage of the wind energy, and promote a clean and sustainable energy future for the society in Canada and worldwide.

1.4 Thesis Organization

The thesis is prepared following the dissertation requirements from the Faculty of Graduate Studies and Research (FGSR) at the University of Alberta. The rest of this thesis is organized as follows:

Chapter 2 presents a detailed literature review on maintenance management, CBM, and current prognostics approaches for the gearbox in wind power industry with focusing on time-varying external load condition. This chapter also devotes to presenting fundamentals of wind turbine systems, some basics of the physical model of gear tooth fracture, and dynamics of gear tooth meshing that are essential in prognostics study for wind energy systems in the thesis.

Chapter 3 presents an opportunistic maintenance method for wind farms considering multi-level imperfect maintenance thresholds. The materials have been published in the journal *Renewable Energy* [1].

Chapter 4 presents an integrated prognostic method for RUL prediction of the gear with tooth crack, which particularly considers time-varying external load condition that wind turbines suffer. The materials have been published in the journal *Renewable Energy* [2].

Chapter 5 presents a further study based on the method presented in Chapter 4 by introducing an additional parameter uncertainty, i.e., CIT.

Chapter 6 presents a CBM approach for wind turbines considering different turbine types and lead times of components in a wind farm, as well as the production loss during the shutdown time. The materials have been published in the journal *Strategic Engineering Asset Management* [3].

Chapter 7 presents a numerical method for solving CBM maintenance cost evaluation problem in a wind farm. A simple case is considered in the chapter to explore the numerical method study.

Chapter 8 concludes the thesis and suggests several future works.

Chapter 2. Literature Review and Background Knowledge

In this chapter, we review literature related to maintenance management for wind turbines, mainly focus on existing CBM approaches, as well as prognostic methods that are usually essential for CBM. In the prognostic study, we focus on the literature considering time-varying external load conditions. Gear tooth fracture is the primary damage mode in the selected literature of prognostic studies. Some essential background knowledge is given as well.

2.1 Literature review

2.1.1 Maintenance optimization for wind turbine systems

2.1.1.1 Traditional corrective & regular maintenance approaches

Primary maintenance strategies employed in the wind power industry are currently corrective maintenance and time-based maintenance. Within these categories, Jardine and Tsang presented many maintenance optimization approaches and their applications, e.g., optimizing the preventive replacement interval & age, spare parts provisioning, etc., to minimize the overall maintenance cost or downtime [20]. The application studies for wind industry have been receiving significant attention thus far; however individual maintenance optimization models were rarely developed mainly due to adverse accessibility and huge maintenance cost. Ding improved a corrective maintenance strategy by finding an optimal number of failures to be replaced together at a time for a wind farm, the expected average cost is then minimized [21]. Carlos et al. optimized the preventive maintenance interval for an onshore wind farm that the total cost is minimized and the annual energy production is maximized [22].

More and more researchers have been studying opportunistic maintenance for wind turbine systems since economic dependency exists among units in a wind farm, and a fixed cost for sending a crew to the wind farm is dominant. Numerous literature has shown the cost benefits by proposing various opportunistic maintenance models. Ding and Tian, Lu et al., Ko and Byon, and Sarker and Ibn Faiz proposed opportunistic maintenance methods to minimize the expected maintenance cost [23]–[26]. Zhang et al. further considered a joint optimization problem where spare parts inventory constraint is involved [27]. Abdollahzadeh et al. developed a multi-objective opportunistic maintenance method that the expected rate of energy is maximized and the total expected cost is minimized as well [28].

2.1.1.2 CBM approaches

CBM techniques have been growing very fast, Jardine et al., Peng et al., and Sikorska et al. provided the reviews about theoretical development and practical applications [29]–[31]. CBM has become an issue for wind farm's operation in recent years as more and more sensors are employed in modern wind turbines. The availability of health condition monitoring data, i.e., sensing signals, has then empowered CBM study to become a hot research area for the wind industry. Indeed, it is consistent with the findings of Alsyouf and El-Thalji (2008) that CBM has drawn much attention in wind power industry [32]. At present, CBM is the most advanced maintenance scheme as the performance of components can be actively tracked based on the condition monitoring (CM) apparatus. Hence an aging component can be pro-actively replaced before a failure occurs.

A CBM program usually consists of three steps: data acquisition, data processing, and health diagnostics and prognostics [29]. Data related to the system health condition is a critical source

for CBM decision. The data can be acquired by optimally placing the sensors at the appropriate locations [33]. Data processing is to analyze the collected data or samples for better understanding the degradation signature. For details, readers are referred to [29]. Hameed et al. and Costinas et al. provided comprehensive reviews on the diagnostic and condition-monitoring techniques for wind turbines and subsystems [33], [34]. The advances in monitoring technology for turbine subsystems were later reviewed in [35]. Some studies only focused on the critical components such as gearbox [36], [37], generators [38], and blades [39].

In CBM, the component health state should be predicted accurately based on the monitoring data. Some literature modeled the degradation process as a continuous stochastic process, e.g., failure probability distributions [19], [36], [3], [40], and [41], while others considered the degradation as a discrete aging process, e.g., multiple states subject to failures [42], [43]. Various maintenance decision rules were proposed in these studies, and the RUL is served as the basis for scheduling the inspection and parts replacement tasks. Instead of modeling degradation process, some studies leveraged the data-mining algorithms to predict the wind turbine degradation states [44] or trace the failure precursors of the bearing in wind turbines [45]. These studies are presented in details in the followings.

For continuous degradation process, both physical models and data-driven models have been proposed in the literature. With the former, one requires detailed knowledge of the failure mechanisms while the latter needs comprehensive data to validate the model [46]. By monitoring the crack indicators of gearbox, Sørensen formulated an exponential damage model with calibration of a fracture mechanical model of the crack growth [40]. A probabilistic model was proposed to capture the damage state uncertainty, and the Bayesian rule was used to update the probability that the crack size exceeds the limit at a given inspection time. With the proposed

cost models and the specified damage level to prevent, the optimal inspection/service interval was determined when the total expected capitalized profit is maximized. One can refer to [41] to obtain more details on how Bayesian rule can aid the damage model update in offshore wind turbines maintenance decision. Based on [40] and [41], Nielsen and Sørensen gave a quick comment on the potential extension of Bayesian degradation model [47]. For instance, one shall consider multiple components, a turbine fleet within the farm, and weather factors, among others. However, the model complexity and the computational time will quickly increase with the problem size, yet no general insights were provided in [47].

Lucente proposed a CBM optimization approach using Proportional Hazards Model (PHM) for the wind industry [36]. PHM is the most widely used and cited model in a variety of industries. It extrapolates the component lifetime by combining the baseline hazard function with the actual operating condition data, or the so-called covariates. PHM improves the prediction of failure with the given values of covariates and corresponding parameters. The latter indicates the degree of influence that each covariate has on the hazard function. By solving an objective function for minimizing the expected average cost, the threshold hazard rate can be found. The optimal decision is to replace the component whenever the estimated hazard rate exceeds the threshold. Lucente discussed the PHM's possible applications in wind turbine components [36]. According to their viewpoints, the limitation of this approach to wind industry is primarily due to the lack of data. Another issue is how to identify the significant covariates.

Tian et al. proposed a CBM approach for managing the maintenance of a wind farm, where multiple components in each wind turbine were considered [19]. Artificial neural network (ANN) algorithm was used to predict components' RUL at each inspection point for the wind farm. The prediction errors were calculated during ANN training and testing processes, and

therefore the predicted failure probability distribution at component and turbine levels were obtained. An optimal maintenance policy was determined such that preventive maintenance is performed if the turbine failure probability during the maintenance lead time exceeds the threshold, which results in the lowest overall maintenance cost. Amayri et al. proposed a CBM strategy considering different types of wind turbines and maintenance lead times in a wind farm [48], [49]. Later, Ding et al. optimized the CBM by considering both different maintenance lead times and turbine types, as well as inevitable production loss due to maintenance activities [3]. Pazouki et al. proposed a CBM for wind turbine systems consisting of multiple components that show independent stochastic deterioration process [50]. CBM tasks were scheduled through optimizing joint failure probability threshold and maintenance interval to minimize the total cost.

Apart from the continuous failure process defined by literature mentioned above, discrete degradation modeling approach was also considered in many studies, for example, multi-state process. In practice, most mechanical components have more than two states, i.e., new and failed. For example, a generator may have reduced capacity between the new and the failed states; however, it is still functional. Another example is that a gearbox has multiple failure modes, which can also be considered as multi-states. For this reason, it is necessary to characterize the degradation process as a multi-state process, which accommodates different reliability requirements on the components at different states. Hence a more effective maintenance plan can be advised. Markov model is a powerful tool to characterize the degradation behavior for a multi-state system, and it has been used by several recent studies addressing the reliability of wind turbine components [42], [43], [51]. Markovian deterioration model can be formulated as a transition probability matrix, which is also capable of incorporating the associated detection uncertainty of degradation condition. Wu and Zhao

divided the gearbox lifetime equally into six states, and proposed several alternative maintenance actions and accordingly derived the transition probability matrix of each state with alternative maintenance actions [43]. An optimal inspection interval was found by using iterative algorithm to calculate maintenance costs for each combination of maintenance actions. However, the states are not stationary at the different age in reality. The state definition in the study did not take any advantage of condition monitoring, and therefore the resulting model confines its general applications. More practically, Byon and Ding defined normal, alert, alarm conditions and five different failure modes [42]. Initially, a 3×8 state transition matrix was constructed by aggregating a long-run historical operation data. The matrix was further validated with the industry data, and it was re-estimated at the beginning of each decision period using real-time sensory data. With the proposed season-dependent CBM actions, the expected cost was evaluated using backward dynamic programming to attain the optimal CBM policy. However, a Markovian modeling approach requires the precise initial state transition matrix, which is a significant challenge due to the lack of data as well as limited industry inputs.

As mentioned earlier, some literature developed data-driven approaches to accurately predict specific failure index value (e.g., temperature) or turbine states (e.g., normal, faulty) without an explicit degradation model. Y. Sinha and J. A. Steel introduced Failure Modes Effects and Criticality Analysis (FMECA) tool and calculated the Risk Priority Number (RPN) for identifying failures, and used them as a basis for CBM [10]. G. Haddad et al. proposed a wait-to-maintain option maintenance method for wind farms based on prognostic indication value, which is determined using a model that quantifies the benefit from implementing prognostics [11]. [12] collected vibration signals and used time series prediction techniques to predict the health related features trends for prognostics of wind turbine gearbox. Multivariate state estimation technique

was applied to estimate the health state of the unit gearbox bearing using temperature data, and a fault is predicted when the value of selected feature exceeds the threshold [13]. A dynamic Bayesian network was applied as prognostics tool to simulate the degradation of wind turbine gearbox using oil test bed data [14]. [15] utilized statistical techniques and expert system to achieve prognostics and transfer into actionable intelligence. Kusiak and Verma investigated the prediction accuracy using five data-mining algorithms: Neural Network, Support Vector Machine (SVM), Random Forest Algorithm (RFA), Boosting Tree Algorithm (BTA), and General Chi-square Automatic Interaction Detector (CHAID) [44]. The historical sensory data was used to train these models, based on which the turbine states were predicted. As a result, RFA has the best prediction performance, which ensures a better maintenance decision for wind turbines. Kusiak and Verma also built five neural networks with different structures and compared their prediction accuracy for over-temperature points of the bearing with abnormal behaviors [45]. Given a pre-determined error residual limit, on average the best NN model generated the alarm signal 1.5 hours prior to the actual fault. [16] reviewed prognostic approaches commonly used for wind turbine systems, and it concluded that three data-driven methods, i.e., Hidden Markov model, Neural Network, and particle filter, are applicable for gearbox prognostics.

Cost is a crucial metric in maintenance project assessment. Several studies analyzed the trade-off between the CBM benefit and the investment cost to demonstrate the economic reality of CBM in the wind industry. Nilsson and Bertling conducted lifecycle cost analysis by comparing the effects of six different maintenance strategies for a single onshore wind turbine and an offshore wind turbine fleet, respectively [52]. CBM, corrective maintenance, and preventive maintenance were all implemented. The conclusion is that CBM is profitable as long as those maintenance

strategies are managed with specific efforts. However, they did not suggest the exact CBM plan. Andrawus et al. and McMillan and Ault made cost comparisons between a 6-month time-based maintenance strategy and a CBM [53], [54]. Andrawus et al. demonstrated that the overall cost savings of £180,152 over 18 years life cycle for a 26×600kW onshore wind farm was achieved by adopting CBM [53], while McMillan and Ault indicated that an amount of £225,000 operational saving per turbine over 15 years is guaranteed using CBM [54].

There are some other approaches associated with CBM technology. For example, Haddad et al. suggested that the logistics lead time of a blade can be minimized using the health condition prediction information [55]. Byon and Ding, and Byon et al. investigated the weather influence on the management of CBM [42], [51]. [56] adopted power purchase agreement modeling to determine the optimum predictive maintenance opportunity for wind farms, and the uncertainties in the wind speed and the RUL predictions from PHM were considered.

2.1.2 Prognostics considering time-varying load

In the field, substantial wind fluctuations lead to instantaneously varying external load associated with wind turbine systems, which makes it become a big challenge to realize diagnosis and prognosis of components in the system and therefore appropriate CBM schedule.

As the vital part in CBM, prognostics can provide the prediction of remaining useful life (RUL) based on the real-time health condition status of systems. CBM can then be scheduled to retain the system availability best and to reduce maintenance costs most. In prognostics, data-driven methods and physics-based methods are two main categories among the existing studies. Data-driven methods apply machine learning techniques to the historical condition data to empower the capability of predicting future condition. Physics-based methods use physical models such as

Finite Element (FE) model, fault propagation model based on fatigue mechanics to predict the component health condition. The significant challenges exist for physics-based methods when a component is complex to describe its physics and dynamic response, while data-driven methods are not effective either if there are not sufficient data. Noticing these drawbacks an integrated prognostics method is a preference in the thesis, which combines two methods to exceed the limitations. Detailed information about integrated prognostics will be provided in Chapter 4. Particularly, the consideration of time-varying external load in prognostics is one of the key contributions in this study. The review focusing on fault propagation process studies under time-varying external load condition is then given as follows.

A fault propagation model is essential to describe the fault evolution process and used to predict the future health conditions. However, the variations of operating conditions, e.g., varying external load, can greatly challenge the accuracy of fault degradation modeling. [57] developed a frequency-domain fatigue assessment method for a wind turbine gearbox, where the wind turbulence impacts to gearbox dynamic response was modeled as a non-Gaussian loading process. Chen et al. developed a new prognostics model to accommodate varying factors by using incremental learning approach, and battery degradation case is studied to validate their method [58]. Li et al. employed a continuous time hidden semi-Markov model (HSMM) to derive the remaining useful life prediction under varying load for a helicopter gearbox [59]. Al-Tubi et al. studied gear micropitting propagation subject to varying torque loads under a constant rotational speed [60]. Experimental test and analytical evaluation were employed to demonstrate the effects of excessive load, surface roughness and lubricant film thickness on a micropitting process. However, in the study, they considered step-up torque levels rather than time-varying torques. Gəsperin et al. presented a model-based prognostic approach for mechanical drives

under non-stationary operating conditions [61]. A linear state-space model was developed to model the relationship between variable operating conditions and fault status. Therefore, the future features representing the health condition can be predicted if the future profile of the load is known. The authors also claimed that the further experiments were required to conduct the study properly.

In addition, several fault propagation physics models under varying load condition are found in the literature. The failure mode of mechanical components, e.g., gear, in the existing study is mainly crack. Crack growth has been actively studied under constant loading condition taking advantage of well-recognized propagation model, based on which researchers further investigated and improved the models under varying load condition. Some studies considered the varying load by differing under-load and over-load cases. However, this is not the case for the working environment of wind turbines that usually suffer time-varying even non-stationary external load.

The time-varying load studied in the literature is mostly so-called variable amplitude loading, under which two branches are identified: stationary and non-stationary load. In simple words, stationary load means that the magnitude of load randomly changes over time, but the frequency is constant, while non-stationary load changes over time in either magnitude or frequency. A recent review [62] presented the reliability assessment of fatigue under variable amplitude loading. However, it limited the discussion to the stationary load processes as they claimed that the assumption of stationarity is sufficient for most relevant applications. In this case, the amplitude of loading was sampled with a certain distribution, e.g., lognormal, and the crack propagation process was modeled as Basic Paris' Law shown in Equation (2-1). Paris' Law is one

of the first and most widely used fatigue crack propagation model presented by Paris and Erdogan [63].

$$\frac{da}{dN} = C(\Delta k)^n \tag{2-1}$$

where *c* and *n* are material constants, Δk is the range of stress intensity factor.

However, consider the working environment of wind turbine systems, the load is always non-stationary due to wind turbulence. For the crack propagation under non-stationary loading, a few old studies in the 1980s and 1990s are found, but there are not much new findings recently. These studies mainly worked on aerospace problems and materials, e.g., Aluminum Alloys. Couples of modified crack propagation models were proposed but need to be justified. Sobczyk presented a form of crack growth rate under randomly varying load [64]:

$$\frac{dL}{dt} = c\mu(t)g(Q)(k_{rms})^n,\ L(t_0)=L_0 \tag{2-2}$$

k is stress intensity factor (SIF), *L* is crack length. k_{rms} has the form of

$$k_{rms} = \sqrt{\frac{1}{N}\sum_{i=1}^{N} {k_i}^2} \tag{2-3}$$

In the case of random loading, a new stress ratio *Q* characterizing the mean stress effect was used. It was defined as:

$$Q = \frac{\langle S \rangle}{S_{rms}} \tag{2-4}$$

In Equation (2-2), $\mu(t)$ describes the average number of 'cycles' of a stress process per unit time. In the conventional analysis, crack growth rate is usually expressed as *da/dN* as indicated in Equation (2-1), *N* denotes the number of cycles. When the load is randomly varying in time, a

cycle is not straightforward and not unique, and a possible definition can be the load history between two consecutive local maxima.

[65]–[67] presented the crack propagation process in the form of

$$\frac{da}{dN} = C(\Delta k_{rms})^n \tag{2-5}$$

RMS is a prevailing statistics of a continuously varying quantity. Some studies considering varying load concluded that there exists a correlation between Δk_{rms} and the rate of fatigue crack growth. However, [66] found that this approach failed to model the fatigue crack growth data by tested specimens. In other words, the experiment results showed the nature of scattering by plotting Δk_{rms} vs. *da/dN*, and it was not possible to present the data in an analytical form as Equation (2-5). In another study [67], it was suggested that, for material parameter $n \leq 2$, Δk_{rms} could be appropriate but for $n > 2$, Δk_{rms} is underestimated.

Another modified model was studied in [68] and [69], which is given by

$$\frac{dA}{dt} = \mu C(\Delta k)^n Y(t), \text{ where } \Delta k = 2S(t)\sqrt{\pi A(t)} \tag{2-6}$$

$A(t)$ signifies that the crack size growth is a random process due to random loading (stress) $S(t)$, and random process $Y(t)$ accounts for the random material resistance. Besides, μ denotes the average number of cycles per unit time, and it is assumed as a constant. Assuming that $A(t)$ is a slowly varying random process compared with the stress range process $\Delta S(t)$, it is approximately a diffusive Markov process according to the Stratonovich-Khasminski limit theorem. The drift and diffusion coefficients can be determined given that the probability distribution of initial crack, the covariance of $\Delta S(t)$ at two different times, and the mean and covariance of $Y(t)$ are

known. Hence, a Fokker-Planck equation for $\mathrm{A(t)}$ is obtained and solved. The Fokker-Planck equation is

$$\frac{\partial q}{\partial t} = -m\frac{\partial q}{\partial a} + \frac{1}{2}\sigma^2\frac{\partial^2 q}{\partial a^2} \tag{2-7}$$

where m and σ are drift and diffusion coefficients, a denotes the crack size, and q is the transition probability density of $\mathrm{A(t)}$. The information on the covariance of $\Delta\mathrm{S(t)}$ was not available for a general stationary stress process based on the author's knowledge up to date, and a particular case that the random stress was modeled as a Gaussian random process was considered to solve Equation (2-7) for $\mathrm{A(t)}$.

A review provided by [62] also presented a fatigue propagation model under variable amplitude loading:

$$\frac{da}{dN} = f_a(R(N), \delta, \Delta k_a(a, \Delta S(N), \gamma) \tag{2-8}$$

where f_a is the function describing the crack growth rate, δ is a set of parameters describing material properties, e.g., C and n in Equation (2-5), γ is a set of parameters describing the geometry of the component containing the crack. R and ΔS are stress ratio and stress range, respectively. They are presented as random processes and functions of N.

Apart from above mentioned modified models, some literature directly used the basic Paris' Law to represent the crack growth process under variable loading condition, e.g., [70]. Though the study treated the random loading and crack growth rate as random variables, the random time-varying feature was ignored.

Even though the researchers developed multiple models in the case the load is time-varying, but

these models have not straight forward evolvement relationship, and they did not give the details of how to implement them. In addition, the hypothesis about the random processes involved are limited in the real applications. In this thesis, we propose another modified model to address the crack propagation problem under time-varying external load condition, and case studies are given to demonstrate its effectiveness.

Except for the approach of applying fatigue crack propagation model to predict RUL of gear, it should be noted that there is another approach dealing with high cycle fatigue assessment under variable amplitude loading, which is defined as an S-N damage accumulation approach in the review by Altamura and Straub [62]. This approach is based on empirically determined S-N curves and fatigue damage criteria, i.e., Palmgren-Miner's rule. According to Sutherland and Burwinkle, American Gear Manufacturers Association (AGMA) Standard (1976) adopted Miner's Rule "to ascertain the effects of variable loading on the life of the gearing" for the design of spur and helical gears [71]. The varying load sequences are typically extracted to a series of S-stress range and corresponding N-number of cycles using cycle counting techniques. Rainflow counting is the best cycle counting method used in the industry. In this scenario, [72] quantified short-time gearbox fatigue damage using the data from Supervised Control and Data Acquisition system (SCADA). Fatigue damage d of a certain amplitude of load i is calculated by

$$d_i = n_i/N_i \tag{2-9}$$

where, n is the applied load cycles of the specific load amplitude i, N is the number of cycles to failure when the applied load equals to i, S_i is the stress corresponding to load i. Regarding the relationship between load and stress, Sutherland and Burwinkle simply suggested a linear multiplier for converting gear shaft torque (load) to the stress in a gear tooth based on AGMA

Standard (1976). Miner's rule then summarizes the accumulated damage from each cycle for all different load amplitudes as

$$D = \sum \frac{n_i}{N_i} \leq 1 \tag{2-10}$$

Theoretically, the component is failed when D is larger than 1.

S-N curve damage accumulation approach will not be given many insights in this thesis since the prediction results are usually inaccurate or conservative if S-N curve information is not appropriately determined. In addition, D values need to be very carefully selected in reality as they may be as low as far from 1.

2.2 Background knowledge

In this section, a brief introduction to the basics of wind turbine systems including the critical components and their major failure modes is given, as well as the typical maintenance research challenges regarding wind turbine working conditions. Some basics about physics of gear tooth crack and dynamic process of gear tooth meshing follow.

2.2.1 Introduction of WT system

2.2.1.1 Typical configuration of a WT system and major failures of critical components

Wind turbines are stand-alone machines which are typically installed and formed as a group in a place named as a *Wind Farm* or *Wind Park*. Generally speaking, a wind turbine system is a rotary device that extracts energy from the wind and converts to electricity.

Wind turbine systems are basically classified into horizontal axis wind turbines and vertical axis wind turbines according to the axis of rotation of the wind rotor. Some old design of wind rotors have the feature of the vertical rotation axis, and it can work well in wind turbulence but less efficient than horizontal-axis-turbine, which can generate more electricity by increasing the rotor height up to hundreds of meters where the wind is much stronger. Nowadays horizontal-axis wind turbine is the dominant type in global wind projects because of its outstanding power production. Nevertheless, this form of turbines suffers severely in turbulent wind conditions and therefore challenges the research on maintenance significantly. In this thesis, we focus on horizontal-axis wind turbines.

Typical configurations of a horizontal-axis wind turbine system are shown in Figure 1. The followings present details on four critical components in a wind turbine: the rotor blades, the main bearing, the gearbox and the generator [73].

- **Rotor Blades**

Wind turbine blades collect energy from the wind and then transmit the rotational energy to the gearbox via the hub and main shaft. The number of blades and their sweeping area affects wind turbine performance. Most wind turbines have only two or three blades on their rotors. The reason is that the space between blades should be big enough to avoid turbulence so that one blade will not encounter the disturbed and weaker air flow caused by the blade which passed before it. In an offshore environment where corrosion is a critical factor, blade material often prefers the ones that are corrosion resistant, also that have the possibility of achieving high strength and stiffness-to-weight ratio.

Blade Failures and Causes

Rotor blades are highly stressed due to the constant wind contact, as well as environmental conditions such as ice, UV radiation, lightning, etc. Crack arising from fatigue and materials deficiency, impacts on the blade surface because of ice build-up, lightning strikes and rain erosion and so on are known to cause failures.

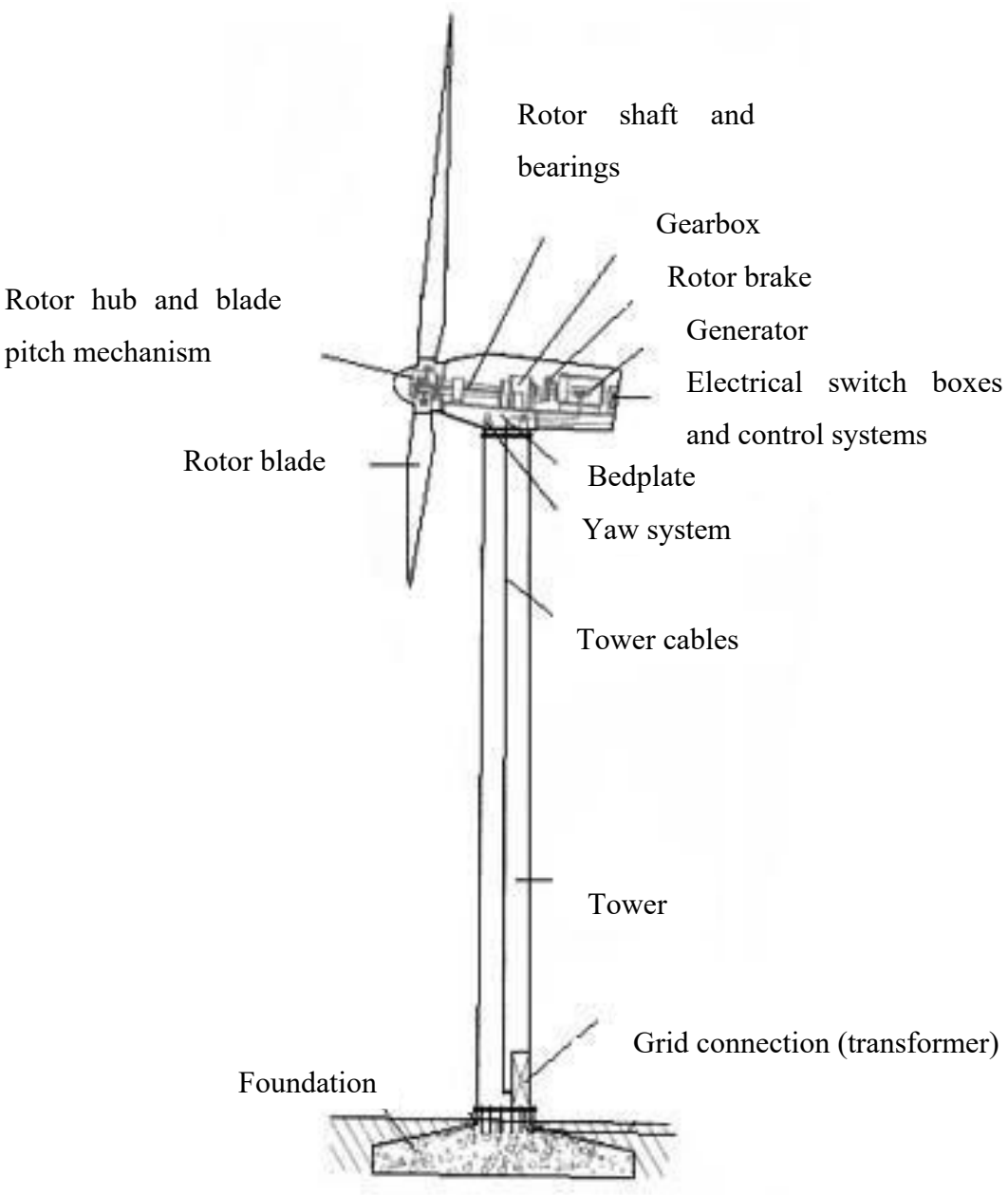

Figure 1. Components of a horizontal-axis wind turbine [74]

- **Main Bearing**

All modern wind turbines have spherical roller bearings as main bearings. The main bearing is mounted in the bearing housing bolted to the mainframe, and it reduces the frictional resistance between the blades, the main shaft, and the gearbox while it undergoes relative motion. The designs of different types of wind turbines vary regarding the number of bearings and bearing seats.

Main Bearings Failures and Causes

National Renewable Energy Laboratory (NREL) of USA conducted a series of investigations of wind turbine failures [75]. According to the study results, axial cracks formed on the bearings due to overloading during high- and intermediate-speed stages dominantly causes bearing failures, which eventually causes the majority of wind turbine gearbox failures (76%). This information was given in 2015 and can be retrieved online titled "Statistics Show Bearing Problems Cause the Majority of Wind Turbine Gearbox Failures". Poor lubrication, wear, pitting, deformation of the outer race and rolling elements may also cause bearing failures.

- **Gearbox**

The gearbox is typically placed in a wind turbine drive train to increase speed from a low-speed rotor to high-speed generator. Some designs of so-called direct-drive machines do not have a gearbox, the generator turns at the same speed as the turbine rotor. There is a trade-off between the reliability and the cost of slower generators. Besides, wind turbines usually need more than one gear stage to achieve an overall high gear ratio, among which planetary gear outperform parallel-shaft-gear taking advantage of its high gear ratio of up to 1:12, typically [74]. In the

megawatt power class, the multi-stage planetary gearbox prevails while in smaller power classes parallel-shaft gears are preferred because of cost.

Gearbox Failures and Causes

Fractures, scuffing, micropitting on gear tooth surface and bearing failures are mostly reported failure problems. Torque from the rotor is very high to drive the power generation system, and this challenges the wind turbine gearbox due to the excessive loading. A poor design would make the gearbox poorly support these loads, and thus internal components can become misaligned, which eventually causes failures. In addition, unreliable seals and lubrication systems, as well as manufacturing errors, are also considerable causes.

- **Generator**

The generator transforms mechanical energy into electrical energy. The blades transfer the kinetic energy from the wind into rotational energy, and then the generator supplies the energy from the wind turbine to the electrical grid. The generator produces either alternating current (AC) or direct current (DC), and they are available in a broad range of output power ratings. The generator's rating or size depends on the length of wind turbine blades, longer blades capture more energy.

Generator Failures and Causes

The generator is a very critical component of the wind turbine with high failure rates, which follows the gearbox and the rotor blades as the 3rd top-ranked component causes production loss at Canadian wind farms [8]. The main reason is that the generator works with a highly fluctuating mechanical power. Early bearing fatigue may result from poor lubrication contributes

to the mechanical failure of the generator, while poor insulation systems create an increase of the leakage currents and then arises the safety issue of goods and persons as well as production loss.

2.2.1.2 Maintenance research challenges regarding wind turbine working Conditions

The external environment of erected wind turbines is complex and uncontrollable, e.g., time-varying wind speed and direction, wind shear, wind veer, temperature, ice, humidity and so on. All these significantly affect the reliability of the components. Modeling and analysis of the component failure process become very challenging. For example, gear tooth crack propagation is apparently different under time-varying external load condition comparing to the constant load condition. Therefore, developing an appropriate fault growth model with knowledge of the impacts of such conditions is essential for predicting the failure in wind turbines. Another example is that, to evaluate the reliability of power production not only an accurate power generation model is required, but a local wind distribution around the wind turbine needs to be appropriately determined, which is usually difficult. In addition, condition monitoring data are essential to implement fault diagnostics, prognostics, and schedule CBM; however, these data are generally not accessible or proprietary in the wind industry, and they may not stand in good quality. Van Kuik and Peinke presented the long-term research challenges in wind energy in a whole scenario, which includes materials and structures, design, aerodynamics environmental aspects and so on [76]. Followings list some significant challenges or limitations of maintenance study, in particular, considering the external working conditions of wind turbines, but not limited.

- Acquiring accurate condition monitoring data well indicates the working and healthy condition of the study object;
- Reliability analysis and uncertainty modeling for accurate failure prediction;
- Accurate cost model especially for offshore wind power due to limited accessibility and more severe consequences of a failure. It is more critical for economic-oriented maintenance optimization;
- Comprehensive knowledge about external conditions;
- High demand for data mining techniques in case of an incomplete or limited data source;
- Require appropriate fault degradation models addressing the issue of time-varying external conditions.

2.2.2 Introduction of Dynamics of gear tooth meshing and physics of tooth fracture

2.2.2.1 Physics of Fracture

As one of the common and severe failure modes of mechanical components, the fracture has been given much research efforts to control and predict its occurrence. Fracture mechanics is an important tool in modern materials science, and it applies the theories of elasticity and plasticity to the microscopic defects in real materials to predict the further mechanical behavior. In this thesis, we focus on the theory of linear elastic fracture mechanics.

Crack propagation causes the fracture. There are three forms of enabling a crack to propagate according to the loading modes, which are shown in Figure 2.

Mode I - Opening mode: tensile stress normal to the plane of the crack,

Mode II - Sliding mode: shear stress acting parallel to the plane of the crack and perpendicular to the crack front,

Mode III - Tearing mode: shear stress acting parallel to the plane of the crack and parallel to the crack front.

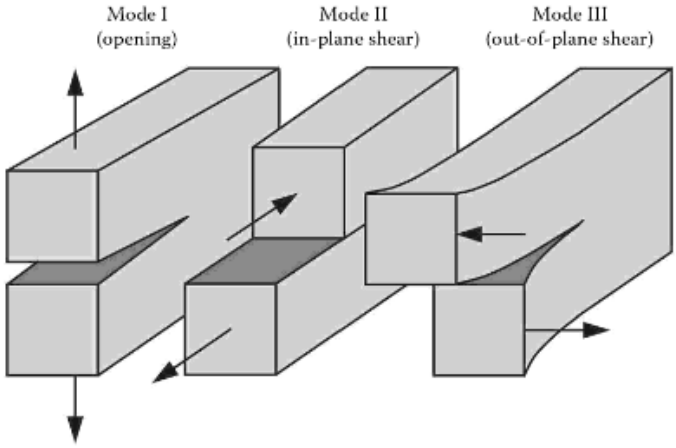

Figure 2. Three modes of loading applying to a crack [77]

A cracked object can be in any one of these modes, or a combination of two or three modes. To predict the crack process, stress should be the first to analyze. The stress intensity factor (SIF), denoted by *K*, is a quantity to describe the stress field in the area near the crack tip, and it is usually given a subscript to denote the loading mode, i.e., opening mode $K_{\square}$, sliding mode $K_{\square}$ and tearing mode $K_{\square}$. The solution of the stress field near the crack tip in any linear elastic cracked body exhibits a $1/\sqrt{r}$ singularity, the normal stress σ_{xx}, $\sigma_{yy}$and shear stress σ_{xy} for mode

I and Mode II in a linear elastic and isotropic material, which are expressed as follows. Figure 3 schematically shows an element near the tip of a crack together with the in-plane stresses on this element.

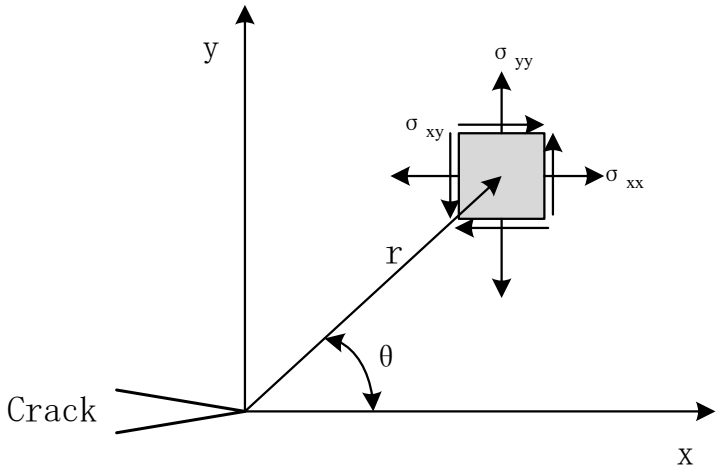

Figure 3. Two-dimensional stresses near the tip of a crack in an elastic material [77]

If K is known, it is possible to solve for all stress components as a function of r and θ[77]. In the part of solving the problem of gear prognostic in this thesis, FRANC2D is used for the gear FE model, which is a widely used numerical method to obtain solutions for the stresses and strains when a body is subject to complex loading conditions. The method adopted in FE model to calculate K employs a singular element to model stress singularity near the crack tip [78], the idea is to correlate the local displacements with their theoretical asymptotic values. The stress intensity factors, K, therefore can be expressed as functions of the nodal displacements, the details can refer to [79].

The crack propagation direction can then be estimated after K_{I} and K_{II} are obtained under mixed-mode loading. There are several criteria for mixed mode fracture on the basis of stress-

strain field, for example, maximum tangential stress criterion, maximum strain criterion, and strain energy density criterion, and so on [80]. In this study, the maximum tangential stress energy criterion is applied to determine the crack propagation direction, which is given by the angle θ that maximizes the effective stress intensity factor with respect to θ [81]. The crack extends from the crack tip and grows in the direction normal to the maximum tangential tensile stress, and the propagation angle θ can be written as [78].

$$\theta = 2tan^{-1}\left[\frac{1}{4}\left(\frac{K_{\mathrm{I}}}{K_{\mathrm{II}}} \pm \sqrt{\left(\frac{K_{\mathrm{I}}}{K_{\mathrm{II}}}\right)^2 + 8}\right)\right] \tag{2-11}$$

In addition, the thickness of the gear rim, represented by the backup ratio (m), has great impact on the crack propagation path according to [79]. If the rim is thin (m is small), the crack tends to grow towards to the rim, the failure is very harmful, and the consequence is more severe than the case that the crack grows across the tooth thickness, where the rim is thick (m is large).

The crack propagation model is another important topic in fracture mechanics. In the prognostic study for a mechanical component suffering crack fracture, a crack propagation prediction model is always essential. The overall fatigue life of the mechanical component having a failure mode of crack has three stages: crack initiation, crack propagation and crack acceleration. Crack prediction study commonly targets the crack propagation stage to prevent the catastrophic failure before the crack goes to the final stage. As mentioned in Section 2.1.2, the fundamental crack propagation model is expressed as Equation (2-1), which is well known as Paris' law proposed by [63]. As we can see, Paris' law describes that the crack evolution process with loading cycles is linear with the stress intensity factor in a log-log scale. In this scenario, a critical crack size is usually defined as a threshold value representing an actual failure, the remaining loading cycles, in other words, the RUL, can be evaluated at each crack level.

2.2.2.2 Dynamics of a one-stage gearbox and gear tooth meshing

Vibration signal of the mechanical system is the most used data source to diagnose and predict the faults since the fault will be reflected in the overall vibration of the system. As one of the major failure modes, tooth crack on a spur gear of a one-stage gearbox is studied in this thesis for prognostics. The crack affects the tooth meshing stiffness, which is time-varying and one of the vibration excitation sources. Dynamic models of gear meshing process help to understand and identify the vibration sources in gear transmission.

Crack usually happens close to the tooth root where the highest bending stress exists due to cyclic loading. The total mesh stiffness varies when the cracked tooth comes into meshing. Thus, the force acting on the tooth is affected because it is determined by the mesh stiffness and the tooth deflection. Accordingly, the crack changes the dynamic load on the tooth. There are many types of gear, e.g., spur gear, helical gear, bevel gear, etc., among which spur gears are the most common type of gears. They are cylindrical shaped gear, and the teeth are parallel to the axis of the rotating shaft. The advantage of the spur gear is that it is easy to design and produce, and the cost of manufacture and maintenance is relatively low. In this thesis, we focus on the spur gear.

Assuming the mating tooth is an isotropic elastic body in this thesis, the tooth with a crack is considered as a cantilevered beam, and the beam does not experience any deflection. Potential energy is the stored energy when a body is deformed. The total potential energy stored in a meshing spur gear pair includes four parts: Hertzian energy, bending energy, axial compressive energy and shear energy. All these types of energy are proven to be significant contributions to the total effective mesh stiffness [82]. Tian assumed the crack growth path as a straight line. However, as illustrated in Section 2.2.2.1, $K_{\square}$ and $K_{\square}$ determine crack propagation direction in a

mixed-loading mode fracture, the crack therefore actually grows at a varying intersection angle to upright vertical due to the variability of $K_{\square}$ and $K_{\square}$. The details of potential energy and stiffness calculation with a curved crack was introduced in [78] and [83].

An example of calculated total effective mesh stiffness with a crack of 3.0mm over one rotation period is shown in Figure 4. As we can see, the mesh stiffness is substantially reduced when the cracked tooth is in meshing.

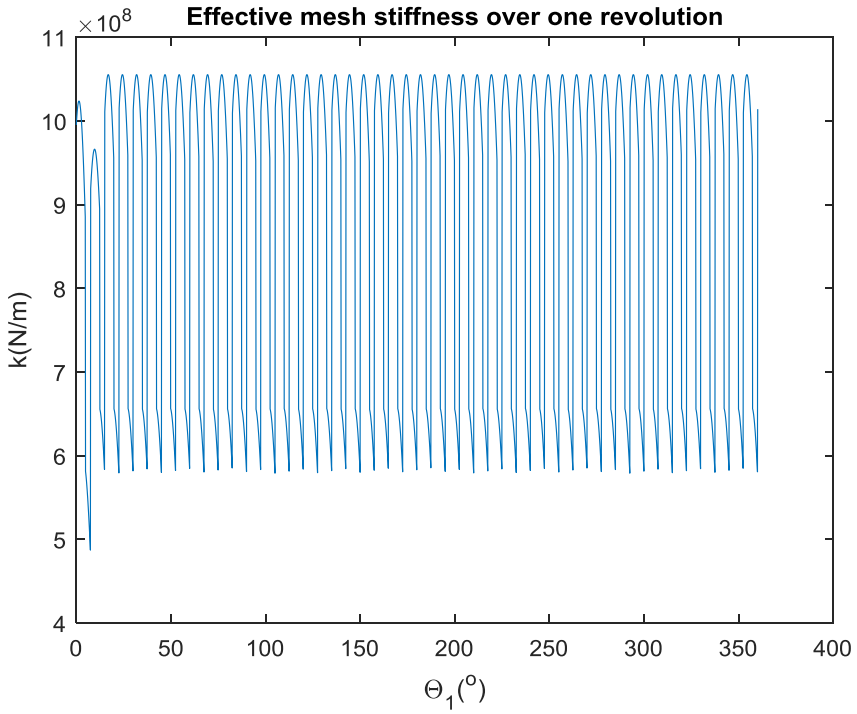

Figure 4. Total effective mesh stiffness for the 48-teeth gear with a crack of 3.0mm

Wu at al. developed a 6-degree-of-freedom dynamic model for a one-stage gearbox to describe its motions, which is so-called a lumped parameter model [84]. In this thesis, this model is used to simulate the vibration signals considering a cracked tooth. Further, the formulas given by Lin et al. [85] are used to calculate the dynamic load F to drive the crack propagation, which is implemented in FE model. The 6-DOF one-stage gearbox system is shown in Figure 5.

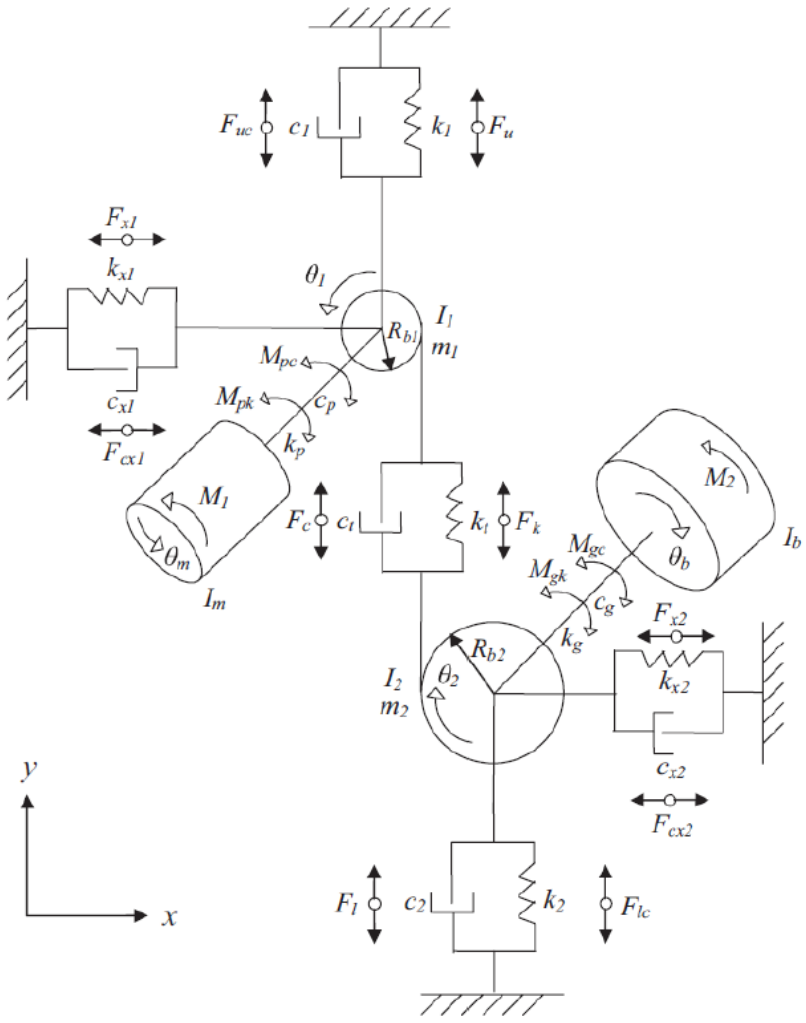

Figure 5. The one-stage gearbox system [84], [86]

The modeled vibrations include torsional and lateral motions. The pinion and the gear are perfectly mounted on the shafts that are coupled with the motor shaft and the output shaft on both sides respectively. The system is driven by a motor with the torque M_1 and loaded with the torque M_2. The bearings support the shafts. Stiffness and damping are involved in the model. The friction is ignored for simplicity, so the vibration in the x-direction is free and disappears due to the damping [84]. The details of the mathematical dynamic model refer to [84] and [86], the dynamic load over one mesh period is then calculated and shown in Figure 6 as an example.

The static load shared by the tooth pairs is crucial in a load transmission [87], and it is also shown in the figure as blue dash line for comparison. The method of calculating the static load can be found in [87]–[89]. [89] gave the calculation process using the variable "tooth pair compliance", while the other two solved the problem using the variable "tooth mesh stiffness". The tooth carries the full load when the tooth pair is in single-tooth-meshing, while the tooth shares the load when they are in double-tooth-meshing.

As shown in Figure 6, the maximum dynamic load is larger than the maximum static load, which has to be considered in the crack propagation process since the larger load accelerates the crack growth. Therefore, to prevent the critical crack an actual larger dynamic load is selected to apply in FE model to drive the crack propagates.

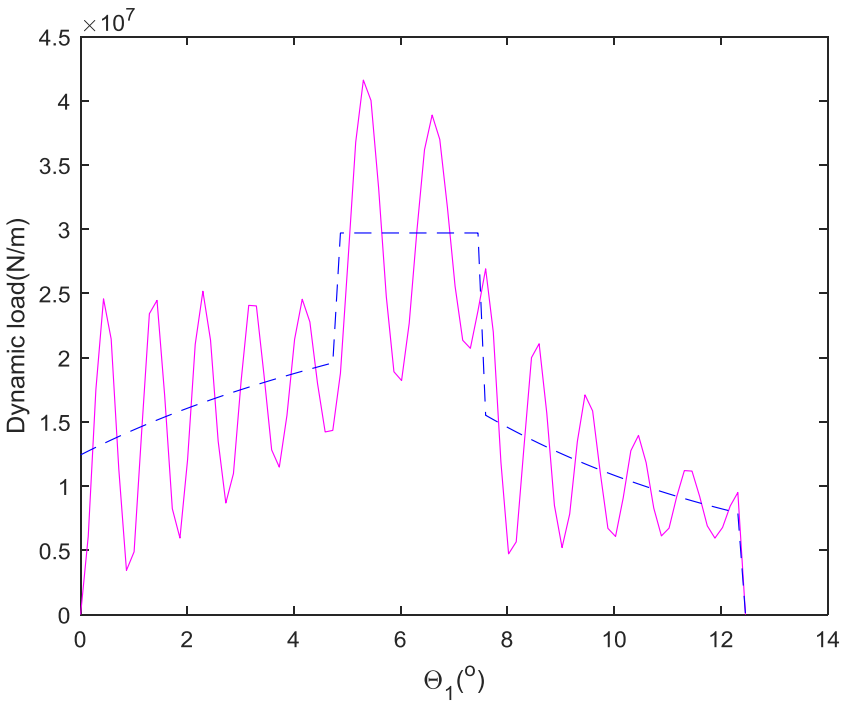

Figure 6. Static and dynamic load on the cracked tooth

2.3 Summary

In this chapter, literature is reviewed in the field of maintenance optimization for wind power industry. Traditional maintenance and the most advanced maintenance CBM are first studied. In CBM, prognostics is essential to predict the remaining useful life of a studied object. Therefore, a review of prognostics, of which particularly the existing methods of modeling the crack propagation of a gearbox focusing on time-varying external load condition are introduced. The typical wind turbine configurations and critical components are introduced, as well as the fracture mechanism and dynamic models of a gearbox for better understanding the whole study.

Chapter 3. Opportunistic Maintenance for Wind Farms Considering Multi-level Imperfect Maintenance Thresholds

3.1 Overview

Nowadays wind industry mainly adopts regularly scheduled maintenance strategy, e.g., every 6 months, to prevent catastrophic loss and hence reduce overall investment cost. Advanced condition-based maintenance faces significant challenges of lack of availability of condition monitoring data and knowledge of failure modes. The study on appropriate and practical maintenance strategies without implementation difficulty has drawn increasing interests. Fixed-interval maintenance can prevent severe failures but is also costly due to excessive or unnecessary maintenance activities, particularly in the case of extreme conditions and high load associated with offshore wind farms. Corrective maintenance and time-based preventive maintenance, which are widely used in wind power industry because of its ease of management, have not been studied adequately, and few methods were developed to optimize the maintenance policies.

Four maintenance strategies for European offshore wind farms were proposed in Europe Wind Energy Report (2001), among which one is opportunistic maintenance. In opportunistic maintenance, whenever a failure occurs in the wind farm, the maintenance team is sent onsite to perform corrective maintenance, and take this opportunity to simultaneously perform preventive maintenance on the other components in the failed turbines and the running turbines that show relatively high risks. There are typically multiple wind turbines in a wind farm, and a wind turbine has multiple components. Economic dependencies exist among various components and

systems in the farm. When the failed components create a failure replacement opportunity, maintenance team may perform preventive maintenance for other components satisfying pre-specified decision conditions, such as certain age thresholds. As a result, a substantial cost can be saved compared to separate maintenance for the components.

In the general maintenance engineering field, various opportunistic maintenance policies and applications have been reported. Laggoune et al. considered hydrogen compressors with different component failure distributions, and made maintenance decisions based on if performing replacements can lower the expected costs [90]. An age-based policy was used by Crocker and Kumar to optimize the maintenance of a military aero-engine, and they concluded that opportunistic maintenance should be performed on relatively cheap components in their application [91]. Mohamed-Salah et al. proposed an opportunistic maintenance policy for ball bearings based on the time difference between expected preventive maintenance time and failure instant [92]. Haque et al. assumed that the components are identical and follow the same Weibull distribution, and presented a maintenance method for multi-unit systems [93]. However, very few studies were reported on opportunistic maintenance for wind power systems. Besnard et al. proposed an opportunistic maintenance method for off-shore wind turbine systems based on both failure probability and real wind data [94]. They presented an optimization model with a series of constraints aiming at minimizing the cost, and an optimal maintenance schedule for a 5 turbines wind farm was obtained. Tian et al. developed a CBM method for wind farms by considering the economic dependencies among components, and determined the maintenance actions based on the optimized failure probability threshold values and the condition monitoring data [19].

In most existing studies on preventive maintenance for wind turbines, one disadvantage is that preventive maintenance actions were generally considered to be the replacement, which is the

perfect action to return a component to the as-good-as-new state. In practice, however, preventive maintenance does not always return components to the as-good-as-new status. According to [95], repair actions for wind turbine components may include addition of a new part, exchange of parts, removal of a damaged part, changes or adjustment to the settings, software update, lubrication or cleaning, etc. Ding and Tian developed opportunistic maintenance methods for wind farms considering imperfect maintenance actions [23]. However, they did not distinguish between the failed turbines and working turbines, and used the same maintenance thresholds for all the wind turbines.

In this chapter, opportunistic maintenance approaches are developed for wind farms to take advantage of the maintenance opportunities and consider imperfect maintenance actions. In the proposed methods, opportunistic maintenance policies are defined by the component's age threshold values, and different imperfect maintenance thresholds are introduced for failure turbines and working turbines, respectively. Three types of preventive maintenance actions are considered, including perfect, imperfect and two-level action. Simulation methods are developed to evaluate the costs of proposed opportunistic maintenance policies. Numerical examples are provided to illustrate the proposed approaches.

This chapter is organized as follows. Section 3.2 introduces the proposed opportunistic maintenance approaches. In Section 3.3, numerical examples are given to demonstrate the effectiveness of the developed method, and comparative study among different proposed strategies as well as corrective maintenance strategy are conducted. Conclusions are presented in Section 3.4. The materials in this chapter have been published in [1].

Nomenclature:

C_{pv}: the variable preventive replacement cost

C_{pf} : the fixed preventive maintenance cost

C_f : failure replacement cost

C_{Access} : the access cost to a wind turbine

C_{fix} : the fixed cost of sending a maintenance crew to wind farm

C_E: the total expected maintenance cost per turbine per day

$MTTF_i$: mean time to failure of Component i

q: ratio of age reduction

p: ratio of mean time to failure

T_{Renew}: the lifetime of a new one by a replacement

T_{Old}: the original lifetime prior to the maintenance

3.2 The Proposed Opportunistic Maintenance Approaches

In this study, three opportunistic maintenance strategies for wind farms are proposed, where a preventive maintenance action is considered as perfect, imperfect, and two-level action, respectively. At each failure instant in the wind farm, a preventive maintenance task for a specific operational component is determined based on whether its age exceeds the age threshold, which is defined to be different between the components in the failed turbine and

running turbines. Simulation methods are developed to evaluate the maintenance cost of each proposed maintenance strategy. The optimal age thresholds corresponding to the lowest average cost can be found by solving the optimization problems.

In the case of an imperfect maintenance action, a ratio of age reduction, q ($0 \leq q \leq 1$), is defined. The component's failure age after maintenance is updated, and the imperfect action cost varies according to different age reduction effort. In practice, a maintenance represented by age reduction is usually an estimate, and the occurrence time of next failure after this maintenance is also an expected value but not deterministic. In this scenario, we formulate an updated lifetime because of a maintenance action as $q \times \mathrm{T_{Renew}} + (1-q) \times \mathrm{T_{Old}}$. This is not arbitrary and especially describes well two extreme cases: 100% age reduction maintenance, i.e., perfect maintenance, is equivalent to preventive replacement so the lifetime is completely updated as of a new one $\mathrm{T_{Renew}}$, while 0% age reduction maintenance means there is no maintenance and the lifetime remains the same as its original value $\mathrm{T_{Old}}$. In general, an example is provided to illustrate how the maintenance effort, q, affects the age and lifetime in this study. Suppose a generator has original lifetime, $\mathrm{T_{Old}}$, of 20 years, and a replaced new one also has lifetime, $\mathrm{T_{Renew}}$, of 20 years. The current age right before maintenance is 8 years, the maintenance is defined as 80% age reduction. Therefore, after the maintenance, the age of this generator will be 8×20%=1.6 years, the lifetime will be 20×20%+20×0.8=20 years. The remaining useful life (RUL)=20-1.6=18.4 years with maintenance while RUL is 20-8=12 years without maintenance. In addition, the cost of imperfect action is defined as a function of q, which is given by

$$Cp = \begin{cases} q^2 C_{pv} + C_{pf} & 0 < q \leq 1 \\ 0 & q = 0 \end{cases} \tag{3-1}$$

where, C_{pv} is the variable preventive replacement cost, and C_{pf} is the fixed maintenance cost. The total preventive replacement cost is $C_{pv} + C_{pf}$, which corresponds to 100% age reduction (q=1). C_{pf} is incurred as long as an imperfect action is required for the component. The more the age of component is reduced, the faster the cost increases, and this leads to an increasing nonlinear feature of the maintenance cost.

3.2.1 Overview of the Proposed Approaches

As mentioned earlier, the proposed opportunistic maintenance actions are determined by the age threshold values, which are proposed to be different between the failed turbines and running turbines. Figure 7 generally illustrates the proposed policy. Suppose there is a failure occurring in the farm at present. The maintenance crew is sent to perform failure replacement, and take this opportunity to perform preventive maintenance on other qualified components. For example, component i and j are in the same wind turbine with a failed component, which is defined as the failed turbine, while component k is in one of the running (working) turbines. Component i will be performed a preventive maintenance action because its age reaches the threshold, which is a ratio of its mean time to failure, denoted by $p_1 \times MTTF_i$ at this moment. The age of component j does not reach the threshold $p_1 \times MTTF_j$ so that a maintenance task will not be performed and it will continue to work till the next opportunity, or it may fail first in the farm.

For all the rest components in the running turbines (e.g., component k), a different age threshold $p_2 \times MTTF$ is applied, which is expected to take fewer actions on running wind turbine such that the cost could be lower. In two-level action method, similarly, four age thresholds p_{1L}, p_{1H} (for the failed turbine) and p_{2L}, p_{2H} (for the running turbines) are applied ($p_{2H}>p_{2L}$, $p_{1H}>p_{1L}$). A

preventive replacement is to be performed if the current age reaches the large age threshold $p_{1H} \times MTTF$ for the components in the failed turbine or $p_{2H} \times MTTF$ for the components in the running turbines. Otherwise, an imperfect maintenance action is to be performed since the age reaches the small age threshold $p_{1L} \times MTTF$ or $p_{2L} \times MTTF$.

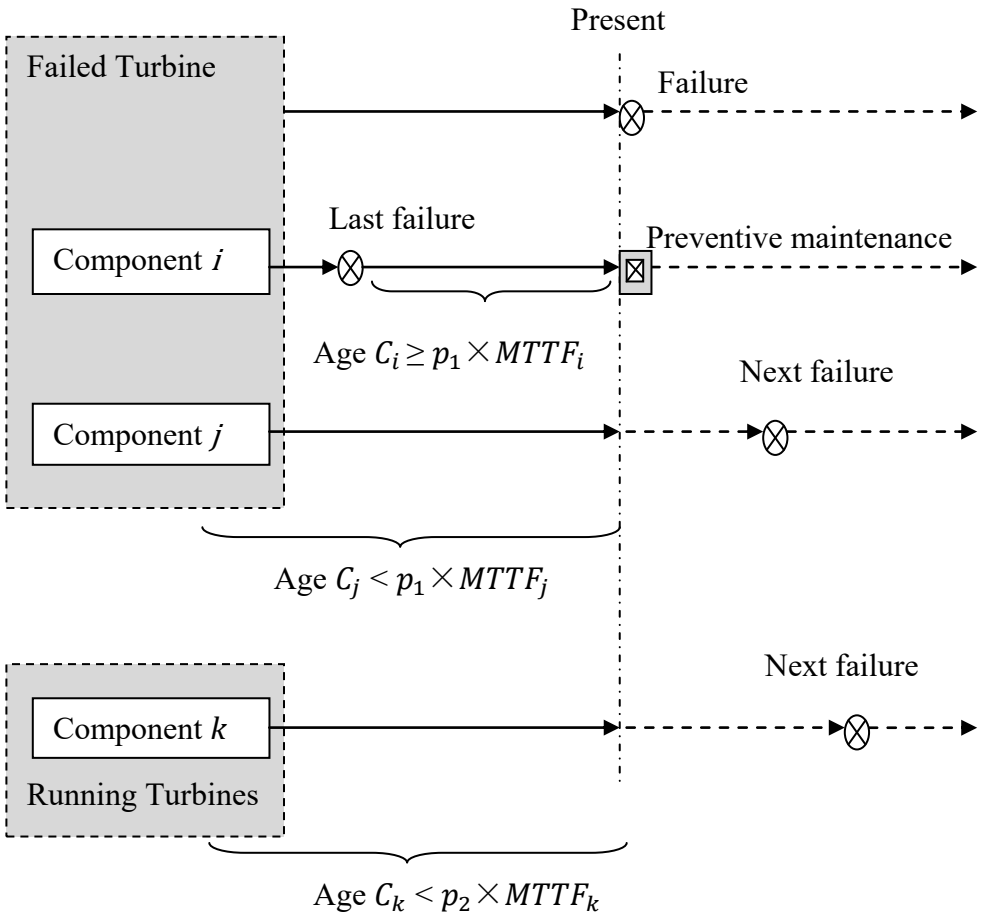

Figure 7. The proposed opportunistic maintenance concept

The proposed policies are based on the following assumptions or properties. (1). All components follow the Weibull distribution, and the failure rate increases over time (i.e., β >1); (2). All wind turbines in the farm are identical, and the deterioration process of each component is independent; (3). Any component failure leads to turbine system failure; (4). The maintenance time is negligible comparing the long lifetime of components.

Suppose there are M wind turbines in the wind farm, and K critical components are considered for each turbine. The related costs are defined as following: C_f, C_{pv}, and C_{pf} are the failure replacement cost, the variable preventive maintenance cost and the fixed preventive maintenance cost for a component, respectively. C_{Access} is the access cost to a wind turbine, and C_{fix} is the fixed cost of sending a maintenance team to wind farm.

Regarding preventive maintenance actions, three proposed strategies are discussed in the following subsections.

3.2.2 Construction of Models and The Solution Methods

3.2.2.1 Strategy 1: Opportunistic Maintenance with Perfect Action Only

The maintenance policy is described as follows. 1. Perform failure replacement if a component fails. 2. At the moment of failure, this opportunity is taken to perform preventive replacement (i.e., perfect action) on component k (k=1,...,K) in wind turbine m (m=1,...,M) if $age_{k,m} \geq MTTF_k \times p$. p=p_1 if the components are in the failed turbine, and p=p_2 if the components are in the running turbines. 3. If the component is not performed preventive maintenance on, it will continue working until the next failure occurs in the wind farm.

The brief objective function is given by:

$$\min C_E(p_1, p_2) \tag{3-2}$$

where, C_E is the total expected maintenance cost per turbine per day, and p_1 and p_2 are design variables corresponding to the failed turbine and running turbines, respectively. The objective is

to determine the optimal age threshold p_1 and p_2 to minimize the total expected maintenance cost per turbine per day.

Due to the complexity of optimization problems, it is extremely hard to develop accurate numerical methods for cost evaluation of different maintenance policies. Thus, in this work, simulation methods are developed to evaluate the average cost C_E. Suppose the failure distribution of components are known, the age values of each component at each failure instant can be obtained, and thus the optimal policy can be decided when the corresponding average maintenance cost C_E is the lowest. Figure 8 shows the flowchart of the simulation procedure in general. Strategy 2 and 3 are also included, and the detailed descriptions for them are given in the related subsequent subsections.

The simulation process of strategy 1 is explained in detail as follows.

Step 1: Initialize the simulation. Specify all of the parameters used in the simulation process, which includes the maximum simulation iterations *I*, the number of wind turbines *M,* the number of components *K* in a system, and the upper bound of design variables, p_1 and p_2. Specify all of the related cost mentioned previously in Section 3.2.1: C_f, $C_{pv,}$ and C_{pf} for each component in the turbine, C_{fix} and C_{Access} as well. The total cost C_T at the beginning is set to be 0 and is updated during the simulation process. The Weibull distribution parameters α_k and β_k of each component are given, which are presented in Section 3.3.1. The absolute time, $TA_{k,m}$, is defined as the accumulative time of every failure for that component *k* in turbine *m*. In the beginning, generate the lifetimes $TL_{k,m}$ for each component in each turbine by sampling the Weibull distribution for component *k* with parameter α_k and β_k. Thus, the age values for all components

are zero at the beginning, that is, $age_{k,m}$=0, and , $TA_{k,m}$=$TL_{k,m}$ at the moment of the first failure.

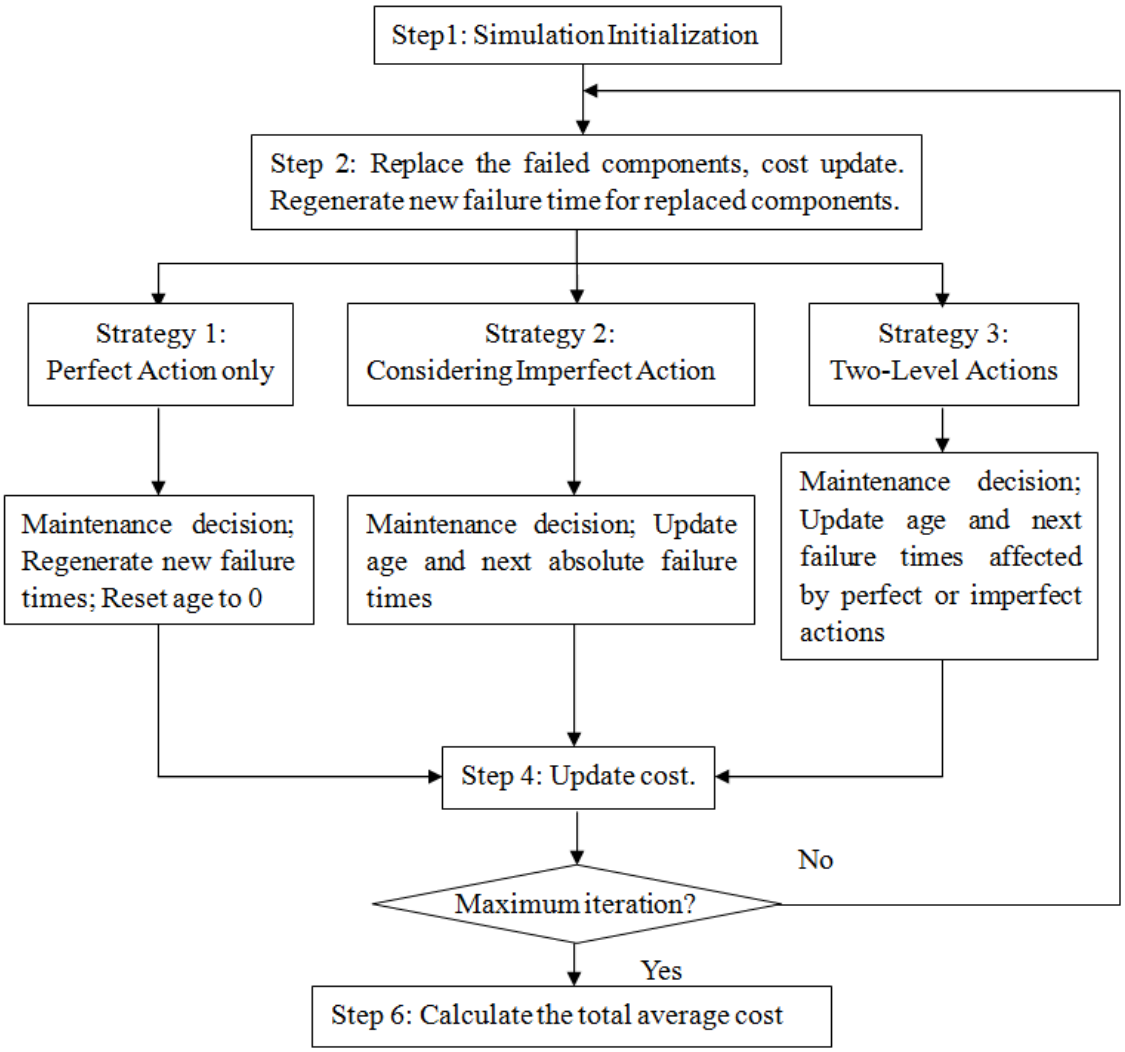

Figure 8. Simulation process for cost evaluation

Step 2: Replace the failed component and cost update. The failure of the ith iteration occurs at t_i, and t_i= min ($TA_{k,m}$). Δt_i represents the time to failure of the ith iteration, Δt_i = t_i-t_{i-1}, and t_0=0. Once there is a failed component in the wind farm, for instance, component k in turbine m fails, the failure replacement cost C_{fk} and the fixed cost of sending a maintenance team to the

wind farm, C_{fix}, are incurred simultaneously. The total cost due to failure replacement is updated as:

$$C_T = C_T + C_{fk} + C_{fix} \tag{3-3}$$

Regenerate a new lifetime $TL_{k,m}$ by sampling the Weibull distribution for this component with parameter α_k and β_k, and reset its age to 0. Its absolute time is moved to next failure, i.e., $TA_{k,m} = t_i + TL_{k,m}$.

Step 3: Make the decision on maintenance activities for the rest of the components in the wind farm. According to the policy described earlier in this section, at the moment of failure instant, a perfect action (i.e., preventive replacement) is determined to perform on component *k* in turbine *M* if $age_{k,m} \geq MTTF_k \times p$. $p = p_1$ for the components in the failed turbine, and $p = p_2$ for the components in the running turbines. Regenerate a new lifetime $TL_{k,m}$ for this component with parameter α_k and β_k, and reset its age to 0. Its absolute time will be moved to next failure, i.e., $TA_{k,m} = t_i + TL_{k,m}$.

Step 4: Cost update. The total cost due to perfect preventive maintenance action is updated as:

$$C_T = C_T = + \sum_{m=1}^{M} \left(\sum_{k=1}^{K} Cp_k \times IP_{k,m} + C_{\text{Access}} \times IA_m \right) \tag{3-4}$$

where $IP_{k,m}$=1 if preventive maintenance is to be performed on component *k* in turbine *m*; Otherwise it equals 0. IA_m =1 if any preventive maintenance is to be performed on turbine *m*, and otherwise it equals 0. Note that Cp_k represents the total preventive maintenance cost, and it equals to $C_{pv} + C_{pf}$ in this strategy.

Step 5: After performing perfect maintenance on all qualified components, set i=i+1. If i does not exceed the maximum simulation iteration I, repeat step 2, 3 and 4.

Step 6: Total expected average cost calculation. The simulation process with current variable value is completed when the maximum simulation iteration is reached, which is i =I. The total expected cost per wind turbine per day can be calculated as:

$$C_E = \frac{C_T}{M \times t_I} \tag{3-5}$$

If variable's upper bound is not reached, repeat step 2, 3, 4, 5 and 6.

With the method for cost evaluation and the general optimization model described in Equation (3-2), the optimal variable value can be searched which corresponds to the minimal expected total cost per turbine per day C_E. The optimal maintenance strategy is determined once the optimal values of variables p_1, p_2 are found.

3.2.2.2 Strategy 2: Opportunistic Maintenance Considering Imperfect Actions

The maintenance policy is described as follows. 1. Perform failure replacement if a component fails. 2. At the moment of failure, this opportunity is taken to perform an imperfect preventive maintenance action (i.e., reducing the component age by q) on component k (k=1,…,K) in wind turbine m (m=1,…,M) if $age_{k,m} \geq MTTF_k \times p$. p=p_1 for the components in the failed turbine, and p=p_2 for the components are in the running turbines. 3. If the component is not performed preventive maintenance, it will continue working until the next failure occurs in the wind farm.

The brief objective function is

$$\min C_E\,(p_1, p_2, q) \tag{3-6}$$

where, p_1,p_2,and q are design variables. Similarly, $p_1$and p_2 represent the age thresholds of the components in the failed turbine and running turbine, respectively, and q is the percentage of age reduction. The objective is to determine the optimal age threshold p_1, p_2 and age reduction ratio q to minimize the total expected maintenance cost per turbine per day.

The simulation process is much similar to the Strategy 1. Only the differences in the procedure in the related steps are described.

Step 1: Initialize the simulation. In addition to the all of parameters specified in Strategy 1, one more design variable q, the ratio of age reduction requires specifying. Moreover, the other term $FA_{k,m}$ is applied in Strategy 2, which denotes the new failure age of the component *k* in turbine *m* after imperfect maintenance action, and $FA_{k,m}$=$TL_{k,m}$ at the beginning.

Step 3: Make the decision on maintenance activities for the rest of the components in the wind farm. If $age_{k,m} \geq MTTF_k \times p$, where p=$p_1$for the component in the failed turbine, and p=p_2 for the component in the running turbines, imperfect maintenance is performed on component *k* in turbine *m*. Regenerate a new lifetime $TL_{k,m}$, and its age, failure age and absolute time are updated as:

$$age_{k,m} = age_{k,m} \times (1-q) \tag{3-7}$$

$$FA_{k,m} = q \times TL_{k,m} + (1-q) \times FA_{k,m} \tag{3-8}$$

$$TA_{k,m} = t_i + FA_{k,m} - age_{k,m} \tag{3-9}$$

Step 4: Cost update. Note that in this strategy, Equation (3-4) is also applicable. However, Cp_k varies with different ratio q according to Equation (3-1), where q can be considered to be maintenance effort.

Step 2, 5, 6 and 7 are similar to those in Strategy 1.

3.2.2.3 Strategy 3: Opportunistic Maintenance with Two-level Actions

The maintenance policy is described as follows. 1. Perform failure replacement if a component fails. 2. At the moment of failure in the wind farm, perform imperfect preventive maintenance action, which reduces the age by q on component k (k=1,…,K) in wind turbine m (m=1,…,M) if $MTTF_k \times p_{1H} \geq age_{k,m} \geq MTTF_k \times p_{1L}$ when the components are in the failed turbine, and if $MTTF_k \times p_{2H} \geq age_{k,m} \geq MTTF_k \times p_{2L}$ when the components are in the running turbines. Perform preventive replacement on this component if $age_{k,m} \geq MTTF_k \times p_{1H}$ (for the failed turbine) and $age_{k,m} \geq MTTF_k \times p_{2H}$ (for the running turbines). This policy implies that the older a component is, the more it tends to be replaced. Note that in this policy, " q ", described as the maintenance effort, is a certain value rather than a variable. 3. If the component is not performed preventive maintenance on, it will continue working until the next failure occurs in the wind farm.

The brief objective function is

$$\min C_E(p_{1L}, p_{1H}, p_{2L}, p_{2H}, q) \tag{3-10}$$

s.t.

$$0<p_{1L}<p_{1H}<1 \text{ and } 0<p_{2L}<p_{2H}<1$$

where, p_{1L}, p_{1H}, and p_{2L}, p_{2H} are design variables corresponding to two age thresholds of the components in the failed turbine and running turbines, respectively. The objective is to determine the optimal variable values to minimize the total expected maintenance cost per turbine per day.

Similarly, only the differences from Strategy 1 are described.

Step 1: Initialize the simulation. In addition to the all of parameters specified in Strategy 1, the design variables are modified since more design variables are introduced. The term $FA_{k,m}$ is also applied in Strategy 3, which denotes the new failure age of the component *k* in turbine *m* after imperfect maintenance action, and $FA_{k,m}$=$TL_{k,m}$at the beginning.

Step 3: Make the decision on maintenance activities for the rest of the components in the wind farm:

If $MTTF_k \times p_{1H} \geq age_{k,m} \geq MTTF_k \times p_{1L}$ for the component in the failed turbine and if $MTTF_k \times p_{2H} \geq age_{k,m} \geq MTTF_k \times p_{2L}$ for the component in the running turbines, imperfect maintenance is performed on the component. Regenerate a new failure time $TL_{k,m}$. Age, failure age and absolute time are updated similarly according to Equations (3-7), (3-8) and (3-9).

If $age_{k,m} \geq MTTF_k \times p_{1H}$ for the component in the failed turbine and if $age_{k,m} \geq MTTF_k \times p_{2H}$ for the component in the running turbines, preventive replacement is performed on the component. Regenerate a new lifetime $TL_{k,m}$, and reset its age to 0. Its failure age is updated as $TL_{k,m}$, denoted by $FA_{k,m} = TL_{k,m}$. The absolute time is updated as: $TA_{k,m}$=t_i + $FA_{k,m}$.

Step 4: Cost update. In this strategy, Equation (3-4) is applicable, and Cp_k varies with different ratio q according to Equation (3-1).

Step 2, 5, 6 and 7 are similar to those in Strategy 1.

For all three proposed maintenance strategies, once the minimum cost is find out, the algorithm outputs the optimal values of the design variables simultaneously.

3.3 Numerical Examples

In this section, examples are provided to illustrate the proposed approach. A comparative study is conducted with the policy using the same age threshold for failed turbines and operational turbines, and with the corrective maintenance strategy as well. The comparison results demonstrate the advantage of proposed approaches, and significant cost savings are achieved.

3.3.1 Optimization Results with the Proposed Approaches

Consider ten 2MW turbines in a wind farm at a remote site. Four key components in each component are studied to simplify the discussion: the rotor, the main bearing, the gearbox and the generator (National instruments products for wind turbine condition monitoring, 2010). Assume all components follow Weibull distributions with increasing failure rates (β>1), and all components and turbines are identical and independently deteriorate. The related cost and failure distribution parameters α (scale parameter) and β (shape parameter) are given in Table 1 based on the data in [19] and [74]. Note that C_{pf} in Table 1 is the fixed preventive maintenance cost for a wind turbine, and it is shared by all the components in the turbine.

The total maintenance cost can be evaluated using the proposed simulation method presented in Section 3.2.2. The optimization results for each proposed opportunistic maintenance strategy are presented as follows. Note that due to more than two design variables in each proposed strategy,

it is impossible to show the cost versus all variables in one figure. Thus the following figures are the cost versus one variable while the other variables are kept at the optimal values.

Table 1. Failure distribution parameters and cost data for major components ($k)

Component	α (days)	β (days)	C_f	C_{pv}	C_{pf}	C_{fix}	C_{Access}
Rotor	3000	3	112	28			
Bearing	3750	2	60	15	40	50	7
Gearbox	2400	3	152	38			
Generator	3300	2	100	25			

Strategy 1. Perfect maintenance only

As shown in Figure 9, the optimal average maintenance cost per unit time is $167.2/day. The corresponding policy is that, when there is a requirement of failure replacement in the wind farm, the preventive replacement is performed on the components in the failed turbine if its age exceeds 50% of the mean lifetime, and on the components in the running turbines if its age exceeds 60% of the mean lifetime. Note that the optimal values are rounded to integer percentage values.

Strategy 2. Considering imperfect maintenance

As can be seen in Figure 10, when there is a failure occurs, the 50% age reduction maintenance actions are performed on the component reach 30% of its mean lifetime in the failed turbine, and on the component reach 40% of its mean lifetime in the running turbine. This optimal maintenance policy leads to the minimum cost of $123.4/day.

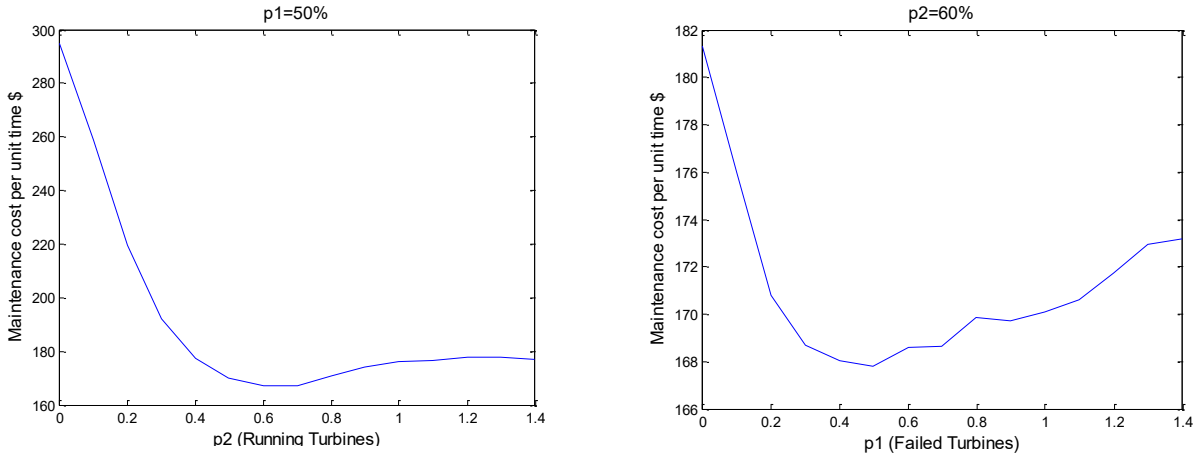

Figure 9. Cost versus p_1 and p_2 respectively

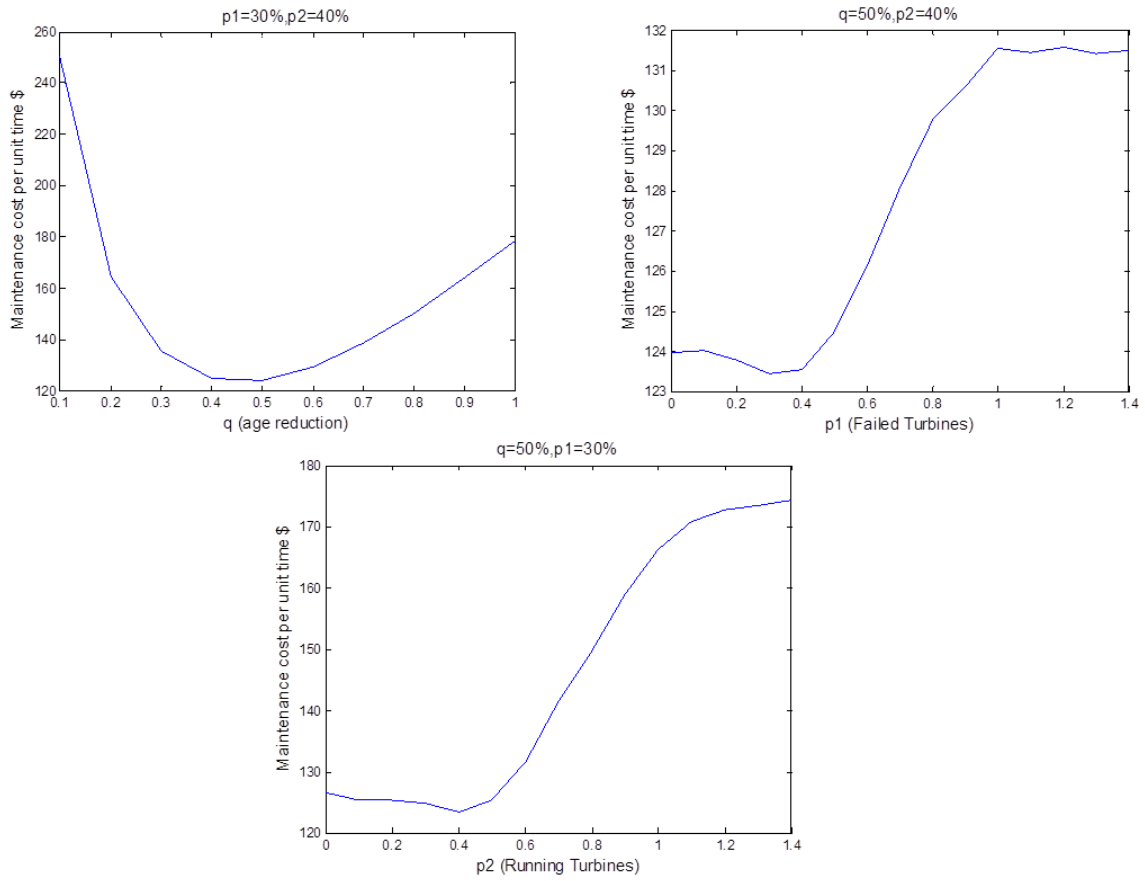

Figure 10. Cost versus p_1, p_2, and q

Strategy 3. Two-level maintenance

Two-level maintenance defines that the low-level maintenance is imperfect and the high level is perfect, and they are supposed to be performed at different age thresholds. A replacement will be considered when a component is older, while the imperfect action tends to be performed at the younger age. There are 4 age thresholds, two for the components in the failed turbine, denoted by p_{1L} and p_{1H}, while the other two for the components in the running turbines which are denoted by p_{2L} and p_{2H}. Based on the optimization result of strategy 2, the imperfect maintenance action of reducing the component's age by 50% is applied to this optimization problem.

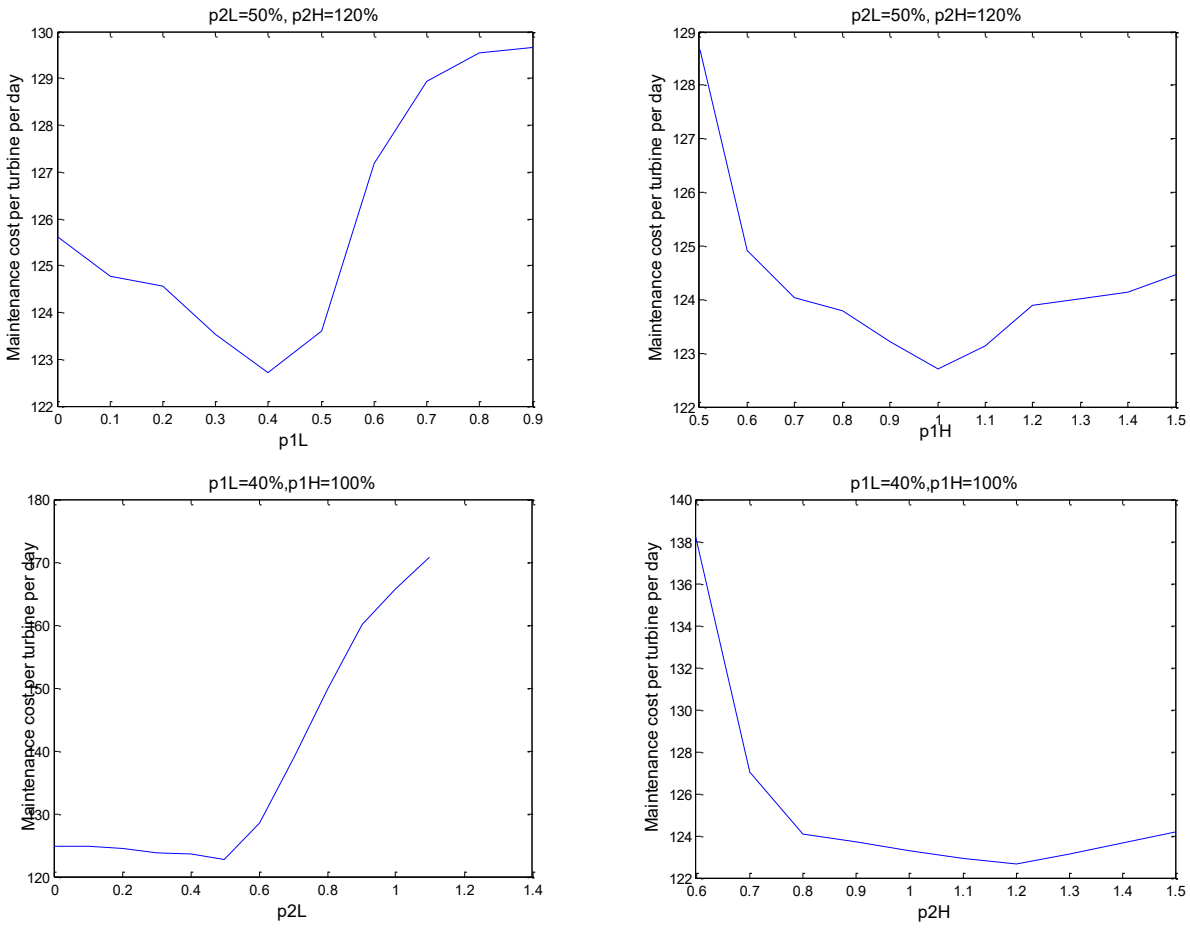

Figure 11. Cost versus p_{1L}, p_{1H}, p_{2L}, p_{2H} respectively

As can be seen in Figure 11, the two-level maintenance optimization model leads to the minimum cost of $122.7/day. The optimal policy shows that at the moment of a failure in the farm, imperfect preventive maintenance action is taken on the component whose age is between 40% and 100% of its mean lifetime in the failed turbine, and on the component whose age is between 50% and 120% in the running turbines. Otherwise, preventive replacement is performed on the component whose age exceeds 100% and 120% of its mean lifetime in the failed and running turbines respectively.

3.3.2 Comparative study

As mentioned earlier, [23] developed opportunistic maintenance methods for wind farms considering imperfect maintenance actions without distinguishing the age thresholds between the failed turbines and working turbines. In this section, the average maintenance cost is investigated considering only one age threshold for all components in the farm, regardless the failure turbine or working turbines. The advantage of the proposed methods is also investigated compared to the corrective maintenance policy, where only failure replacement is performed when a component fails in the wind farm. A comparison table is given to show the significant cost-saving of proposed approaches in this paper.

3.3.2.1 Optimization Results of The Same Threshold for All Turbines

Perfect maintenance only:

The minimum cost is $168.8/day, and a preventive replacement will be performed on all components older than 60% of their mean lifetime. The results are shown in Figure 12.

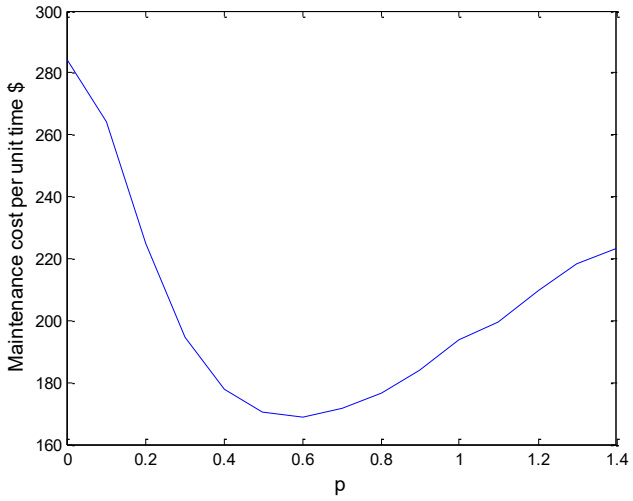

Figure 12. Cost versus preventive replacement age threshold value (p)

Considering imperfect maintenance:

The minimum cost is \$125.1/day, and the 40% age reduction maintenance actions will be performed on all components older than 40% of their mean lifetime.

Two-level maintenance:

In the optimal policy, 40% age reduction maintenance action is performed on the components according to the optimal result in Strategy 2A. The optimal cost is \$123.6/day, and all the components with age between 50% and 120% will be performed the imperfect action, while the components with age above 120% will be performed the preventive replacement.

3.3.2.2 Corrective Maintenance Cost Result

The total average cost of corrective maintenance policy is calculated for the same wind farm studied in previous examples. By applying the corrective maintenance policy, the optimal total average cost per turbine per unit time is found to be \$237/day.

3.3.2.3 Comparison Results

The optimal cost results of each proposed strategy are given in Table 2. In Section 3.3.1, the optimization results show the optimal average cost of \$167.2/day, \$123.4/day, and \$122.7/day for the proposed strategies with perfect action only, imperfect action and two-level action policies, respectively. Thus, significant cost savings of 29.4%, 47.9%, and 48.2% can be achieved compared to the corrective maintenance policy, and the two-level action method produces the lowest cost. It is found that the optimal results considering the same age thresholds are close to those distinguishing the failed turbines and running turbines. Thus, if the wind farm operators want to be accurate in wind farm performance evaluation and optimization, the accurate models considering the difference between failed turbines and running turbines should be preferred.

Table 2. Optimal cost of proposed opportunistic maintenance strategies

Corrective Maintenance		\$237/day		
Proposed Methods		Perfect	Considering	Two-Level
	Minimum Cost	\$167.2	\$123.4	\$122.7
	Cost-savings	29.4%	47.9%	48.2%
Same Age Threshold for Failed and Operational Turbines		\$168.8	\$125.1	\$123.6
Fixed Imperfect Actions (Age Reduction)	25%	/	\$144.2	\$144.9
	50%	/	\$123.4	\$122.7
	75%	/	\$143.2	\$142.1

Also, imperfect maintenance actions, i.e., variable q, are considered as discrete values rather than continuous variable, where only specific ratios of age reduction actions can be implemented in an imperfect maintenance task. In many real-world applications, a particular age reduction level corresponds to a particular preventive maintenance technology or routine, and it also takes into account the ease of control and administration of imperfect maintenance actions. For this specific example, it is assumed that there are three possible age reduction options, 25%, 50%, and 75%. In this example with the specific settings, the 50% age reduction imperfect action is found to be the most cost-effective, while 25% and 75% age reduction actions cost 16.6% more.

3.4 Conclusions

In this chapter, opportunistic maintenance optimization approaches are developed for wind farms to take advantage of the maintenance opportunities to perform preventive maintenance actions. Imperfect maintenance actions are considered, which addresses the practical issue that preventive maintenance does not always return components to as-good-as-new status. The proposed opportunistic maintenance policies are defined by the component's age threshold values, and different imperfect maintenance thresholds are introduced for failure turbines and working turbines, respectively. Three types of preventive maintenance actions are considered, including perfect, imperfect and two-level action. Simulation methods are developed to evaluate the costs of proposed opportunistic maintenance policies. The numerical examples illustrate the proposed approaches. The comparative study with the widely used corrective maintenance policy demonstrates the advantage of the proposed opportunistic maintenance methods in significantly reducing the maintenance cost. The developed methods have great potential to bring immediate benefits to wind power industry.

One should be noted that, the variable values, q and p, in the study are considered as discrete values with interval of 10%. This is to reduce the computation burden, and besides, an integer times of 10% would be easy to implement regarding an age reduction maintenance and evaluation of component's age compared to its mean lifetime by the maintenance crew in practice. However, there is a limitation of finding the global optimal solution without considering the continuity of the variable values. It is suggested that future work could consider continuous variables in the optimization procedure by means of more efficient optimization algorithm, if the precise maintenance cost is extremely concerned by the industry.

Chapter 4. Integrated prognostics study for the gearbox in wind turbines considering instantaneously varying load condition

4.1 Overview

There are many studies on CBM of wind turbines. In this study, we focus on the fatigue crack damage in wind turbine gearboxes, which are critical components and can lead to high failure and maintenance costs. Fatigue crack propagation is generally governed by the Paris' law, where the stress intensity factor (SIF) plays a key role in crack propagation. Many existing approaches developed for wind turbine component prognostic problems mainly assume constant loading condition. In reality, many engineering systems work under unstable environment, e.g., time-varying speed, load, temperature, etc. Specifically, wind turbines work under varying wind conditions in terms of wind speed and direction, which leads to varying torque applied to the mechanical components in the hub. The torque is changing over time, even during one revolution period. The existing approaches are generally not accurate representations of the problems in such an instantaneously time-varying environment. Using constant load over time as an approximation of the time-varying load case is not accurate since the crack propagation process is affected by the loading condition. This is reflected by different SIF values when different loads are applied, and thus the crack growth rate is affected according to crack propagation law. Stepwise time-varying load was considered by Zhao et al. [96], but the load is still assumed to be constant in each operation period. Such load condition approximation is usually not the case of wind turbine operating condition, since the rotor torque caused by the wind keeps changing instantaneously. In addition, the instant of load change was mapped to a certain cycle to

represent the varying load process in [96]. However, the exact number of cycles of that change occurs is very likely unknown in practice, and load changes happen on a continuous basis.

Considering the instantaneous time-varying load, Alawi and Shaban, Altamura and Straub, Huang and Hancock, Khan et al., Lei and Zhu, Sobczyk, Zhao et al., and Zhu et al. proposed various modified crack propagation process based on the basic Paris' law[62], [64], [66]–[70], [78]. Material constant C and Δk were expressed as the functions of load cycle N in the model proposed in [62]. In [64], the growth rate of fatigue crack was denoted by crack length growth per unit of time, rather than increasing number of load cycles, because a cycle is not straightforward and unique when the load is randomly varying in time. [66] claimed that there exists a correlation between the root mean square of SIF range (Δk) and growth rate of a fatigue crack, but they concluded that Δk_{rms} vs. $\mathrm{da/dN}$ approach fail to model the experimental data. However, [67] suggested that if the constant in the model, m, is less than 2, $\Delta \mathrm{k_{rms}}$ can be appropriate. An extra random process Y(t) accounting for the random material resistance were considered in the model [67], [68]. In [70], The basic Paris' model was applied, and treated the random loading and crack growth rate were treated as random variables, but the random time-varying feature was ignored. In this study, we do not apply any mentioned approaches due to their limitations and lack of implementation details. Instead, a new scaling method is proposed to model the crack propagation process, where Δk at each crack level is represented by a scaled distribution corresponding to the varying external load profile. More details are given in Section 4.3.

Model-based prognosis and Data-driven prognosis are well-known methods in CBM study. Data-driven methods generally apply machine learning techniques or statistical models to the historical condition data to empower the capability of predicting future condition. Model-based

methods, however, use physical models, such as finite element (FE) models and fatigue propagation models based on fatigue mechanics, to predict the component health condition. Significant challenges exist for model-based methods when a component is complex for modeling its physics and dynamic response, while data-driven methods are not effective when data are not sufficient, or the data-driven models are not suitable. In this study, an integrated prognostics method based on the framework in [78] is developed to fuse the condition monitoring data via Bayesian inference to update the physical model in an integrated way, and improve the prediction with limited available historical data.

Considering the drawbacks and challenges of existing works mentioned above, in this study, an integrated varying-load approach is proposed for predicting wind turbine gearbox reliability by explicitly considering instantaneously varying external load. The damage propagation process under instantaneously time-varying external load condition is explicitly considered. We focus on the prognosis for a spur gear with a crack at the tooth root. FE model is built to calculate the SIF, and it is used in a modified Paris' propagation model proposed in this study to deal with time-varying load conditions. Material parameter distribution in the crack propagation model is updated by means of Bayesian inference method by fusing new available condition monitoring data at each inspection interval, and the predicted failure time of the cracked gear is then updated accordingly. An example will be used to demonstrate the effectiveness of the proposed method.

This chapter is organized as follows. Section 4.2 presents the framework of the proposed prognostics approach, which is adapted from the existing study but considers time-varying loading conditions. Section 4.3 gives the analysis details about varying external load profile for the gearbox in a wind turbine, and introduces a useful load simulation tool FAST which produces a dataset of the instantaneously varying load applied for the examples in this study. In Section

4.4, the proposed integrated prognostic approach consider time-varying load condition is introduced. Section 4.5 gives a numerical example to demonstrate the developed method. A comparative study between the proposed time-varying load method and constant load approximation method with two different crack measurement error cases is conducted in Section 4.6. Conclusions are given in Section 4.7. The materials in this chapter has been published in [2].

Nomenclature:

P_w: the wind power passes through the turbine

P_m: mechanical power generated by the rotor

ω_m: the turbine angular velocity

C_p: the power coefficient

R: the maximum radius of blade sweeping area (blade tip)

v: wind speed

c and m: gear material parameters

Δk: the range of stress intensity factor

$\Delta a/\Delta N$: crack growth rate

f_{post}: posterior distribution in Bayesian updating process

f_{prior}: prior distribution in Bayesian updating process

4.2 Framework of the proposed integrated prognostics approach

The framework of the proposed integrated prognostics approach is presented in this section, and the flowchart of the framework is shown in Figure 13. The framework is adapted from the existing one presented in [78] by considering time-varying loading conditions. There are two parts in the prognosis process, the data-driven part and model-based part. Data-driven part processes the collected condition monitoring data and applies the crack estimation techniques to evaluate the crack length with uncertainty. In the model-based part, the crack at the gear tooth root affects the mesh stiffness significantly, and thus the dynamic load applied to the cracked tooth. The dynamic model is used to determine the dynamic load accounting for the load change due to crack growth by solving a set of dynamic motion equations. FE model is used to perform stress analysis corresponding to a specific crack length and load, and produces the SIF value at the crack tip. SIF is then used in the proposed crack propagation model dealing with varying external load condition. The failure time and the remaining useful life (RUL) distribution can be predicted through the degradation model at the current crack length, which is described in Section 4.4. Bayesian inference is used to update the distributions of the material parameter, one of the major uncertainty factors in this work, and thus achieve a more accurate RUL prediction.

The wind turbine modeling and consideration of varying external load are described in Section 4.3. The degradation model and crack propagation prediction are presented in Section 4.4. For related information such as FE model performing stress analysis, gear dynamic model, etc., one can refer to [78]. Uncertainty factors considered in this prognostic study include material parameter uncertainty, crack propagation model uncertainty $\mathcal{E}$, and measurement uncertainty τ.

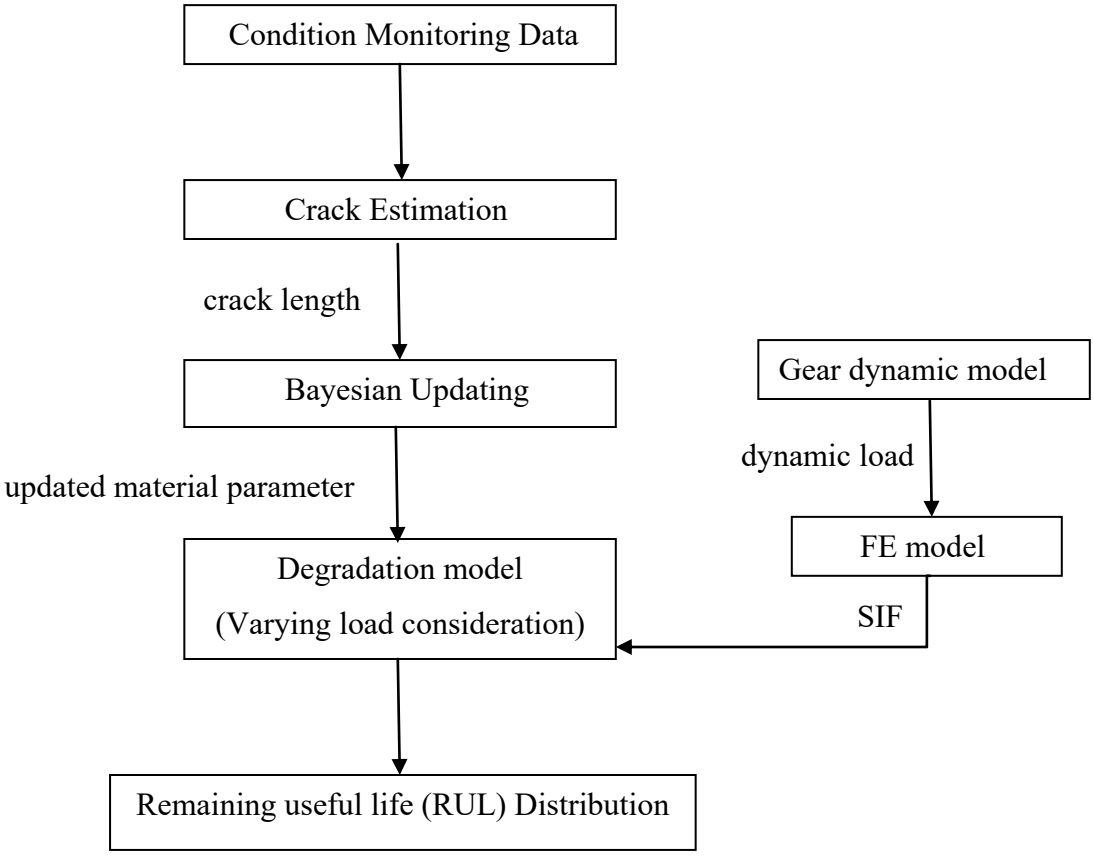

Figure 13. Flowchart of the integrated prognostics framework

4.3 Wind turbine and varying load profile modeling

Wind turbines can generally be in operational or parked status. When the wind speed is below cut-in speed or above cut-out speed, wind turbines stop through its control strategy. Jiang et al. considered both operational and parked cases in contact fatigue analysis of a planetary bearing in a wind turbine drive train, and they concluded that the parked cases have negligible contributions to the fatigue life while the operational cases are the dominant case [97]. We consider only the operational cases in this study for RUL prediction. The time-varying torque applied to the low-speed shaft (LSS) connected to the gearbox is the key input in this study, called LSS torque. A

brief explanation is given as follows to understand the varying torque profile. Wind turbines are typically designed to work at two kinds of operational modes, working in a constant rotor speed regardless of the wind speed fluctuations, or variable rotor speed which is proportional to the wind speed. Some studies use a proportion of wind power to represent the aerodynamic load applied to the rotor in the wind. Note that this method can only be applied to variable rotation speed wind turbines, which is designed to operate at a rotor speed proportional to the wind speed. This is because changes in the aerodynamic power are absorbed as changes in the angular velocity of the rotor, while assuming the turbine is well controlled with the power optimized, i.e., the pitch angle θ and the tip speed ratio λ are kept constant at optimal values [98]. The followings illustrate the load calculation in the case that a wind turbine works at variable rotor speed.

4.3.1 Time-varying torque applied to the transmission system

Figure 14 shows the power conversion system of a wind turbine (WT), and we can consider a gearbox system as a transmission unit [99]. After the wind power P_w passes through the turbine, mechanical power P_m at the turbine angular velocity ω_m is then supplied to the transmission system. $P_m = C_p \cdot P_w$.

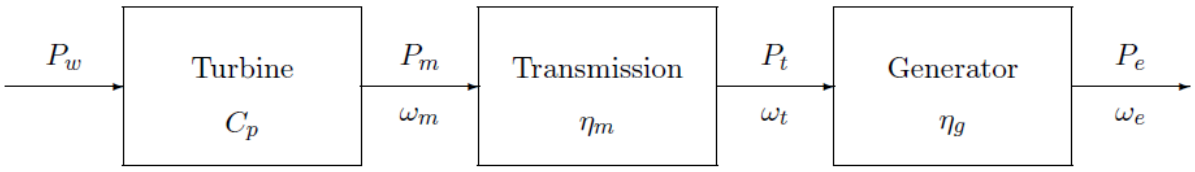

Figure 14. Wind Electric System [99]

The power in the wind P_w is

$$p_w = \frac{1}{2}\rho A {v_w}^3, \tag{4-1}$$

and $P_m = C_p \cdot P_w$. So

$$P_m = C_P\left(\frac{1}{2}\rho A {v_w}^3\right) = \frac{1}{2}\rho\pi R^2 {v_w}^3 C_P(\lambda,\beta), \tag{4-2}$$

where C_p is the power coefficient, i.e., the ratio of the extractable mechanical power to the power contained in the air stream [74], which is a function of tip speed ratio λ and blade pitch angle β (degree) [100]. λ is formulated as:

$$\lambda = \frac{w_r R}{v} \tag{4-3}$$

where w_r is angular velocity of wind turbine rotor (revolution per time), R is the maximum radius of blade sweeping area (blade tip), and v is wind speed.

Thus, the aerodynamic torque applied to the rotor is [101]:

$$\text{torque} = P_m/w_r, \quad w_r \text{ is angular velocity (arc/s).} \tag{4-4}$$

However, when the wind speed is above the designed rated wind speed corresponding to the rated power (say, 2MW), the power is not a function of wind speed but remains a fixed value. The torque calculation described above is not applicable any more, and aerodynamic load, which is a main role of the torque, varies by means of power control mechanism.

4.3.2 The relationship between load and power control

Wind turbines are in general designed to yield a maximum power output, rated power, at a certain rated speed. To prevent damage to the wind turbine due to excessive winds, the rotor speed is designed to remain constant in order to shed part of the excess energy, and stall when wind velocity exceeds cut-out speed. Thus, wind turbines need power control. Basically, there are three control strategies: yaw control, generator torque control and pitch control [98], [101]. Control methods optimize the power output by adjusting the relevant angle, e.g., yaw angle and pitch angle of the blade, in response to the time-varying wind speed and direction. These all affect the load applied to the rotor. Thus, the load change is a very complex and dynamic process.

The varying cyclic load, which dominantly leads to fatigue, consists of a deterministic part due to gravity loads and a stochastic part due to aerodynamic loads [98]. Gravity load is given as:

$$F_g = M_{blade} \cdot g \tag{4-5}$$

Aerodynamic loads are based on the blade element momentum method. The rotor swept plane is divided into a number of ring elements, the torque on the ring element is

$$dQ = 4\pi r^3 \rho V_0 \omega (1 - a) a' dr, \tag{4-6}$$

where r is the radius of the ring element, a and a' are the axial and tangential induction factors, respectively, and are mainly related to pitch angle θ and inflow angle α, which vary by means of pitch in response to the varying wind speed and direction.

As we can see, when a turbine has constant rotation speed, the aerodynamic load due to the wind speed fluctuations is certainly varying due to the working mechanism of power control system,

e.g., blade pitch θ adaptation. The varying load applied to the rotor can be thus calculated by summing the load over the blades using Equation (4-6), and it will be induced to the gearbox transmission system. However, there is almost no way to get the parameter values of θ and α analytically. The existing studies usually use FEM and modeling software, e.g., FAST, to simulate the instantaneous loading. Given these issues on quantifying the varying load, FAST is used in this study to generate the varying torque data. A brief introduction of FAST is given in the following subsection.

4.3.3 FAST simulation tool

As mentioned earlier, the varying load applied to the wind turbine rotor due to varying wind speed and its complicated control mechanism is very hard to be presented by analytical model only, as the parameters involved are not in steady state over time and their values almost cannot be captured analytically. No mathematical models are found in existing studies on modeling the varying load in wind turbine thus far.

However, FAST, simulation tool developed by NWTC/NREL, was found to be very helpful to provide simulated instantaneously varying load outputs, which resolve this vital issue in our prognosis study for WT application. [102] Used FAST to address dynamic conditions in the study of gear contact fatigue analysis for a wind turbine drive train. FAST archive is free for download online, and a set of 17 sample models are provided including all pertinent input files, such as tower, blade, turbine control, aerodynamics parameters, mass, wind profiles, etc., [103]. In this study, sample model "test13" is selected, Table 3 gives a general description of this wind turbine based on the provided input file in the open accessed FAST archive.

Table 3. General configuration of the wind turbine (Model-Test13)

Type	Three-blade
Rated Power	1.5MW
Rotor Diameter	70m
Rated Rotor Speed	20rpm
Power Control	Simple variable speed & pitch control
Hub Height	84.2876m
Gearbox Ratio	87.965
Wind Condition	Wind speed at the hub height
	Min=10.16m/s, Max=24.90m/s, Mean=18.2m/s

Given the specific wind data profile and wind turbine model, 700s time-series of torque on the main shaft is simulated in FAST, and the first 100s is discarded due to possible transient effects in the simulation. The generated torque time-series data is plotted in Figure 15. Such torque is then transmitted to the input shaft for the high-speed stage gear pair, by introducing a linear factor considering the gear transmission ratio in between and the energy loss. The output shaft for the high-speed gearbox stage is the high-speed shaft (HSS). Thus the focus of this study is on the integrated prognostics study for the faulty gear in the high-speed gearbox stage. The torque is then applied as the input to gear dynamic model, which describes the dynamics of the studied high-speed gearbox stage, for calculating the load applied on gear tooth and subsequently the SIF to be used in crack propagation calculation [78].

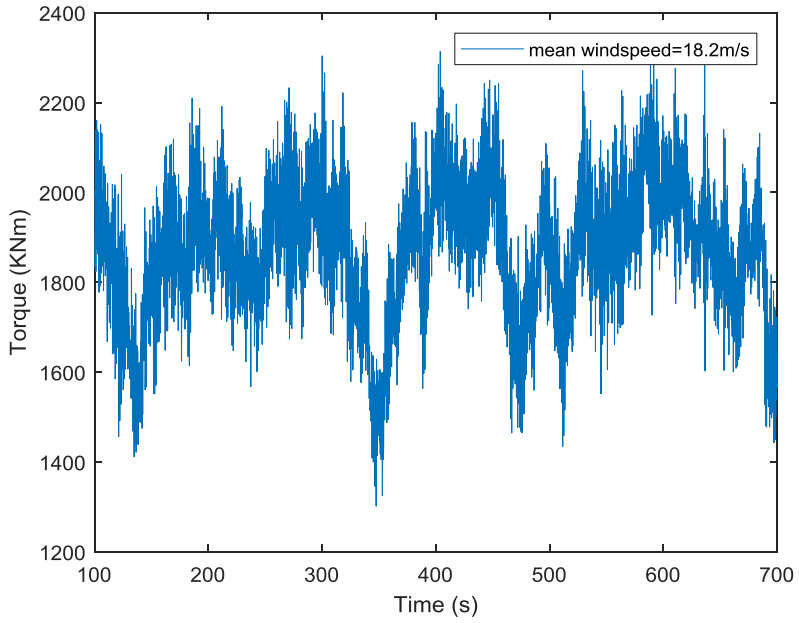

Figure 15. FAST simulated varying torque

4.4 Gear degradation and parameter updating considering time-varying load

The gear degradation model proposed in this study is for predicting crack propagation in a gear tooth over time considering the time-varying external load condition. Experimental results of fatigue crack tests have shown that the crack propagation has three distinct regions. Most of the existing crack propagation models are based on the Paris' law [63], which is one of the first and most widely used fatigue crack propagation models and work at the stable region where the log-log plots of crack growth rate versus cycles are linear.

In this study, a scaling method is proposed to model the crack propagation process based on the basic Paris' law, and the form is given by

$$\frac{\Delta a}{\Delta N} = C \cdot E[(\Delta k)^m], \tag{4-7}$$

where *da/dN* is crack growth rate, *c* and *m* are material parameters and generally experimentally estimated by fitting fatigue test data, and *E* is the expectation of $(\Delta k)^m$ at a certain crack level considering the time-varying load condition. With the integrated prognostics framework, SIF with respect to a certain load can be obtained by scaling the pre-calculated SIF with respect to a baseline load, and thus Δk can be obtained in an efficient way [96]. Equation (4-7) can also be reformatted in a discrete form as

$$\Delta a = \Delta N \cdot C \cdot (p_1(\Delta k_1)^m + p_2(\Delta k_2)^m + \cdots + p_n(\Delta k_n)^m), \tag{4-8}$$

where p_i is the PDF value when $\Delta k = \Delta k_i$.

Considering the time-varying load, the sampled real time-varying external torque data set is used as input for the tooth meshing dynamic process and dynamic load calculation, and stress analysis will be subsequently conducted in FRANC2D physical model. The resulting Δk over one revolution of gear meshing can reflect the varying load impact. In addition, during each crack level, the load keeps changing. In this case, the varying load over one revolution is to be sampled multiple times from same varying torque data pool, which is simulated by FAST with a given common wind sample. Note that we assume these simulated varying torque values can reflect typical patterns, which is reasonable since wind profile in a certain location usually is same over a period of time. By sampling load data with appropriate times and applying these data sets repeatedly at each crack level, we can properly model a gear subject to consistent varying input torque condition during its damage propagation process.

Suppose that during each crack increment $\Delta a = 0.2mm$, the same 100 sets of time-varying external torque over one gear revolution are sampled, and these samples represent the consistent external condition that the gear suffers at each crack level. Suppose Δk values at initiation stage

$a = 0.2mm$ are obtained given 100 data sets of sampled varying torque, we can easily find the distribution of $\Delta k \sim N(\mu, \sigma^2)$ by normal fitting, with a significant reduction of computation complexity.

In addition, it is found that Δk monotonously increases as the crack grows when the constant external load is considered in the FE model, which is briefly described in Section 5.2. The larger the crack is, the faster Δk increases. In this study, the mean of 100 sets of sampled external torque data is applied as the constant load to the FE model first, Δk is then analyzed at each crack level by applying the method developed in [78]. Thus, the pairs of calculated $\overline{\Delta k}$ vs. crack length are obtained and then fitted by polynomial approximation. The distribution of Δk at each crack level is thus be obtained *N(rate* $\cdot \mu$, $rate^2 \cdot \sigma^2$*),* where *rate*= Δk at current crack level/Δk at initial crack level (0.2mm).

The process of calculating crack increment using the proposed damage propagation model is illustrated as follows.

Step1: Initiate crack at a=0.2mm. Sample 100 external torque data sets from the simulated torque pool.

Step 2: Calculate Δk values corresponding to the 100 mean torques for crack length =0.2mm, and fit them to get μ and σ of Δk distribution, which is assumed to be normal.

Step 3: Divide the Δk over the range (μ-3 σ, μ +3 σ) with *n* data points, and here we set *n* =500.

Step 4: For each Δk in [μ-3 σ, μ +3 σ], calculate its PDF, denoted by *p*.

Step 5: Calculate Δa using Equation (4-8), and

$$\mathrm{E}(\Delta a)=\Delta N \cdot C \cdot \int_1^n p \cdot (\Delta k)^m \, d\Delta k \tag{4-9}$$

Step 6: With the growth random variable Δa and the current crack length, the predicted crack length distribution at the next inspection interval can be obtained, denoted by $\boldsymbol{a}_{NX}$, which is used for updating material uncertainty parameter m, based on the observed crack length at the next inspection interval a_{ab}. Bayesian inference is used:

$$f_{post}(m|a_{ab}) = \frac{\mathrm{l}(a_{ab}|m) f_{prior}(m)}{\int \mathrm{l}(a_{ab}|m) f_{prior}(m) dm} \tag{4-10}$$

where $\mathrm{l}(a_{ab}|m)$ is the likelihood function, which is determined based on crack length random variable at the next inspection point $\boldsymbol{a}_{NX}$. a_{ab} is the observed crack length at the next inspection point.

Step 7: Go to Step 2.

The uncertainties in the model are the major causes of inaccurate failure time prediction, and these are the consequences of variations in the production process as well as human errors. In this degradation model, material uncertainty, model uncertainty, and measurement uncertainty are considered. Condition monitoring data are the unit-specific information that can be used to determine and update the material parameter distributions for the specific unit. In this chapter, the gear at the high-speed stage in a wind turbine is studied. Bayesian updating method will be used to update material parameter distributions at every inspection interval as long as the crack length is estimated with available condition monitoring data.

4.5 Numerical Examples

In this section, numerical examples are presented on gear life prediction using the proposed integrated prognostics approach considering time-varying load. Simulated degradation paths are generated by considering the various uncertainty factors. A degradation path contains the information on inspection time and the associated crack length. The generated degradation paths are divided into two sets: the training set used to obtain the prior distribution for parameters, and the test set to test the prediction performance of the proposed prognostics approach.

4.5.1 Introduction

In the examples, a 2D FE model of a single cracked tooth is built in the FRANC2D software program. The singular mesh near the crack tip will be generated automatically. Based on the stress analysis, the crack will be propagated, and the associated $\overline{\Delta K}$ at each crack length will be recorded accordingly since the mean torque is used representing the varying load profile in FE model. The material and geometry properties of this specific spur gear used in this example are listed in Table 4 [78], [86]. In a wind turbine, the gearbox is configured to increase rotation speed at the output shaft for power generation by the generator. Thus, the driving gear size is supposed to be bigger than the driven gear size. The tooth number of the studied gear with crack, the driving gear, is 48, while the driven gear in the gear pair has 19 teeth.

In a wind turbine, the fixed axis gear pairs are usually applied at the intermediate and high-speed stages after planetary gear stage, which is at low-speed stage directly connected to the rotor shaft. An overview of a typical gearbox with internal components of many megawatt-sized wind turbines is shown in Figure 16 [104], and this is also the configuration of gearbox we considered in this study. There are three gear stages: the low-speed planetary gear stage, the intermediate

and high-speed parallel gear stages. In this case, we consider the driving gear at the high-speed stage. The varying rotor torque applied to the low-speed shaft (simulated by FAST) is transmitted to the input shaft at the high-speed stage by introducing a linear factor based on gear ratio and energy transmission loss.

Table 4. Material properties, and main geometry parameters [78], [86]

Young's modulus (Pa)	Poisson's ratio	Module (mm)	Diametral pitch (in^{-1})	Base circle radius (mm)	Outer circle (mm)	Pressure angle (degree)	Teeth No.
2.068e11	0.3	3.2	8	71.6	79.4	20	48

Suppose the critical crack length is 5.8mm, which is about 70% of the full base tooth thickness. Beyond this failure threshold, the crack will propagate very fast, and the tooth break is imminent. The FE model is shown in Figure 17.

The gear dynamic system model is used to calculate the dynamic load on this cracked tooth [78]. The varying input torque during one revolution period is sampled from the FAST simulated RotTorq output shown in Figure 15. At each crack level, the load is constantly changing. 100 varying torque datasets are periodically sampled within 600s simulation duration, and these same 100 datasets are used at each crack level, which represents the gear under consistent varying input torque profile during one crack degradation unit period (0.2mm). SIF values are calculated in FRANC2D. The mean of 100 sampled torque data sets is applied as a constant load for stress analysis in FE model to get the curve of $\overline{\Delta k}$ vs. crack length, as mentioned in Section 4. This

curve is to be used as a baseline in evaluating crack growth with the proposed damage propagation model. During the crack propagation process, at each crack level, to drive the crack to propagate at an appropriate direction under time-varying external load, it is also reasonable that we consider the calculated maximum dynamic load under that mean torque as the load applied at the contact point. 0.2 mm crack increment is then implemented in FRANC2D model.

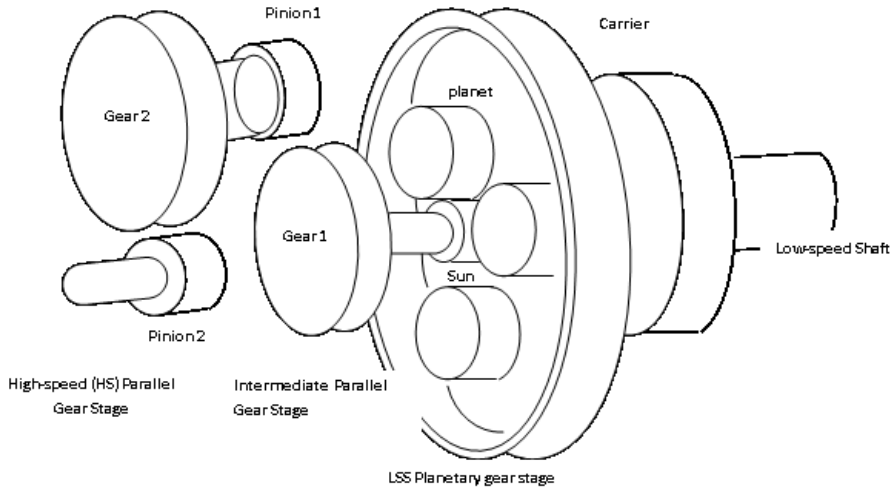

Figure 16. Wind turbine gearbox configuration [104]

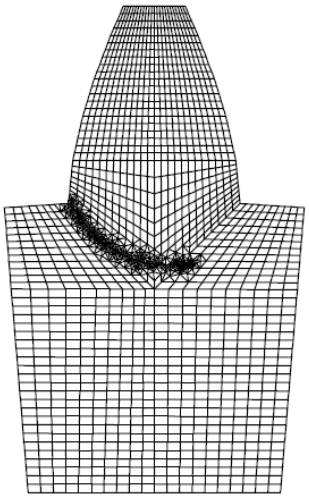

Figure 17. 2D FE model for spur gear tooth, critical crack length=5.8mm

Besides the torque, other values for the parameters in the dynamic system can be found in [86]. The crack is introduced at the root of the second tooth on the driving gear, and the crack growth will end when it reaches the critical length of 5.8 m. Crack greatly reduces the mesh stiffness, as can be seen in Figure 18 showing the crack of 3.6mm, and the total mesh stiffness is represented by the solid blue line while the mesh stiffness of the gear pair with the cracked tooth is represented by the mauve dash line. The details of calculation for time-varying stiffness at different crack length can be found in [78].

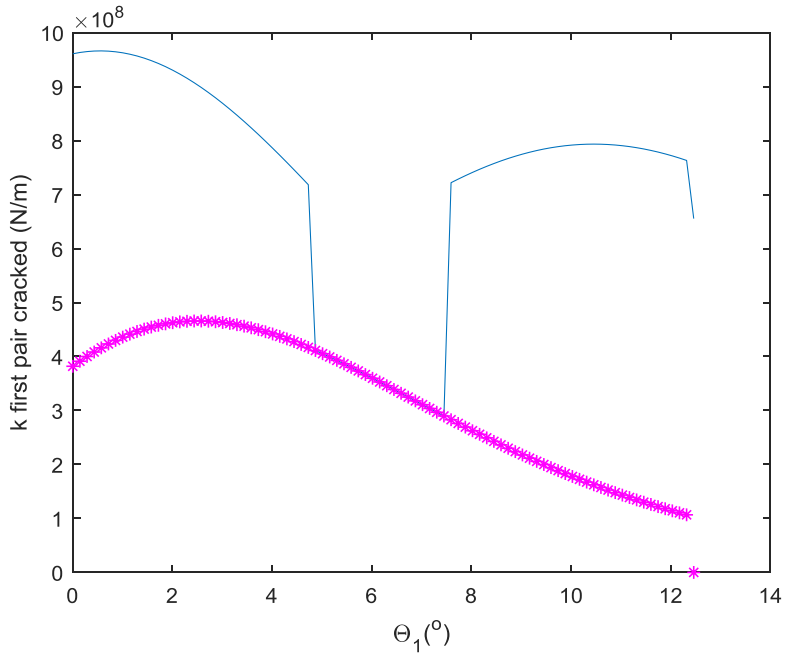

Figure 18. Meshing stiffness of gear pair with a cracked tooth, crack length=3.6mm

MATLAB's ODE15s function is used to solve the dynamic equations listed in [78] with time-varying mesh stiffness at different crack lengths calculated. Dynamic loads at every contact points, in other words, at every rotation angle, can then be obtained. Figure 19 shows the static load and dynamic load on the cracked tooth when it has a crack of 3.6mm meshes. There appears

the maximum dynamic load at the rotation angle of 5.6 degrees, and it is higher than the maximum static load.

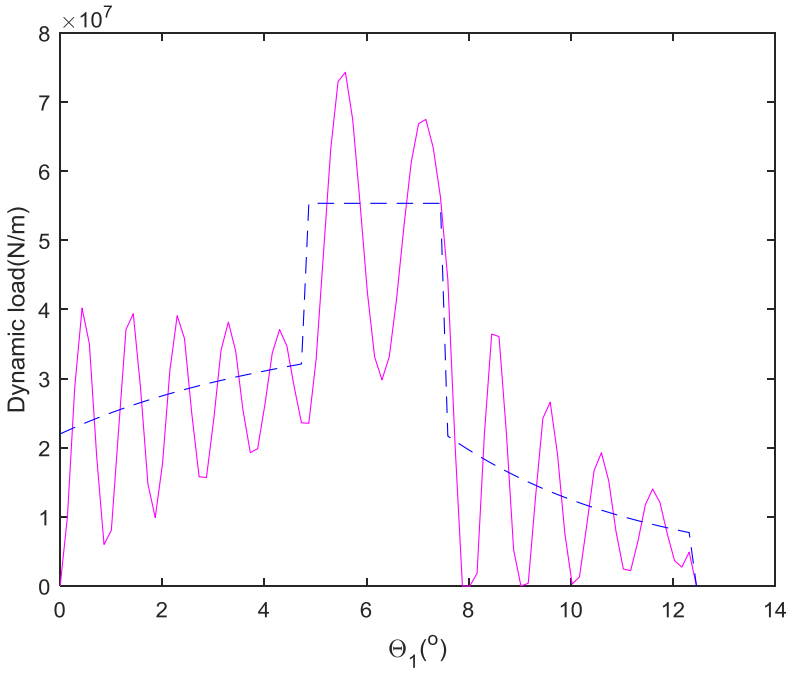

Figure 19. Dynamic load on gear tooth with a crack of 3.6mm

By conducting the experiments for the entire crack path, it is found that the position of maximum dynamic load only moves forward a little bit with the movement of less than 1 degree as the crack grows. It is not arbitrary that we consider the maximum load is always applied at a fixed position for the whole crack path, which corresponds to the rotation angle of around 6 degrees. As mentioned earlier in Section 4.4, the time-varying external torque over one revolution is sampled multiple times, and same data sets are used for each crack level to represent the consistent varying load profile applied to the wind turbine. The mean of the varying torque is applied using the constant-load approach developed in [78] to find out SIF vs. crack length curve. The result is shown in Figure 20, which is $\overline{\Delta k}$ vs. crack length. As can be seen in Figure

20, the mode I's SIF is dominant comparing to the mode Ⅱ stress intensity factor, so only K_I is used to calculate the crack growth rate. As we can see, Δk equals K_I that is obtained with the input of the maximum dynamic load, since the minimum dynamic load during the cracked tooth mesh period is zero. In addition, the maximum dynamic load is larger than the static load, which results in a larger Δk compared to that obtained with the static load, and thus the crack grows faster that will lead to a relatively shorter RUL.

As mentioned previously, the curve K_I vs. crack length in Figure 20 represents $\overline{\Delta k}$ vs. crack length when the mean of time-varying torque is applied, and it will serve as the baseline to estimate the crack increment Δa using the proposed damage propagation model described in Section 4.3.2.

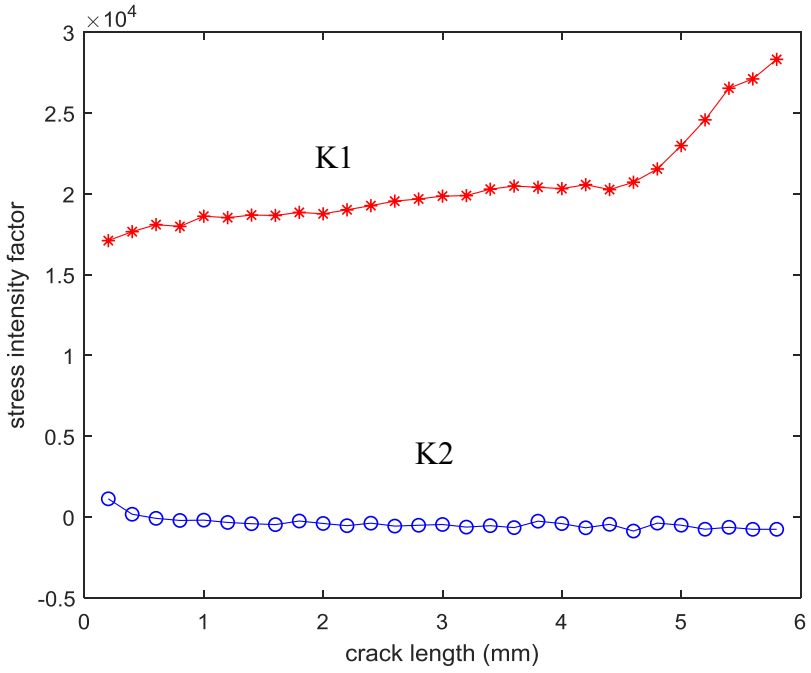

Figure 20. $\overline{\Delta k}$ vs. crack length (the unit of Δk is Mpa$\sqrt{\text{mm}}$)

To validate the proposed integrated approach, a set of crack degradation paths P are generated using the modified Paris' law described in Equation (4-7), and it can be formed as follows:

$$a((i+1)\Delta N)=a(i\Delta N)+(\Delta N)C\cdot E[\Delta k(a(i\Delta N))]^m\varepsilon,\ i=0, 1, 2, ..., \lambda\text{-}1$$

$$a_{\text{mea}}(\lambda\Delta N)= a(\lambda\Delta N)+e$$

$$a(0)=0.2 \tag{4-11}$$

where $E[\Delta k(a(i\Delta N))]^m = p_1(\Delta k_1)^m + p_2(\Delta k_2)^m + \cdots + p_n(\Delta k_n)^m$, p_i is the PDF of $\Delta k = \Delta k_j$ when the crack length $a(i\Delta N)$, and a_{mea} is the measured crack length at every inspection time. To generate degradation path i, parameter m_i is randomly sampled once from its population distribution, and the value is kept constant until crack grows to the critical length. At each propagation step, model error ε sampled from its distribution is introduced, and a random measurement error e is added to the generated measured crack length at each inspection time as well. All generated crack paths i and values of sampled m_i, termed as *real* m_i, are used in the training process to obtain a prior distribution of parameter m and validating the approach. The following values and distributions for the parameters are used in this example to generate the degradation paths: $C = 9.12e\text{-}19$, $e \sim N(0, 0.2^2)$, i.e., $\tau = 0.2$, $m \sim N(3.2354, 0.2^2)$, and $\varepsilon \sim N(2.5, 0.5^2)$.

Ten degradation paths are generated according to Equation (4-9), until the critical crack length of 5.8mm, as shown in Figure 21. Table 5 shows the ten real values of m for generating these ten paths. They are divided into two sets: #(H)=7, #(R)=3, of which #5, #7, #9 are the three test paths. Thus, for each path i belongs to H, the optimal m_{i_op} value, i=1,2,3,4,6,8,10 satisfying minimum least square (MLS) criteria can be found. 7 Trained m_i are then used to obtain a prior

distribution m by fitting with the normal distribution. Finally, the prior distribution for m is $f_{prior}(m) \sim N(3.1255, 0.0535^2)$.

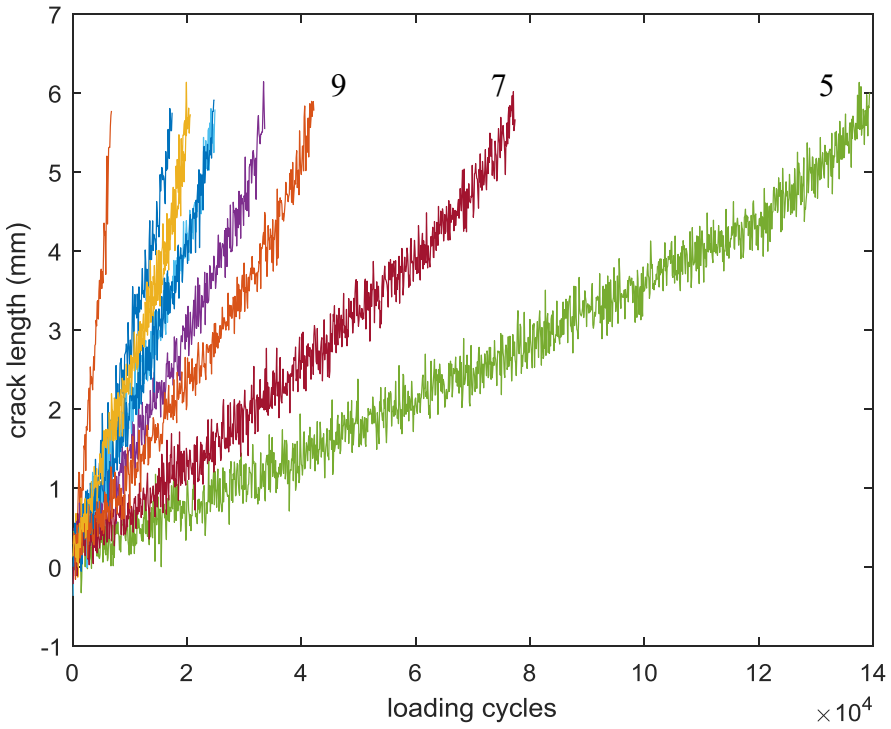

Figure 21. 10 Simulated degradation paths

4.5.2 Results

To validate the proposed prognostics approach, we take paths #5, #7, and #9 for testing. At each inspection cycle for updating, the posterior distribution of m will be the prior distribution for the next updating time. Here, Path #7 is given as an example to demonstrate the updated posterior distribution of m. In path #7, the updating history is shown in Table 6. The Bayesian updates adjusted the mean value of m from the initial value 3.1255 to its real value gradually at every inspection interval of 1.9×10^4 cycles, as the condition monitoring data on the crack length are available. Because the RUL is very sensitive to the value of m, the distribution adjustment for m

is critical for maintenance optimization. Moreover, the standard deviation of *m* is reduced, which means that the uncertainty in *m* is reduced through Bayesian updating given the measured crack length. To demonstrate this, Figure 22 shows the updated distribution of for path #7, from which we can see that with the updates for distribution of *m* at certain inspection times, the predicted failure time distribution becomes narrower, and the mean is approaching the real failure time. The updated RUL distribution at each inspection time for path #7 is also computed as shown in Figure 23.

Table 5. Real and trained m of each degradation path

Path #	Real *m*	Trained *m*
1	3.1434	3.1437
2	3.2353	3.2330
3	3.1279	3.1283
4	3.0803	3.0816
5	2.9427	-
6	3.1088	3.1117
7	2.9993	-
8	3.1096	3.1085
9	3.0581	-
10	3.1305	3.0718

Table 6. Test for Path #7 (real m=2.9993)

Inspection cycle	Crack length (mm)	m_μ	m_σ
0	0.2	3.1255	0.0535
$1.9*10^4$	1.4621	3.0219	0.0123
$3.8*10^4$	1.9521	2.9953	0.0067
$5.7*10^4$	3.6476	3.0014	0.0060
$7.6*10^4$	5.6214	3.0028	0.0042

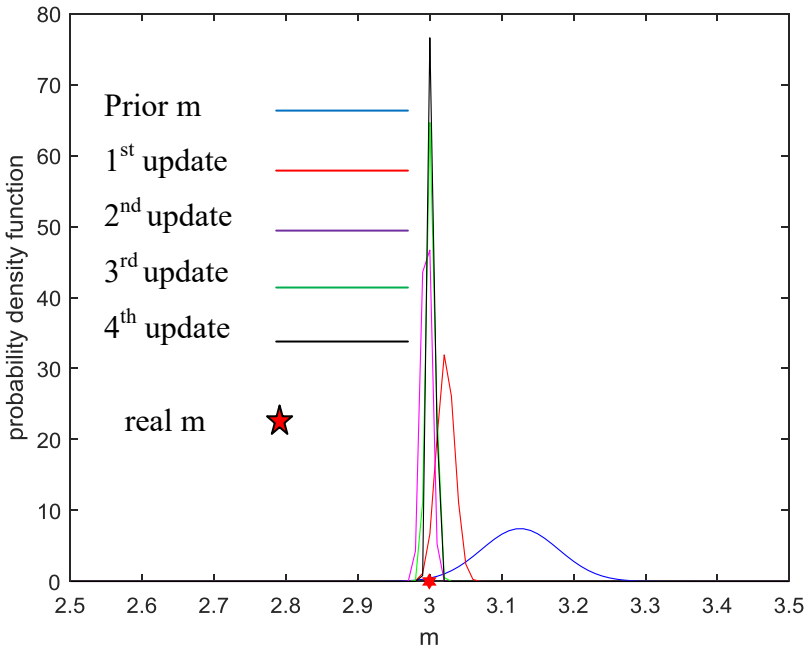

Figure 22. Updated distribution of m for path #7

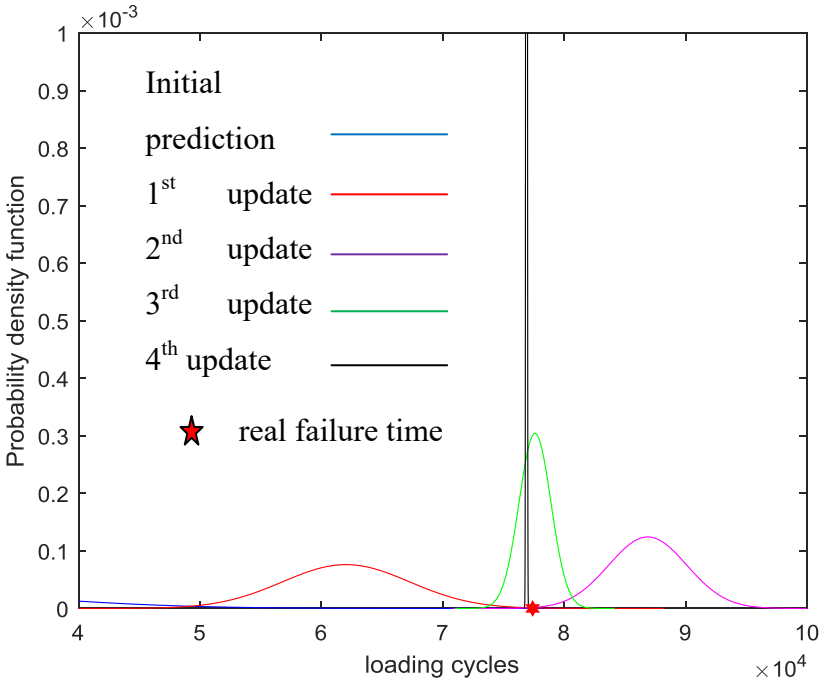

Figure 23. Updated failure time distribution for path #7

4.6 Comparative Study

In this section, based on 10 degradation paths shown in Figure 21, the constant-load approach presented in [78] is applied to update the uncertain parameter m and the predicted RUL at each inspection interval, which is an approximated way to deal with time-varying external load problem. In this approximation, the form of the basic Paris' Law, as shown in Equation (4-12), is directly used to estimate the crack increments. Δk with respect to a certain crack level is now a deterministic value, obtained at the mean torque value.

$$\frac{\Delta a}{\Delta N} = C \cdot [(\Delta k)^m] \tag{4-12}$$

Following the same process, the results obtained using the constant-load approach are compared with the previous results by the proposed varying-load approach. Figure 24 shows one sample

crack degradation path using varying-load approach and constant-load approach respectively, where parameters are all set to be the same values. The results show that the crack propagates faster under varying load conditions.

Next, we conduct the comparisons for two different cases: one considers measurement uncertainty τ=0.2, that is, the measured crack length follows a normal distribution $a_{measure} \sim N(a_{real,}\, \tau^2)$; and the other considers a larger measurement error τ=0.3. Measurement error cannot be avoided, and these measured condition data have a significant impact on the prediction result.

Case 1. τ =0.2

This case is the one presented in Section 5.5. Taking Path #7 as an example, the updated *m* at each inspection interval applying constant-load approach is listed in Table 7, and the plots of *m* distribution are shown in Figure 25. As we can see, updating *m* using constant-load approach gives a bigger bias to the real *m* compared to the updated *m* values using the proposed varying-load approach shown in Table 6. Consequently, the estimated mean lifetime at each inspection interval using varying-load approach shows a discrepancy between two sets of updated m values. The one using the updated *m* generated by constant-load method gives the larger error to the actual failure time. The plots of predicted lifetime distribution are shown in Figure 26. Table 8 shows the differences of the updated predicted lifetimes at each inspection interval between the two approaches. Similarly, the comparison for Path #5 and Path #9 in Figure 21 are conducted, the failure time prediction results are shown in Table 9 and Table 10 respectively. As we can see, the accuracy of the average of failure time prediction results is improved significantly compared to the constant-load approximation method. It is noted that there are few negative accuracy

improvement at some inspection points occasionally, these may due to the variations of sampled model parameter value which are given certain distributions in the study. Overall, the prediction accuracy are apparently improved.

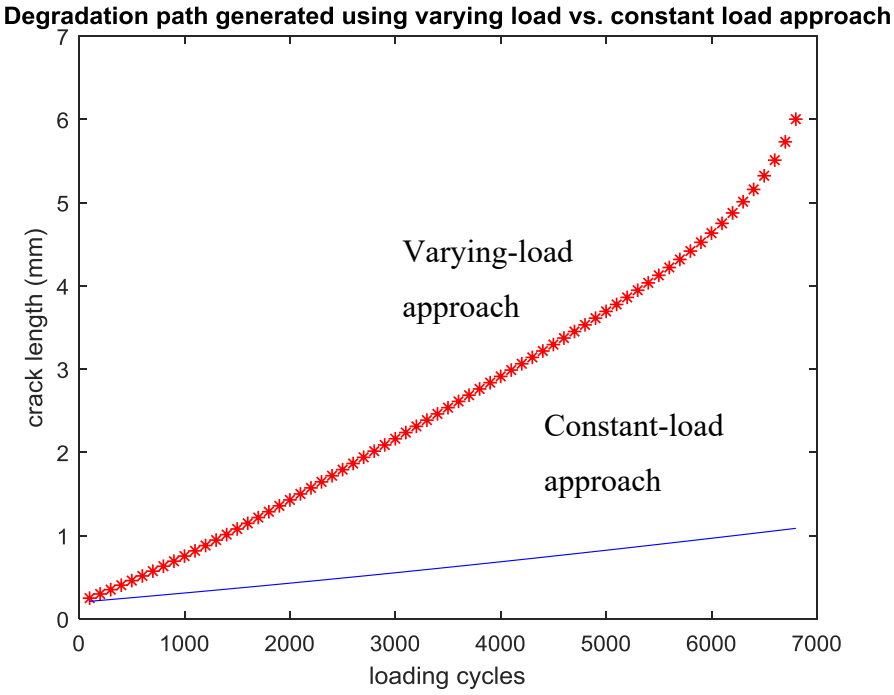

Figure 24. Sample simulated degradation paths for the two approaches with same parameters

Table 7. Test for Path #7 (real *m*=2.9993)

Inspection cycle	Crack length (mm)	m_μ	m_σ
0	0.2	3.2823	0.0514
$1.9*10^4$	1.4621	3.1669	0.0122
$3.8*10^4$	1.9521	3.1400	0.0065
$5.7*10^4$	3.6476	3.1452	0.0059
$7.6*10^4$	5.6214	3.1444	0.0039

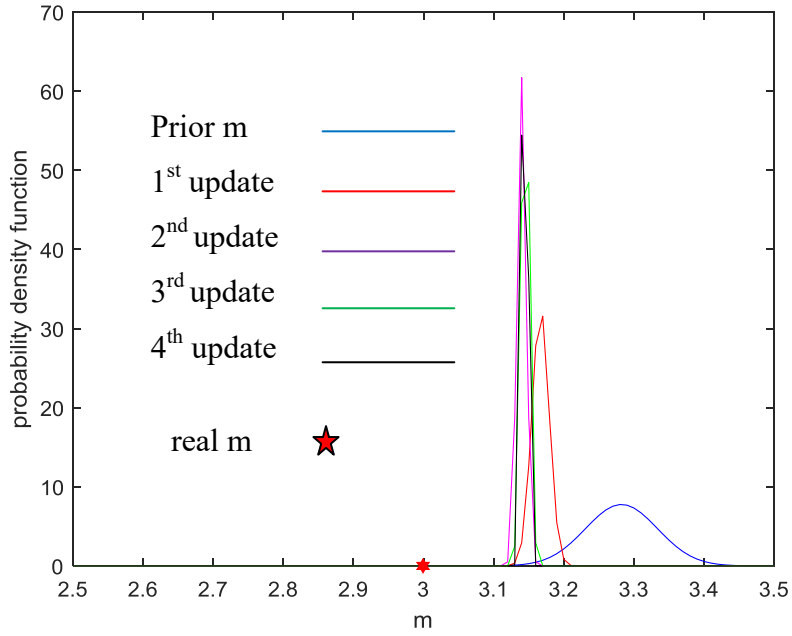

Figure 25. Updated distribution of *m* for path #7 (Constant-load approach)

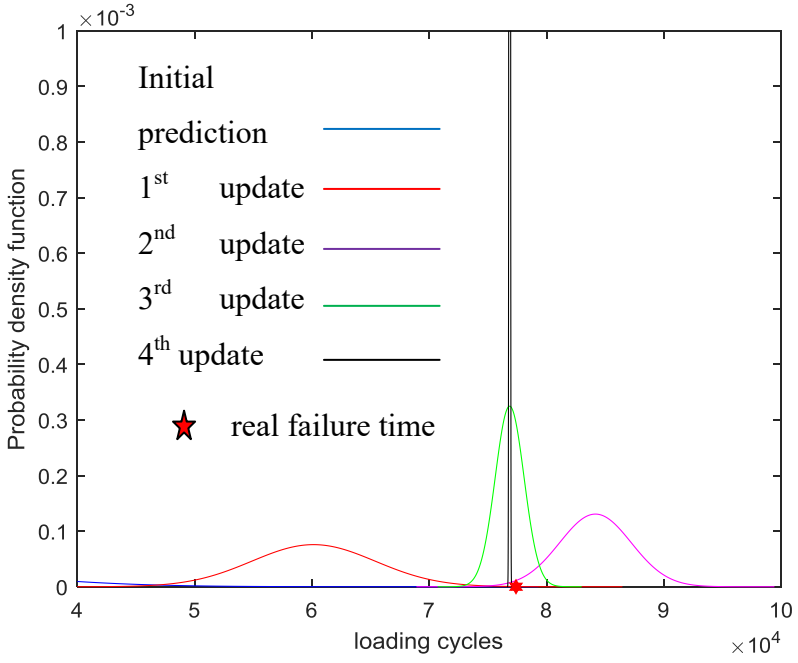

Figure 26. Updated failure time distribution for path #7 (Constant-load approach)

Table 8. Predicted RUL results comparison for path #7 (Actual failure time = 77400cycles)

	Constant-load approach		Proposed varying-load approach		Accuracy improvement
Inspection cycle	μ (cycles)	|μ-actual|	μ (cycles)	|μ-actual|	
0	21342	56058	22795	54605	3.6%
$1.9*10^4$	60136	17264	62030	15370	11%
$3.8*10^4$	84172	6772	86880	9480	-39%
$5.7*10^4$	76857	543	77596	196	64%
$7.6*10^4$	76860	540	76898	502	7%

Table 9. Predicted RUL results comparison for path #5 (Actual failure time = 139400cycles)

	Constant-load approach		Proposed varying-load approach		Accuracy improvement
Inspection cycle	μ (cycles)	|μ-actual|	μ (cycles)	|μ-actual|	
0	22630	116770	25120	114280	2.13%
$3.4*10^4$	91360	48040	106340	33060	31.18%
$6.8*10^4$	109060	30340	120220	19180	36.78%
$10.2*10^4$	127660	11740	134440	4960	57.75%
$13.6*10^4$	137200	2200	137460	1940	11.82%

Table 10. Predicted RUL results comparison for path #9 (Actual failure time = 42200cycles)

	Constant-load approach		Proposed varying-load approach		Accuracy improvement
Inspection cycle	μ (cycles)	|μ-actual|	μ (cycles)	|μ-actual|	
0	21577	20623	24545	17655	14.39%
10000	59112	16912	62116	19916	-17.76%
20000	46501	4301	45952	3752	12.76%
30000	38102	4098	38334	3866	5.7%
40000	43347	1147	43230	1030	10.2%

Case 2. τ =0.3

Ten new degradation paths are generated according to the method, and they are shown in Figure 27. Table 11 shows ten real values of *m* for generating these ten paths, and the seven trained values for the seven paths in the training set.

Similarly, we take path #9 as an example to compare the updated *m* and predicted lifetime results between the proposed varying-load approach and constant-load approach. Figures 28 and 29, and Tables 12 and 13, show the updated *m* distributions and values at each inspection interval, by applying the proposed varying-load method and the constant-load approximation method, respectively. Figures 30 and 31 show the updated predicted failure time distributions by applying two methods, respectively. Table 14 shows the differences of the updated predicted lifetime at each inspection intervals. Table 15 and Table 16 show the comparison results of predicted lifetime for Path #4 and Path #6 respectively. As can be seen, the accuracy of the average of the failure time prediction results is improved compared to the constant-load approximation method in the case of τ =*0.3*, where the measurement error is larger. In both cases, the varying-load approach always gives smaller errors comparing to the constant-load approach for failure time estimation at each inspection interval.

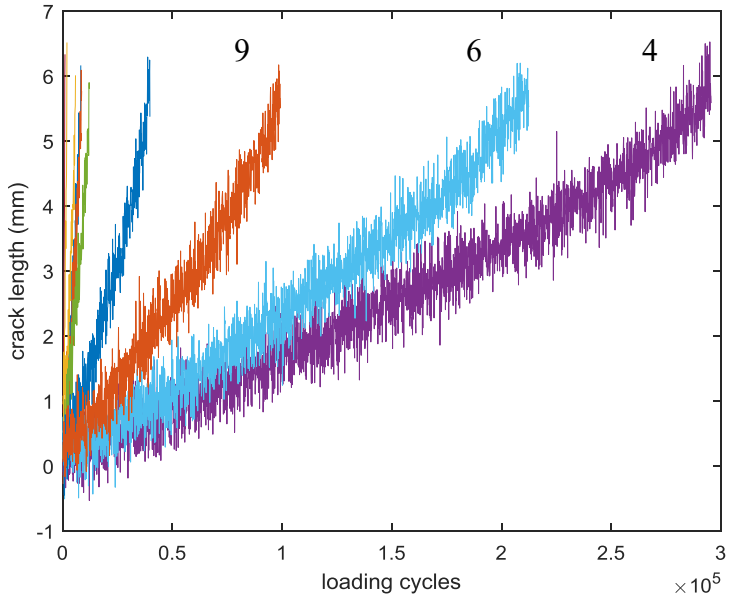

Figure 27. Ten simulated degradation paths (τ=0.3)

Table 11. Real and trained m of each degradation path

Path #	Real m	Trained m (varying-load approach)	Trained m (constant-load approach)
1	3.2178	3.2135	3.3722
2	3.2129	3.2088	3.3601
3	3.2511	3.2562	3.3988
4	2.8702	-	-
5	3.1787	3.1800	3.3287
6	2.9021	-	-
7	3.4239	3.4272	3.5828
8	3.0643	3.0664	3.2087
9	2.9759	-	-
10	3.3587	3.3611	3.5060

Table 12. Test for Path #9 by the proposed varying-load approach (real m=2.9759)

Inspection cycle	Crack length (mm)	m_μ	m_σ
0	0.2	3.2447	0.1192
24000	0.8905	2.9551	0.0267
48000	2.5471	2.9864	0.0178
72000	3.4851	2.9713	0.0129
96000	5.3763	2.9785	0.0088

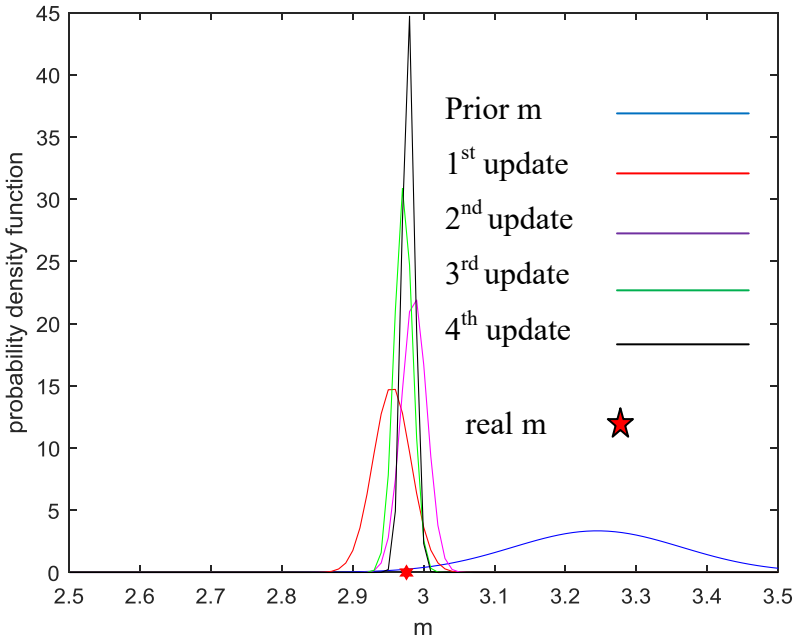

Figure 28. Updated distribution of m for path #9 (Proposed varying-load approach)

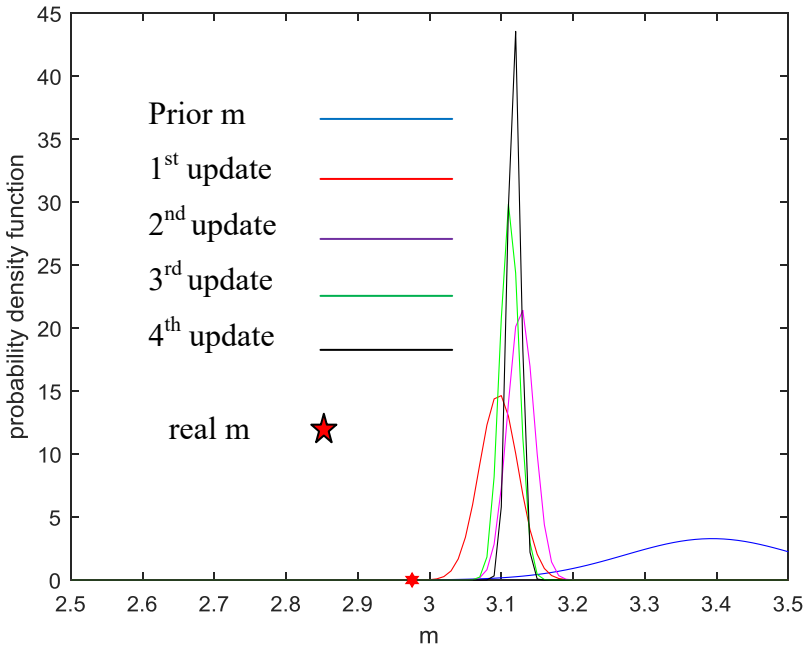

Figure 29. Updated distribution of *m* for path #9 (Constant-load approach)

Table 13. Test for Path #9 by the constant-load approach(real *m*=2.9759)

Inspection cycle	Crack length (mm)	m_μ	m_σ
0	0.2	3.3939	0.1214
24000	0.8905	3.0963	0.0270
48000	2.5471	3.1271	0.0184
72000	3.4851	3.1114	0.0133
96000	5.3763	3.1181	0.0089

Table 14. Predicted RUL results comparison for path #9 (Actual failure time = 99100cycles)

	Constant-load approach		Proposed varying-load approach		Accuracy improvement
Inspection cycle	μ (cycles)	|μ-actual|	μ (cycles)	|μ-actual|	
0	9880	89220	14030	85070	4.6%
24000	128160	29060	129920	30820	-6%
48000	89490	9610	91390	7710	20%
72000	105220	6120	103630	4530	26%
96000	98920	180	99130	30	83%

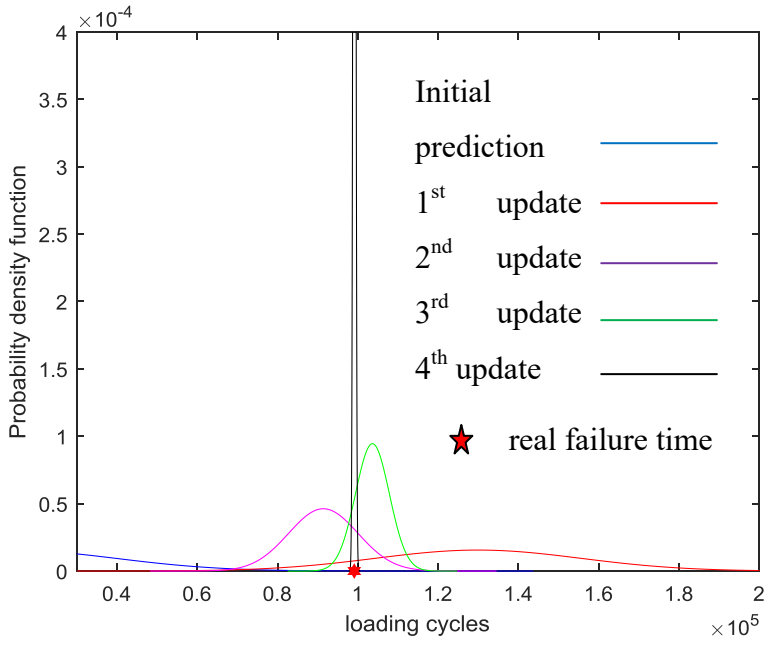

Figure 30. Updated failure time distribution for path #9 (Proposed varying-load approach)

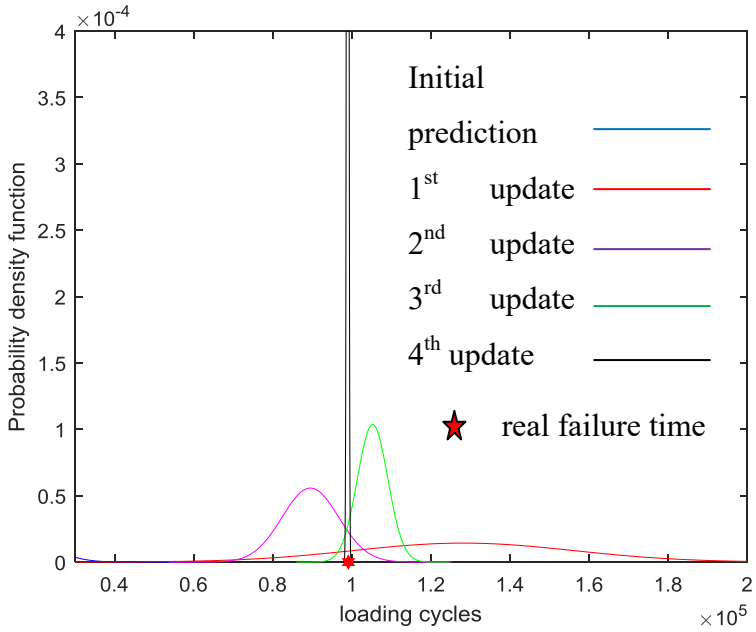

Figure 31. Updated failure time distribution for path #9 (Constant-load approach)

Table 15. Predicted RUL results comparison for path #4 (Actual failure time = 295500cycles)

	Constant-load approach		Proposed varying-load approach		Accuracy improvement
Inspection cycle	μ (cycles)	|μ-actual|	μ (cycles)	|μ-actual|	
0	11080	284420	9910	285590	-0.4%
$7.3*10^4$	221670	73830	228360	67140	9.06%
$14.6*10^4$	251820	43680	257890	37610	13.9%
$21.9*10^4$	314860	19360	310080	14580	24.69%
$29.2*10^4$	294460	1040	294670	830	20.19%

Table 16. Predicted RUL results comparison for path #6 (Actual failure time = 212400cycles)

	Constant-load approach		Proposed varying-load approach		Accuracy improvement
Inspection cycle	μ (cycles)	|μ-actual|	μ (cycles)	|μ-actual|	
0	9500	202900	12190	200210	13.3%
$5.21*10^4$	250800	38400	250370	37930	12.2%
$10.42*10^4$	238670	26270	232590	20190	23.14%
$15.63*10^4$	223890	11490	223100	10700	6.88%
$20.84*10^4$	212060	340	212220	180	47.06%

4.7 Conclusions

Wind power is a significant clean energy source, which provides great promise in protecting the environment while meeting electricity demand. Cost is a key factor to increase the competitiveness of wind energy comparing to other energy sources. Improving reliability through prognostics and CBM provides great potential for cost reduction. In this chapter, an integrated varying-load approach is proposed for predicting the fatigue crack propagation and remaining life of the wind turbine gearbox by specifically considering instantaneously varying external load, which is more realistic. The method integrates physical gear model by taking advantage of stress analysis in finite element modeling and available health condition data. In order to improve the accuracy of RUL prediction, the distribution of the uncertain material parameter modeled in crack degradation process is updated once the new health condition data become available via Bayesian inference. The examples demonstrate the effectiveness of the proposed varying-load approach and its advantages versus the existing constant-load approximation method. Even though gearboxes in wind turbines are considered in this chapter,

the proposed method is also applicable to other systems and structures subject to the instantaneously time-varying load.

One should discuss is the possible impact of varying load on production loss. Wind power production is directly related to the wind speed, and the wind speed does have impact on the external time-varying load as presented in Equation (4-1) to (4-4). However, the varying load simulated by FAST has put the wind profile into consideration, and the power production is well controlled by the power control system in the wind turbines. The power loss during the period of wind speed being between the cut-in and cut-out values is very difficult to quantified, and there is not significance to consider production loss in the prognostics study for the components in a wind turbine. In addition, parked cases in which production is completely zero has negligible contributions to the fatigue life of the gearbox as stated in Section 4.3. In this scenario, we do not consider the production loss in this study, however, it may be considered in the future work in optimizing CBM by minimizing production loss.

Chapter 5. Integrated prognosis for the gearbox in wind turbines under time-varying external load condition considering crack initiation time uncertainty

5.1 Overview

In Chapter 4, a study is conducted where wind turbines suffer from varying environment conditions from time to time, e.g., time-varying wind speed and direction, temperature, etc., which leads to time-varying torque applied to the mechanical components in the hub. Hence, the gearbox fails in a different manner from the one under constant load condition. The prognosis starts at the point when an initial crack is detected, and the crack initiation time is typically considered as an exact value in the previous study. However, the existing fault detection and diagnostic techniques are limited so that a large variation in the accuracy of initial crack detection cannot be ignored.

As illustrated in Figure 32, five crack degradation paths are generated considering both the uncertainty in CIT and the physical model parameters. a_0 and a_C are the initial crack size and the critical crack size, respectively. Two black vertical dash lines represent the CIT and the failure time if the crack propagates on Path 1, respectively. The black dash curve represents CIT distribution due to the variation of CIT which goes on the x-axis, and the y-axis represents the probability density function (PDF). As a result, the failure time, i.e., the time of crack size a reaches a_C, shows a variation as distributed as the red dash curve, of which the x-axis is used as the variable failure time and the y-axis represents the PDF. To reduce the variation, in this chapter, a new parameter, uncertainty of crack initiation time (CIT), is introduced in the

previously developed prognostics model for the gearbox in a wind turbine under time-varying external load condition. The objective is to update the distribution of both CIT and the physical model parameters at each inspection time by applying the new observations into Bayesian inference, so that the means of CIT and the physical model parameters approaches the true value, and thus the prediction of failure is more accurate.

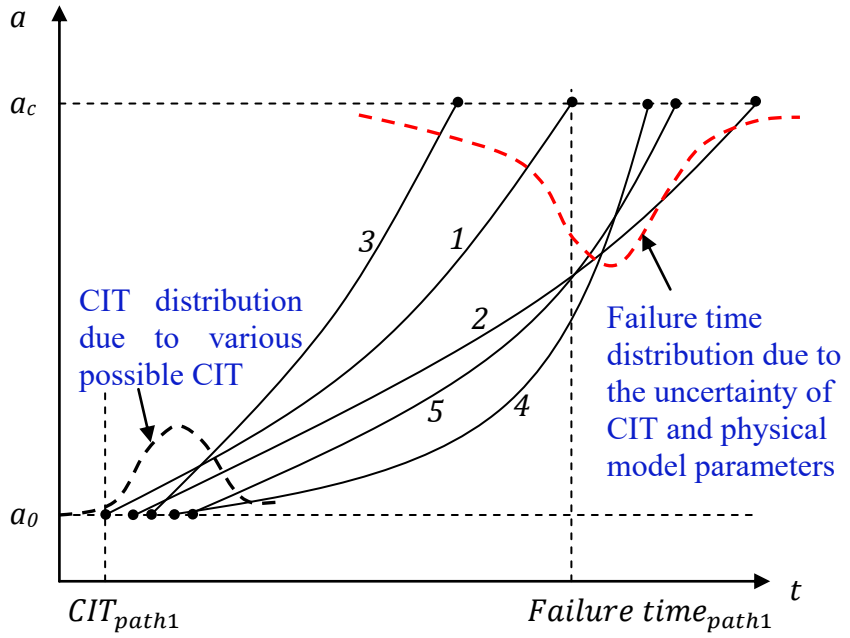

Figure 32. Degradation paths generated by varying CIT and physical model parameters

There is limited literature considered CIT uncertainty in gear prognostics. Lewicki investigated the effects of initial crack angle and position on the gear tooth crack propagation path [105]. Zhao et al. considered CIT uncertainty in their developed prognostics method for a gear but only addressed the problem under the constant load condition [106]. In this chapter, the varying load condition is considered in the gear crack propagation model as introduced in Chapter 4. Therefore, the RUL prediction for the gearbox in Wind Turbines under time-varying external load condition is more rational and accurate.

This chapter is organized as follows. Section 5.2 presents the framework of the integrated prognostics method and the details specifically focusing on CIT consideration. In Section 5.3, an example is given to demonstrate the effectiveness of the method. A comparative study between the proposed varying load model and constant load approximation method is given in Section 5.4. The results show that CIT and material parameters are updated more accurately at each inspection interval compared to the constant load approximation method, and the results of RUL prediction for the gearbox in Wind Turbines are more accurate accordingly. Section 5.5 provides the conclusions.

Nomenclature:

f_{post}: posterior distribution in Bayesian updating process

f_{prior}: prior distribution in Bayesian updating process

a^{obs}: the observed crack size

t_0: crack initiation time

L: time-varying load

C and m: material parameters

5.2 The proposed integrated prognostic method considering crack initiation time uncertainty

The principle and framework of the integrated prognostic method are illustrated in Section 4.2. The main idea in this study is that, for a gear working in the wind turbine under time-varying load condition, the RUL prediction is better by introducing a variable $t_{0,}$ i.e., crack initiation time.

Bayesian updating, therefore, adjusts both the distribution of t_0 and m at each inspection interval when a new observation data is available. In this study, we consider another material parameter C as a constant. The posterior distributions of t_0 and m are then applied in Paris' law to predict the crack size at the next inspection interval until the crack reaches the threshold. RUL of the gearbox is then calculated. A general case of Bayesian updating process is shown in Figure 33.

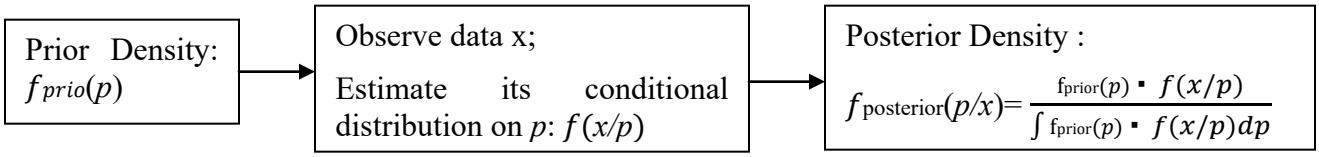

Figure 33. A general Bayesian update process

Specifically, in this study, there are two random variables, t_0 & m, which represent the uncertainty of CIT and model material parameter, respectively. The material parameter C in Paris' model is considered as a fixed value. Suppose that several failure histories are available, which provide the information of inspection times and the associated crack sizes. Then a prior distribution $f_{prio}(t_0, m)$ can be obtained by applying least-square regression and statistical fitting techniques. Assume the crack measurement error follows a zero-mean Gaussian distribution with τ as the standard deviation. Under the time-varying load condition, crack growth is modeled as Equation (4-7) to account for the time-varying load effects. In this scenario, we denote the crack size a by a function of the load L, i.e., *a(L).* At a certain inspection time t_u, the likelihood of observing a crack size of ${a_u}^{obs}(L) = a^{obs}(t_u, L)$ is [106]:

$$l({a_u}^{obs}(L)|t_0, m) = \frac{1}{\sqrt{2\pi}\tau} exp(-\frac{({a_u}^{obs}(L) - a_u(t_0, m, L))^2}{2\tau^2}) \quad (5\text{-}1)$$

In the Bayesian inference framework, a posterior distribution $f_{post}(t_0, m)$ can be obtained by [106]:

$$f_{post}(t_0, m|{a_u}^{obs}(L)) = \frac{l({a_u}^{obs}(L)|t_0,m) f_{prior}(t_0,m)}{\int l({a_u}^{obs}(L)|t_0,m) f_{prior}(t_0,m) dt_0 dm} \quad (5\text{-}2)$$

The updating process is implemented when a new observation of crack size is available. The posterior distribution of the parameters will serve as the prior distribution for the next update process. Importance sampling technique is used to obtain samples which follow the posterior distribution.

In this thesis, Bayesian updating aims at adjusting the distributions of uncertain parameters that affect the crack degradation process, and thus the RUL of the cracked gear can be predicted more accurately. A predicted failure time is the time when the observed crack size reaches the critical length a_C, and the RUL is the time from current inspection point to the predicted failure time. The RUL prediction result can be updated at each inspection time after the parameter distributions are adjusted via Bayesian updating. A modified Paris' law to model crack propagation under time-varying load condition can be written in its reciprocal form as in Equation (5-3),

$$\frac{\Delta a}{\Delta N} = C \cdot E[(\Delta k)^m] \quad (5\text{-}3)$$

In Equation (5-3), Δa represents the crack increment and it can be expressed in the following way,

$$\Delta a = \Delta N \cdot C \cdot (p_1(\Delta k_1)^m + p_2(\Delta k_2)^m + \cdots + p_n(\Delta k_n)^m) \quad (5\text{-}4)$$

where p_i is the PDF value when $\Delta k = \Delta k_i$. Let $N_C(t_0)$ be the current inspection cycle. The RUL is then the summation of ΔN from the current inspection cycle to the failure instant, i.e., the time when $\sum \Delta a\,(L) \geq a_C$. Therefore, the failure time is given by

$$F(t_0,m)= N_C(t_0)+\Sigma_i \Delta N_i(m|t_0) \quad (5\text{-}5)$$

5.3 Numerical Examples

It is not arbitrary to consider that the crack initiation time does not affect the FE modeling process of the gear tooth crack propagation. Hence the 2D FE model used in Chapter 4 is directly applied in this study. The history of SIF is adopted from Chapter 4 shown in Figure 20 is considered, as well as the main gear geometry and properties listed in Table 4.

Suppose CIT of a spur gear tooth described in Chapter 4 follows a normal distribution N(2e6, 2e5) cycles, and material parameter *m*~ N(3.0354, 0.2). Another measurement error is similarly considered as in Chapter 4, and it follows a normal distribution N(0, 0.2).

First, a real crack degradation path is generated with CIT of 1.7e6 cycles as shown in Figure 34. Each red circle point denotes the real crack size every after an inspection interval of 1e4 cycles. Blue star points are actual observed crack size with the sampled measurement error. These data are to be used as the observations to update CIT and *m* distributions at each inspection interval.

Based on the updating process illustrated in the previous section, the updating history of CIT and *m* are shown in Table 17. Figure 35 and 36 show the updated distribution of CIT and *m*, respectively. As can be seen, under the time-varying load condition, the Bayesian updates adjusted the mean value of m and CIT gradually to its real value as the new crack length observations are used. Moreover, the distributions of the updated variables become narrower and narrower, which means that the uncertainty is reduced.

The updated failure time prediction results are listed in Table 18, and Figure 37 shows the lifetime distribution at each inspection interval. As can be seen, lifetime prediction result

becomes more and more accurate, the mean is approaching the real failure time, and the uncertainty is much reduced.

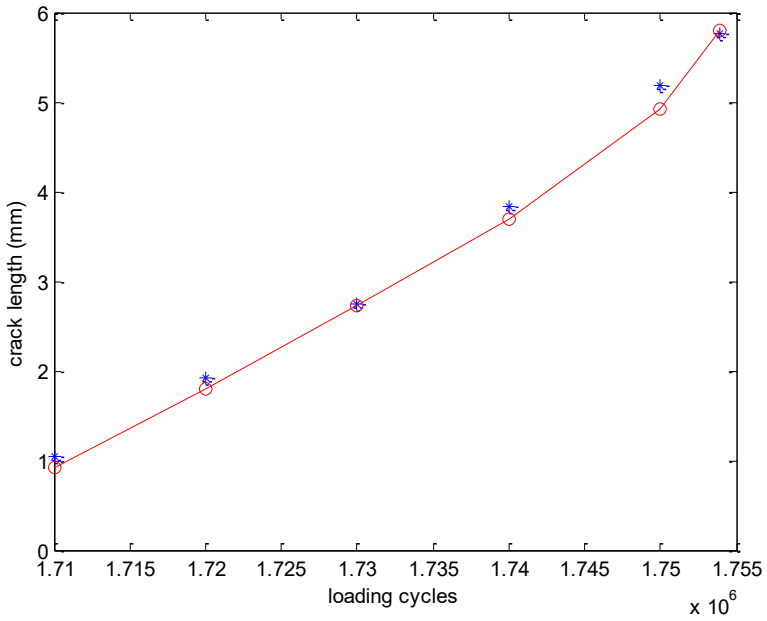

Figure 34. One real crack propagation path

Table 17. Updating history of crack initiation time and *m* at each inspection time

(real *m*=3.2354, t_0=1.7e7 cycles)

Inspection	t_{0_μ}	t_{0_σ}	m_μ	m_σ
1	2.0005e6	2.0544e5	3.0465	0.1938
2	1.5826e6	1.0410e5	3.0289	0.1120
3	1.6917e6	0.0977e5	3.1965	0.0177
4	1.6918e6	0.0295e5	3.2061	0.0103
5	1.6924e6	0.0212e5	3.2104	0.0062
6	1.6932e6	0.0145e5	3.2176	0.0037

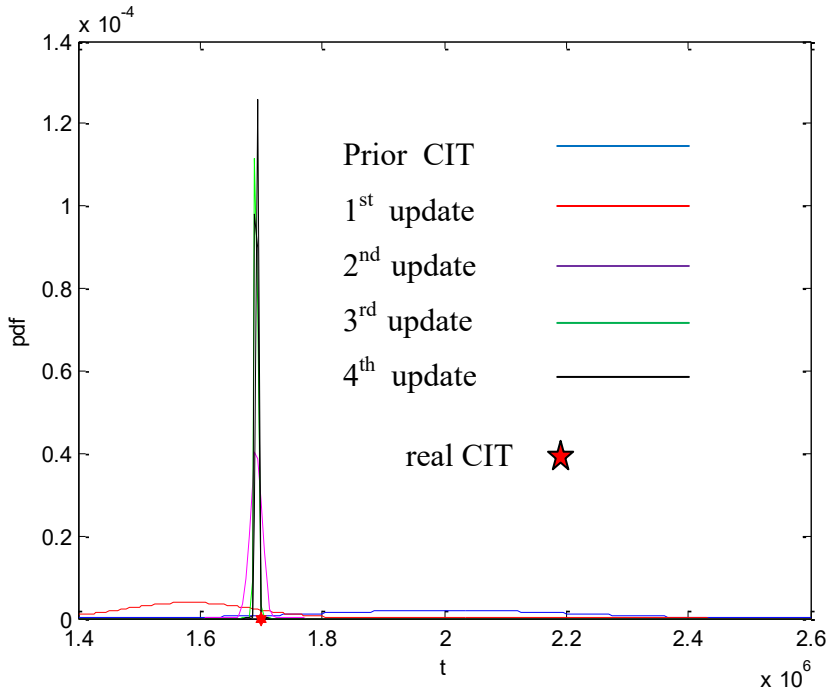

Figure 35. Updated distribution of CIT

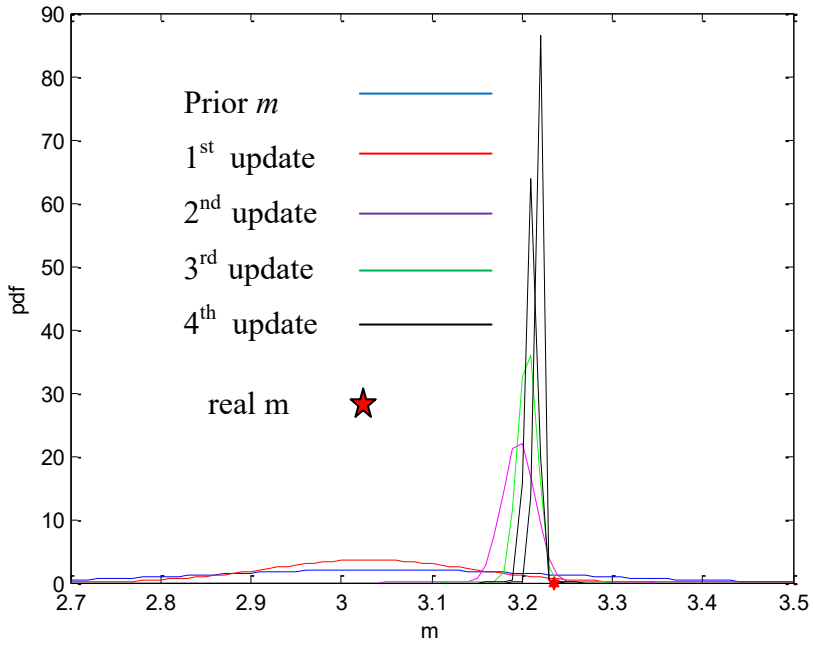

Figure 36. Updated distribution of *m*

Table 18. Updated failure time prediction at each inspection time (real failure time=1753890)

Inspection	$lifetime_{\mu}$	$lifetime_{\sigma}$
1	2867261	15155610
2	2272654	733065
3	1771620	9464
4	1765121	3579
5	1760957	1271
6	1756613	487

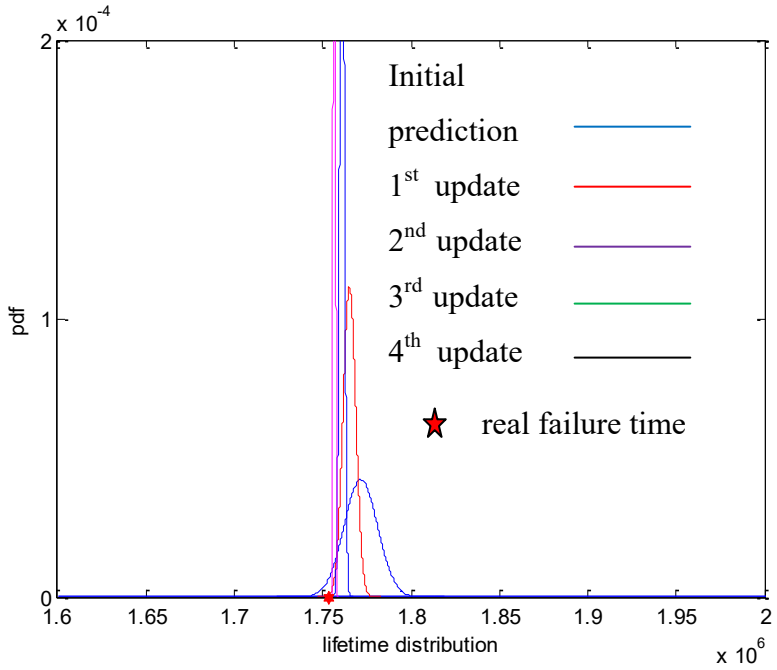

Figure 37. Updated distribution of failure time

5.4 Comparison Study

In this section, constant load approach presented by [78] is again applied as an approximation way to deal with the time-varying external load. The comparison study is performed to demonstrate the effectiveness of the proposed method.

To make a fair comparison, the same crack propagation observations shown in Figure 34 is consistently used in the Bayesian updating process using the constant load approximation method. As a result, the updated t_0 and m at each inspection interval are listed in Table 19. Compared to the results with the proposed method, the values in Table 13 show the larger error in the actual parameter value. The plots of the predicted lifetime distribution are shown in Figure 38. Table 20 shows the difference of updated predicted lifetime at each interval between the two approaches. As can be seen, the varying load approach always results in smaller error compared to the constant load approach regarding failure time estimation at each inspection interval. Moreover, Table 20 also shows that the proposed time-varying load approach benefits more the prognostics considering the uncertainty of CIT as the accuracy improvement is larger.

Table 19. Updating history of crack initiation time and m at each inspection time

(real m=3.2354, t_0=1.7e7 cycles)

Inspection	t_{0_μ}	t_{0_σ}	m_μ	m_σ
1	2.0005e6	2.0544e5	3.0465	0.1938
2	1.5917e6	1.4304e5	3.0851	0.1334
3	1.5966e6	0.0444e5	3.0472	0.0007
4	1.5906e6	0.0347e5	3.0474	0.0006
5	1.5823e6	0.0240e5	3.0477	0.0005
6	1.5734e6	0.0092e5	3.0486	0.0001

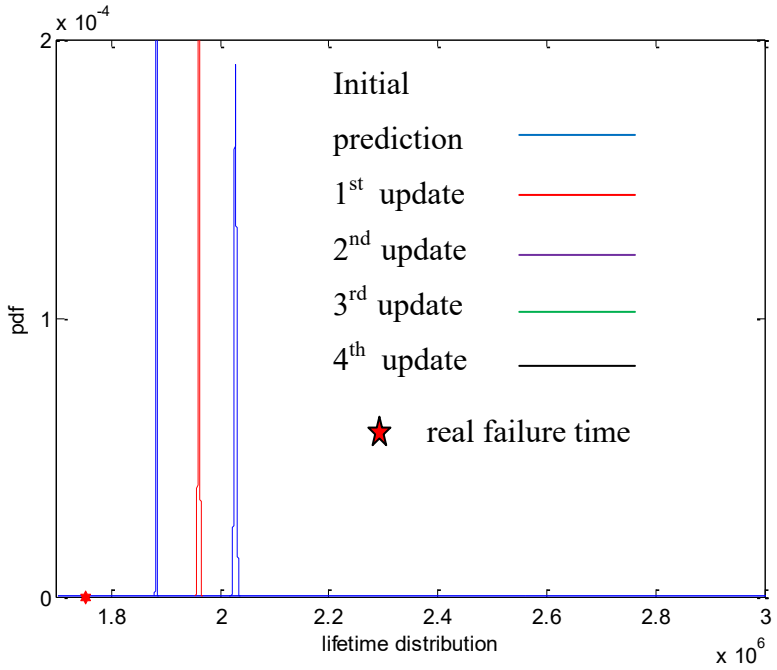

Figure 38. Updated distribution of failure time applying constant load approximation method

Table 20.Comparison of updated failure time prediction between two methods

(real failure time=1753890)

	Constant-load approach		Proposed varying-load approach		Accuracy improvement
Inspection	μ (cycles)	|μ-actual|	μ (cycles)	|μ-actual|	
1	5332071	3578181	2867261	1113371	68.9%
2	2239699	485809	2272654	518764	-6.8%
3	2027711	273821	1771620	17730	93.5%
4	1960548	206658	1765121	11231	94.6%
5	1882469	128579	1760957	7067	94.5%
6	1795000	41110	1756613	2723	93.4%

5.5 Conclusions

The time-varying load is a real problem that has to be dealt with in the prognostics study for wind turbine systems. The crack initiation time of a gear is usually uncertain under complex and time-varying stress conditions. The key contributions of the proposed approach are its outstanding capability to directly relate the time-varying load to the crack propagation, and the significance of considering the CIT uncertainty factor in RUL prediction.

The uncertainty of CIT certainly affects the accuracy of the RUL prediction. In this study, we extend the method presented in the previous study to further consider CIT factor in prognostics for the gearbox. As the new condition monitoring observations are available, the distribution of both material parameter and CIT are updated via Bayesian reference, and the prediction of failure time is updated accordingly. An example is provided to demonstrate that the proposed method has the advantage versus the existing constant load approximation method. Also, it shows that the proposed time-varying load approach benefits more the prognostics considering the uncertainty of CIT, because the accuracy improvement is larger than the one does not consider CIT.

Chapter 6. Condition-based maintenance of wind power generation systems considering different turbine types and lead times

6.1 Overview

In Chapter 3, the developed opportunistic maintenance methods provide cost-effective solutions for wind power systems to schedule maintenance activities, and they bring immediate benefits without further techniques. As the most advanced maintenance strategy, condition-based maintenance (CBM) always deserves more study since it can reduce the most catastrophic loss by preventing failure occurrence, which is achieved by fault diagnosis and accurate failure prediction. Currently, the wind energy industry is switching from corrective maintenance and time-based preventive maintenance strategies to CBM strategy that effectively utilize condition monitoring information. In CBM, condition monitoring measurements such as vibration data, acoustic emission data, oil analysis data, power voltage and current data, etc., can be obtained from the sensors mounted on the wind turbine components. These measurements are utilized to evaluate and predict the health conditions of the components and the turbines [107]–[112]. The objective of CBM is to optimize the maintenance schedule based on the condition monitoring and prediction information to minimize the overall costs of wind power generation systems. Newly deployed turbines are typically equipped with condition monitoring sensors. For legacy turbines, operators and manufacturers are also trying to install such sensors on many of these turbines. There is a significant and growing need to develop effective methods for optimizing maintenance activities by fully utilizing the available condition monitoring information. Nilsson and Bertling proposed a life cycle cost approach for evaluating the financial benefits using condition monitoring system, a tool required in CBM [52]. Byon and Ding applied a multi-state

Markov decision mechanism in estimating the wind turbine degradation process, based on which the optimal maintenance scheme is determined [42]. They also investigated the operations and maintenance of a wind farm using discrete event simulation (DEVS) [113]. Sørensen investigated the framework for risk-based planning of operation and maintenance for offshore wind turbines, which are typically difficult to access [40].

There are typically multiple wind turbines in a wind farm, which is typically located at a remote site. A wind farm can be considered to be a system consisting of multiple wind turbines, and there are multiple components including main bearing, gearbox, generator, shafts, etc., in each wind turbine. Thus, there are economic dependencies among wind turbines and their components in the wind farm. More specifically, there are fixed costs for sending a maintenance team to the wind farm. Thus, it may be cheaper to take the opportunities to maintain multiple turbines and multiple components in a turbine at the same time, based on the evidence presented in the condition monitoring data. Tian et al. developed a CBM approach for wind energy systems considering such economic dependencies [19]. In their work, they focused on a homogeneous wind turbine fleet made by the same manufacturer and assuming a constant lead time for all turbine components. However, it is very likely a wind farm owner acquires different capacities of wind turbines from the same manufacturer or different brands from different manufacturers. Different types of wind turbines have different capacities and typically different types of turbine components. Thus, the CBM decision making criteria are expected to be different for different types of turbines. In addition, various turbine components are likely from various suppliers and thus have different lead times. Amayri et al. developed a CBM method considering different types of turbines [48], and also jointly considered different lead time in [49]. In their work production loss due to shut down for maintenance activities was not considered in the proposed

cost evaluation algorithm. In practice, the production loss is not negligible for cost evaluation especially when different lead times and turbine types are given high values in a maintenance optimization problem.

In this chapter, we extend the approach developed in [49] to further involve production loss. The key contribution in the study is that cost evaluation considers production loss due to maintenance activities that stop the turbines, as well as the downtime before the maintenance occurs. Examples are provided to demonstrate the improved CBM approach. This chapter is organized as follows. Section 6.2 introduces the proposed CBM approaches considering both different types and lead times. In Section 6.3 numerical examples are given to demonstrate the effectiveness of the developed method, and the cases of constant lead times and constant-interval preventive maintenance strategy are also investigated for comparison. Conclusions are given in Section 6.4. The materials in this chapter have been published in [3].

Nomenclature:

$Pr_{k,n}(L)$: the conditional failure probability of turbine *n* of type *k* during the lead time L

d_1^1 and d_2^1, d_1^2 and d_2^2, …, d_1^K and d_2^K: two level failure thresholds of type 1,2,…, *K*, respectively.

C_E: the total expected maintenance cost per unit time per turbine

$TP_{k,n,m}$: the mean of the predicted failure time of component *m* in turbine *n* of type *k*

σ_p : the obtained standard deviations of ANN prediction results

T_p: the distribution of the predicted failure time

$L_{k,m}$: the lead time of component *m* in turbine of type *k*

$Pr_{k,n,m}$: the conditional failure probability of component *m* in turbine *n* of type *k* during its lead time $L_{k,m}$

C_{Loss}: the power production loss

$c_{k,p,m}$: the preventive replacement cost of component *m* in turbine of type *k*

$c_{k,p,T}$: the fixed preventive maintenance cost of turbine of type *k*

$c_{k,f,m}$: the failure replacement cost of component *m* in turbine of type *k*

$\Delta C_{T,F}$: the cost increase due to failure replacements

$\Delta C_{T,P}$: the cost increase due to preventive replacements

$\Delta C_{T,Loss}$: the cost due to the loss of productivity

$C(t_{CI})$: the total preventive maintenance cost of the constant-interval (CI) maintenance policy

6.2 The proposed condition-based maintenance approach

The applied CBM policy is presented first. The evaluation of conditional failure probability at a specific inspection interval is then explained, and the algorithm of maintenance cost evaluation is given at last.

6.2.1 The CBM policy

As mentioned earlier, the CBM policy presented in [49] is consistently applied in this study. To make it clear the policy is briefly explained again as follows.

Suppose wind turbine components are continuously monitored in the wind farm. At a certain inspection point, condition monitoring data are collected and analyzed for the health condition prediction. Suppose there are *K* types of turbines in the wind farm.

- Perform failure replacement if a component fails.
- Send a maintenance team to the wind farm if any wind turbine in the wind farm is determined to be maintained.
- Perform preventive replacements on components in wind turbine $WT_{k,n}$ if $Pr_{k,n}(L) > d_1^k$, where $Pr_{k,n}(L)$ is the conditional failure probability of the wind turbine n of type k during the lead time L given that it is still working at the current inspection point, and d_1^k is the pre-specified level-1 failure probability threshold value at the turbine level for turbine type k. Note that $L \epsilon \{L_{k,n,m}\}$, $L_{k,n,m}$ denotes the lead time of component m in turbine n of type k, and same components in all turbine n have the same lead time. The calculation of $Pr_{k,n}(L)$ is explained in Section 6.2.2.
- If turbine $WT_{k,n}$ is to be performed preventive replacement on, perform preventive replacement on its components to bring the turbine failure probability down to below d_2^k, which is called the level-2 failure probability threshold value at the turbine level for turbine type k.
- If a turbine has a failed component, perform all the possible failure and preventive replacements for the turbine at the same time.

For each turbine type k, two failure probability thresholds d_1^k and d_2^k need to be determined. Thus, there are $2K$ failure probability thresholds in total to define the CBM policy. Let C_E denote the total expected maintenance cost per unit time per turbine, an optimal CBM then satisfy [49] :

$$\min C_E\left(d_1^1, d_2^1, d_1^2, d_2^2, \dots, d_1^K, d_2^K\right)$$

$$\text{s.t.} \tag{6-1}$$

$$0 < d_2^k < d_1^k < 1$$

where d_1^1 and d_2^1, d_1^2 and $d_2^2, \dots, d_1^K$ and d_2^K represent two level failure thresholds of type 1,2,…, K, respectively.

In this policy, the criterion of decision making for scheduling maintenance is the conditional failure probability of the turbine $Pr_{k,n}(L)$ at the inspection time. The conditional failure probability is determined by the predicted failure time distribution through learning historical condition data. The health prediction method is explained in next subsection.

6.2.2 Health prediction and conditional failure probability calculation

As mentioned earlier, condition monitoring data are used to obtain a prediction model. In this study, the artificial neural network (ANN)-based prognostics method developed by [114] is applied. The inputs of the ANN model are the component age values at the current inspection time and the previous inspection time, as well as the selected condition monitoring measurements at these inspection times. The output of the ANN model is the life percentage at the current inspection time. Therefore, the failure time can be calculated by dividing the component's age by the predicted life percentage. The uncertainty associated with the predicted

failure time can be estimated based on the prediction errors obtained during the ANN training and testing processes. Thus, the predicted failure time distribution for components can be obtained. In this work, it is assumed that at a certain inspection point, the prediction uncertainty (error) follows the normal distribution, hence the predicted failure time for a component also follows normal distribution given a known lifetime. The original lifetime can be generated by sampling Weibull distribution [19]. For component m in turbine n of type k, the mean of the predicted failure time is denoted by $TP_{k,n,m}$. The corresponding standard deviation is denoted by $\sigma_{k,n,m} = \sigma_p \cdot TP_{k,n,m}$, where σ_p is the obtained standard deviations of ANN prediction results for each type of system. Thus, at a certain inspection point, the distribution of the predicted failure time, denoted by T_p, can be represented by [19]:

$$T_p \sim N\left(TP_{k,n,m}, \sigma_p \cdot TP_{k,n,m}\right). \tag{6-2}$$

For component m in turbine n of type k, the conditional failure probability during its lead time, denoted by $Pr_{k,n,m}$, can then be formulated as [49]:

$$Pr_{k,n,m} = \frac{\int_{t_{k,n,m}}^{t_{k,n,m}+L_{k,m}} \frac{1}{\sigma_p TP_{k,n,m}\sqrt{2\pi}} e^{-\frac{1}{2}\left(\frac{x-TP_{k,n,m}}{\sigma_p TP_{k,n,m}}\right)^2} dx}{\int_{t_{k,n,m}}^{\infty} \frac{1}{\sigma_p TP_{k,n,m}\sqrt{2\pi}} e^{-\frac{1}{2}\left(\frac{x-TP_{k,n,m}}{\sigma_p TP_{k,n,m}}\right)^2} dx} \tag{6-3}$$

where $t_{k,n,m}$ is the age of the component at the current inspection point. $L_{k,m}$ is the lead time of component m in type k turbine, and it is defined as the interval between the time maintenance decision is made and the time when the maintenance is complete. $Pr_{k,n,m}$ is the predicted conditional probability that the component fails during the lead time given that it is still working at the current inspection point.

At the turbine level, the turbine is considered to be a series system. That is, a wind turbine fails if any of its components fail. At a certain inspection point, the conditional failure probability of a wind turbine can be calculated as follows:

$$Pr_{k,n} = 1 - \prod_{m=1}^{M_k}\left(1 - Pr_{k,n,m}\right) \tag{6-4}$$

where M_k is the total number of components in the turbine of type k.

6.2.3 Cost evaluation for the CBM policy

Cost estimation is one of the main contributions in this study, which considers the production loss due to either failure or maintenance that stops the turbine. The production loss certainly cannot be ignored in practice. To emphasis the work devoted in this extended approach, the details about the existing method can refer to [49]. The procedure of the cost evaluation is outlined in Figure 39.

Step 1: Specify all the parameters, e.g., cost data, lead times, the number of components in a wind turbine, the number of the turbines in the farm and the number of the types of turbines. **Step 2:** Simulation initialization. In this step, all components are new and their next failure time $TL_{k,n,m}$ is generated by sampling predefined failure distribution. The total cost and the component's age will be updated during the simulation process. t_{ABS} is set to be the time index at current inspection point. At time $t_{ABS} = 0$, the age $t_{k,n,m} = 0$.

Step 3: CBM decision making. At a certain inspection point, make the decision for either failure replacement or preventive maintenance according to CBM policy, which is described in Section 6.2.1.

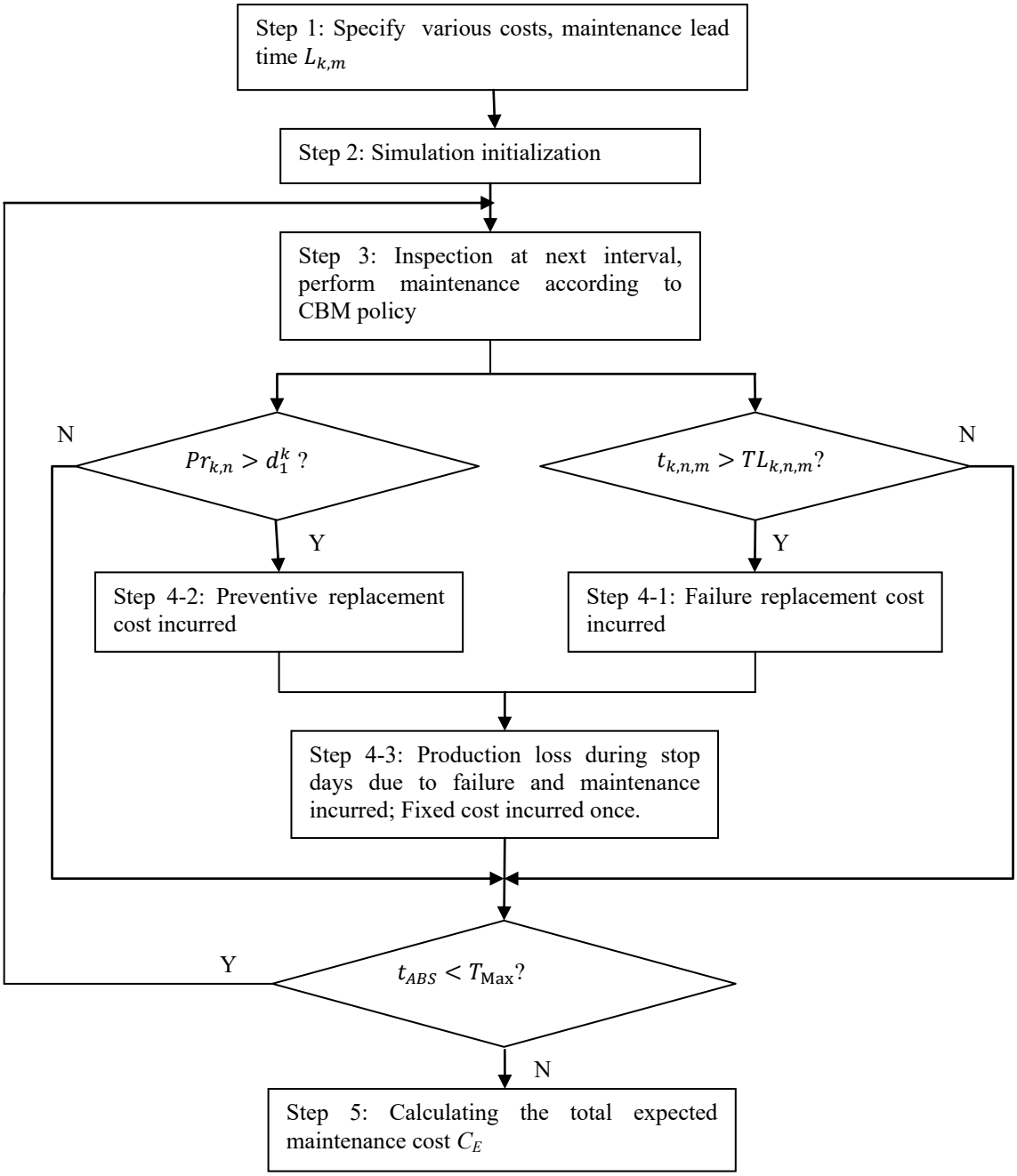

Figure 39. The cost evaluation procedure for the proposed CBM policy

Step 4: Update cost. The cost evaluation algorithm in this study particularly considers the production loss in addition to the existing factors presented in [49]. Thus, the detailed process is given in the followings.

At each inspection point, the CBM decisions can be made based on different situations:

(1) If $t_{k,n,m} > TL_{k,n,m}$, it indicates that a component has failed, and a failure replacement will be performed on the component. Note that the production loss occurs whenever the turbine stops. As the inspection interval is set to be certain days that can be approximately a CBM, a possible shutdown may occur between the two inspections. This is less likely to happen with a CBM policy but still cannot be ignored especially for a large size wind turbine. The production loss occurs before the inspection point, which can be calculated as follows:

$$C_{Loss} = Power\ Rate\ \times 24hrs\ \times \frac{\$50}{MW} \times 30\% \times Stop\ Days \tag{6-5}$$

As a wind turbine system is considered as a series system in this study, any component failure causes system failure. Therefore, the number of stop days right after a turbine shut down is determined by the earliest failed component in the turbine. For the wind turbine with failed components, the number of stop days before the inspection point is then given as:

$$T_{LossBefore,k,n} = Max\{(t_{k,n,m} - TL_{k,n,m}), 0\}\text{, for all m} \tag{6-6}$$

Using above two equations, we can obtain $C_{LossBefore,k,n}$ for the failed turbine n of type k. The cost increase due to failure replacements can be formulated as:

$$\Delta C_{T,F} = \sum_{k=1}^{K} \sum_{n=1}^{N_k} \sum_{m=1}^{M_k} IF_{k,n,m} c_{k,f,m} \tag{6-7}$$

where $IF_{k,n,m} = 1$ if the component m fails, otherwise it equals 0. The cost due to loss of productivity will be added later. er

(2) For wind turbine n, if $Pr_{k,n} > d_1^k$, perform preventive replacement on its components with higher conditional failure probabilities until the turbine failure probability is lower than d_2^k,

which is the lower level failure probability threshold. Accordingly, the preventive replacement costs are incurred. The cost increase due to preventive replacements can be formulated as:

$$\Delta C_{T,P} = \sum_{k=1}^{K} \sum_{n=1}^{N_k} (\sum_{m=1}^{M_k} IP_{k,n,m} c_{k,p,m} + IT_n c_{k,p,T}) \quad (6\text{-}8)$$

where $IP_{k,n,m} = 1$ if a preventive replacement is to be performed on the component *m*, otherwise equals 0; $IT_n = 1$ if preventive replacements are performed, but no failure replacements are performed in the turbine *n*.

(3). For a wind turbine with failed components, it is assumed that the turbine will not start to work until all the failed components have been replaced and all the required preventive replacements have been performed. Thus, the number of the stop days after the current inspection point is equal to the maximum of the lead times of the components that are to be replaced.

$$T_{LossAfter,k,n} = Max\{L_{k,m}\}, \text{ for all components } m\text{s that are to be replaced} \quad (6\text{-}9)$$

where $L_{k,m}$ denotes the lead times of all the components to be maintained in the turbine *n* of type *k*, including preventive maintenance and failure maintenance. Thus, we can calculate the cost due to the loss of productivity as follows:

$$\Delta C_{T,Loss} = C_{Loss} = Power\ Rate\ \times 24hrs\ \times \frac{\$50}{MW} \times 30\% \times \left(T_{Loss,k,n}\right) \quad (6\text{-}10)$$

where $T_{Loss,k,n} = T_{LossAfter,k,n} + T_{LossBefore,k,n}$, representing the total number of stop days for the turbine. Suppose the capacity factor of the wind turbine is 30%, and the price of electricity is \$50/MW.

(4) In addition, there is the fixed cost of sending a maintenance team to the wind farm:

$$\Delta C_{T,Farm} = IF_{farm} C_{farm} \tag{6-11}$$

where $IF_{farm} = 1$ if preventive replacements or failure replacements are to be performed in the wind farm, otherwise equals 0.

Note that after all incurred cost at current inspection point is considered, the next inspection interval will be updated as:

$$L_{farm} = Max\{L_{k,n,m}\} \tag{6-12}$$

where $L_{k,n,m}$ denotes all the lead time values of the components to be determined for maintenance in the wind farm. The next inspection time will move to the point when L_{farm} has passed, i.e.,

$$t_{ABS} = t_{ABS} + L_{farm} \tag{6-13}$$

Otherwise, the next inspection point will move to the time after the regular inspection interval, i.e.,

$$t_{ABS} = t_{ABS} + T_I \tag{6-14}$$

At the new inspection time, if a failure or preventive replacement is decided to be performed on component *m* in turbine *n* of type *k*, regenerate a new real failure time by sampling Weibull distribution with parameters $\alpha_{k,m}$ and $\beta_{k,m}$.

If $t_{ABS} < T_{\text{Max}}$, repeat Step 3 and 4. T_{Max} is the maximum number of simulation iterations.

Step 5: The total expected maintenance cost calculation. When it goes to the maximum simulation iteration T_{Max}, i.e., when $t_{ABS} = T_{\mathrm{Max}}$, the simulation procedure is completed. The total expected maintenance cost per unit time per turbine for the wind farm is therefore:

$$C_E = \frac{C_T}{T_{\mathrm{Max}} \cdot \sum_{k=1}^{K} N_k} \tag{6-15}$$

6.3 Numerical Examples

In this section, we use some examples to demonstrate the proposed CBM approach for a wind farm, where two types of turbines are installed. In total, 6 turbines are considered in the wind farm. Three turbines belong to type 1, low capacity, and the other three turbines belong to type 2, high capacity. To simplify the discussion, we study four key components in series in each wind turbine: rotor, main bearing, gearbox, and generator. We also compare the proposed approach with the widely used constant-interval (CI) preventive maintenance method, and the method considering an approximate constant lead time for all the turbine components.

6.3.1 Example Introduction

In the example, two types of turbines are installed in the wind farm, i.e., low capacity turbines at 2MW and high capacity turbines at 5MW respectively. Thus, the costs and failure distribution parameter values, as well as the lead times of components vary with the different type of wind turbine. Weibull distributions are used to present the component failures of the populations, and the Weibull parameters and maintenance lead times corresponding to each type of turbines are given in Table 21. The cost data are given in Table 22, including the failure replacement costs for the components, the fixed and variable preventive replacement costs for each type, and the fixed cost of sending a maintenance team to the wind farm [49]. The standard deviations of the

ANN life prediction errors, as described in Section 6.2.3, are required to establish the associated prediction uncertainties [114] [115], and their values for each type system are given in Table 23.

All data used in this example are specified based on the data given in our previous study [19], [49], [116]–[118]. [49] collected all required data in this study. Besides, the inspection interval is set to be 10 days.

Table 21 .Weibull failure time distribution parameters and maintenance lead times for major components [49]

Component	Scale parameter α (days)		Shape parameter β	Lead time	
	Type 1	Type 2		Type 1	Type 2
Rotor	3,000	6000	3.0	30	45
Main bearing	3,750	7500	2.0	10	15
Gearbox	2,400	4800	3.0	25	30
Generator	3,300	6600	2.0	15	20

Table 22. Failure replacement and preventive maintenance costs for major components [49]

Component	Failure replacement cost ($k)		Variable preventive maintenance cost ($k)		Fixed preventive maintenance cost ($k)		Fixed cost to the wind farm ($k)	
	Type 1	Type 2	Type 1	Type 2	Type 1	Type 2	Type 1	Type 2
Rotor	112	224	28	56	25	50	50	
Main bearing	60	120	15	30				
Gearbox	152	304	38	76				
Generator	100	200	25	50				

Table 23. ANN life percentage prediction error standard deviation values for major components [49]

Component	Standard deviation	
	Type 1	Type 2
Rotor	0.12	0.15
Main bearing	0.10	0.13
Gearbox	0.10	0.13
Generator	0.12	0.15

6.3.2 The CBM optimization results

The total maintenance cost can be evaluated using the proposed simulation method described in Section 6.2.3. After all the cost being calculated, we search and find the minimum cost and the corresponding variable values, which are the optimal results. The optimal CBM policy can be obtained when the optimization problem is solved. There are 4 design variables in this optimization, and the optimal threshold failure probability values for Type-1 turbines are: $d_1^1 = 0.063$, $d_2^1 = 1.36 \times 10^{-4}$, and the optimal threshold failure probability values for Type-2 turbines are: $d_1^2 = 0.063$, $d_2^2 = 6.3 \times 10^{-6}$. The minimal expected maintenance cost per unit of time per turbine is \$84.8/day/turbine, and thus for the whole farm with 6 turbines, the optimal maintenance cost per unit of time is \$508. 8/day.

6.3.3 Comparison with the CBM approach considering the constant lead time

The CBM approach developed by [19] assumes constant lead time for all the turbine components. When the constant lead time is determined, the maximum lead time among all the components is used, and thus the maintenance work can be considered completed at the end of

the lead time for any component. For a wind farm with different types of turbines and different components, the constant lead time assumption is of course approximate. The CBM approach developed in this work provides more practical insights of the wind farm, and the optimal maintenance cost is 84.8$/day/turbine, as described in Section 6.3.2. If we apply the constant lead time assumption to this example, the lead time would be 45 days, which is the maximum of all the lead time values according to Table 21. At the optimal solution obtained in Section 6.3.2, where $d_1^1 = 0.063$, $d_2^1 = 1.36 \times 10^{-4}$, and $d_1^2 = 0.063$, $d_2^2 = 6.3 \times 10^{-6}$, the cost value obtained under the constant lead time assumption is 90.02$ /day/turbine. As a result, there is approximately 6.2% deviation from the real cost value if we use the constant lead time assumption. Besides, the results of expected maintenance cost between both cases of varying lead times and constant lead time do not show an outstanding difference if the production loss during the turbine stop days is not taken into account [49], which offsets the benefits of the developed method.

6.3.4 Comparative study with the constant-interval policy

In this section, we compare the proposed CBM approach with the constant-interval (CI) policy, which is a type of time-based preventive maintenance policy and is currently widely used in the wind energy industry. The main objective of the CI method is to determine the optimal preventive replacement interval, denoted by t_{CI}, to minimize the total expected cost per unit time. In this section, we investigate the CI maintenance policy using the same lifetime distributions for the components, as given in Table 21. The total expected maintenance cost per unit time for the wind farm can be obtained based on the method in [20], and the equation is given as:

$$C(t_{CI}) = \frac{\sum_{k=1}^{K} N_k \cdot \sum_{m=1}^{M_k} \left(C_{p,k,n,m}^{CI} + C_{f,k,n,m}^{CI} H_{m,k}(t_{CI}) \right)}{t_{CI}} \tag{6-16}$$

where, $C(t_{CI})$ denotes the total preventive maintenance cost, $C_{f,k,n,m}^{CI}$ is the total cost of a failure replacement for component *m* in turbine *n* of type *k*, and $C_{p,k,n,m}^{CI}$ is the total cost of a preventive replacement for component *m* in turbine *n* of type *k*. $H_{m,k}(t_{CI})$ is the expected number of failures for component *m* in type *k* turbine in interval $(0,t_{CI})$, which can be evaluated using the recursive procedure outline in [20]. Thus, the total expected maintenance cost per unit time per turbine, denoted by $C_E(t_{CI})$, can be obtained as:

$$C_E(t_{CI}) = \frac{C(t_{CI})}{\sum_{k=1}^{K} N_k} \tag{6-17}$$

The optimal interval t_{CI} can be obtained using the optimization tool, and it minimizes the expected maintenance cost per unit time.

The cost data is reconstructed based on those in Section 6.3.1 to ensure a fair comparison. The fixed cost of sending the maintenance team to the wind farm, c_{Farm}, is incurred at each time of failure occurrence, so it is regarded as a part of the failure replacement cost. The production loss is also considered. Thus, the failure replacement cost for component *m* in turbine *n* of type *k* can be given as :

$$C_{f,k,n,m}^{CI} = c_{k,f,m} + C_{farm} + Power\ Rate \times 24hrs \times \frac{\$50}{MW} \times 30\% \times L_{k,m} \tag{6-18}$$

At each time of the preventive replacement, the individual component's preventive maintenance cost shares the fixed cost at the farm level c_{farm} and the fixed preventive maintenance cost at the

turbine level shown in Table 22. Besides, the production loss is incurred and is distributed among all the components in the turbine since the components are replaced simultaneously. Therefore, the preventive replacement cost for component m in turbine n of type k can be calculated as:

$$C_{p,k,n,m}^{CI} = c_{p,k,m} + \frac{C_{p,T} + Power\ Rate \times 24hrs \times \frac{\$50}{MW} \times 30\% \times Max\{L_{k,m}\}}{M_k} + \frac{C_{farm}}{\sum_{k=1}^{K} n_k M_k} \quad (6\text{-}19)$$

The calculated failure replacement and preventive maintenance costs data using Equations (6-18) and (6-19) are shown in Table 24.

Table 24. Cost data for the constant-interval maintenance policy

Component	Failure replacement cost ($1000)		Preventive replacement cost ($1000)	
	Type 1	Type 2	Type 1	Type 2
Rotor	378	1,084	90.33	273.08
Main bearing	182	440	77.33	247.08
Gearbox	382	894	100.33	293.08
Generator	258	610	87.33	267.08

The total expected maintenance cost per unit of time can be calculated using Equation (6-17). The cost versus preventive maintenance interval is plotted and shown in Figure 40. By performing optimization, the optimal replacement interval is found to be 3,340 days, and the corresponding optimal cost is 471.89$/day/turbine. Comparing to the optimal cost 84.8

$/day/turbine obtained using the proposed CBM approach, it can be seen that about 82% cost savings are achieved using the proposed CBM approach.

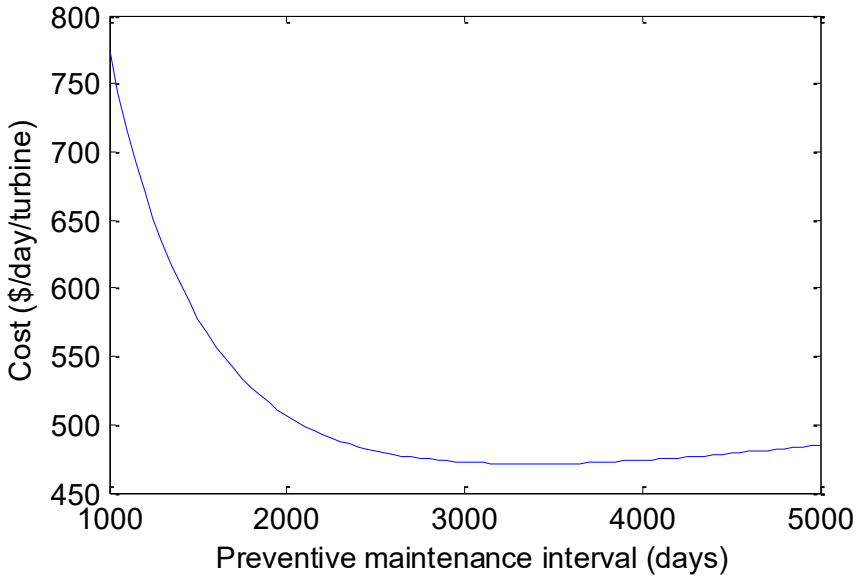

Figure 40. Cost versus preventive maintenance interval for the CI policy

6.4 Conclusions

Currently, the wind energy industry is switching from failure-based maintenance and time-based preventive maintenance strategies to CBM strategy by utilizing condition monitoring information more effectively. In this chapter, we extend the CBM approach presented in [49] to further involve the production loss in the overall maintenance cost evaluation. In practice, the production loss cannot be ignored in cost evaluation especially when different lead times and turbine types are given high values in a maintenance optimization problem. The key contribution of the study is that the cost of production loss during turbine stop days due to failure and maintenance activities is taken into consideration. The optimization results applying the same CBM policy presented in [19] [49] show an outstanding benefit compared to the case of constant

lead time consideration. Without considering the cost of power production loss during the turbine stop days, the results do not show notable average cost difference between the cases of different lead time and constant lead time as shown in [49]. The numerical examples demonstrate the effectiveness

Chapter 7. A numerical method for condition-based maintenance optimization of wind farms

7.1 Overview

Condition-based maintenance (CBM) optimization for wind farms considers multiple turbines in a wind farm, while each turbine involves multiple components. In [19], economic dependency among multiple turbines and multiple components in a turbine were considered, and a simulation-based method was developed for wind farm CBM policy cost evaluation. The simulation-based method was flexible in modeling various scenarios and factors, but due to its sampling-based nature, there are variations in CBM cost evaluation, and the resulting CBM cost function surface is not quite smooth. This could lead to challenge in the optimization process and cause local minima or convergence problems. Thus, an accurate numerical method is desired, which is not based on sampling process, and it could lead to smooth CBM cost function surface and benefit the optimization process. In this chapter, a numerical method is developed to estimate the overall maintenance cost of the CBM policy presented in [19]. Therefore, the optimal maintenance policy corresponding to the minimum maintenance cost is more accurately determined compared to the simulation method. An example of two turbines with two components in each is studied.

Nomenclature:

PrS: matrix describing the RUL probability distribution of component *m* in turbine *n*, with input (k, n, m).

$KV = (1, 2, \dots, K)$: vector indicating the possible RUL values

kr: matrix indicating the combination of all wind turbine component RULs

$T_{\mathrm{Pr}}(kr)$: the transition probability matrix that indicates the probability transitions from the current combination of all wind turbine component RULs, kr, to different component RUL intervals.

$T_{\mathrm{Cost}}(kr)$: the matrix recording the incremental cost incurred when the state of the wind farm transit from RUL combination kr.

Pr_n**:** the predicted failure probability of the wind turbine *n*.

d_1: the pre-specified high-level failure probability threshold at the turbine level.

d_2: the pre-specified low-level failure probability threshold at the turbine level. $d_2 < d_1$.

7.2 The proposed numerical method

Tian et al. proposed a CBM policy by defining two-level turbine failure probability d_1 and d_2 [19]. The policy is briefly explained as follows:

(1). Perform failure replacement if there is a failed component in the wind farm.

(2). At each inspection interval, perform preventive replacement on components in wind turbine n if $Pr_n > d_1$in order to bring the turbine failure probability down to below d_2. The predicted failure probability of the wind turbine is estimated based on the prediction results obtained by the prognosis approach.

According to the CBM policy, the cost rate can be denoted by $C_E(d_1, d_2)$, an optimal CBM satisfy [19],

$$\min C_E(d_1, d_2)$$

$$\text{s.t.} \tag{7-1}$$

$$0 < d_2 < d_1 < 1$$

As can be seen, the best CBM policy is determined when $C_E(d_1, d_2)$ is minimized, which requires an accurate method to evaluate the value. The proposed numerical method for evaluating C_E is presented in this section.

Consider a wind farm involving *N* wind turbines, with *M* critical components considered in each turbine. In this study, assume all turbines are of the same type, and component *m* in a turbine follows Weibull distribution with parameters α_m and β_m. For each component, the possible age is discretized into *K* intervals, and the same *K* is applied to all component types in this study. The first *K*-1 intervals are constant intervals, and the interval length is denoted by T_I. The last interval covers component age $((K-1)T_I, \infty)$.

Let $\mathrm{PrS}(k, n, m)$ denotes the remaining useful life (RUL) probability distribution of component *m* in turbine *n*. *k* is the RUL vector, and its elements can take values from $KV = (1, 2, \ldots, K)$. The first element in vector *KV* covers age $((K-1)T_I, \infty)$, or the last age interval, which means the RUL is 1 unit. The second element corresponds to age *K*-1, …, and the last element corresponds to age interval 1. Matrix PrS will be updated at each inspection point based on the CBM policy, where probability transitions will occur, and the costs incurred will be calculated at the same time.

7.2.1 Main cost evaluation process

The procedure of the cost evaluation is outlined in Figure 41. The details of the process are explained in the following.

Step 1. Determine transition matrices $T_{\mathrm{Pr}}(kr)$ and $T_{\mathrm{Cost}}(kr)$

For this numerical method, first RUL probability transition matrix $T_{\mathrm{Pr}}(kr)$ and cost transition matrix $T_{\mathrm{Cost}}(kr)$ for all components in the wind farm at each inspection point need to be determined, and then they will be used in the following relevant updating process. The procedure details is given in Section 7.2.2.

Step 2. Initialization

At time 0, matrix $\mathrm{PrS}(k,n,m)$ needs to be initialized by specifying the RUL distributions for each of the turbine components. Assume all components are new. The probability is initialized as the probability of the component RUL is in that corresponding interval, based on its Weibull lifetime distribution.

Step 3. Update the RUL probability distribution at intervals

At each inspection time, matrix $\mathrm{PrS}(k,n,m)$ will be updated to account for the probability transitions, i.e., probability transitions from each RUL interval to other RUL intervals due to aging and component replacements. The incremental costs will also be calculated.

Let $T_{\mathrm{Pr}}(kr)$ denotes the transition probability matrix that indicate the probability transitions from the current RUL combination of all wind turbine components to different component RUL intervals.

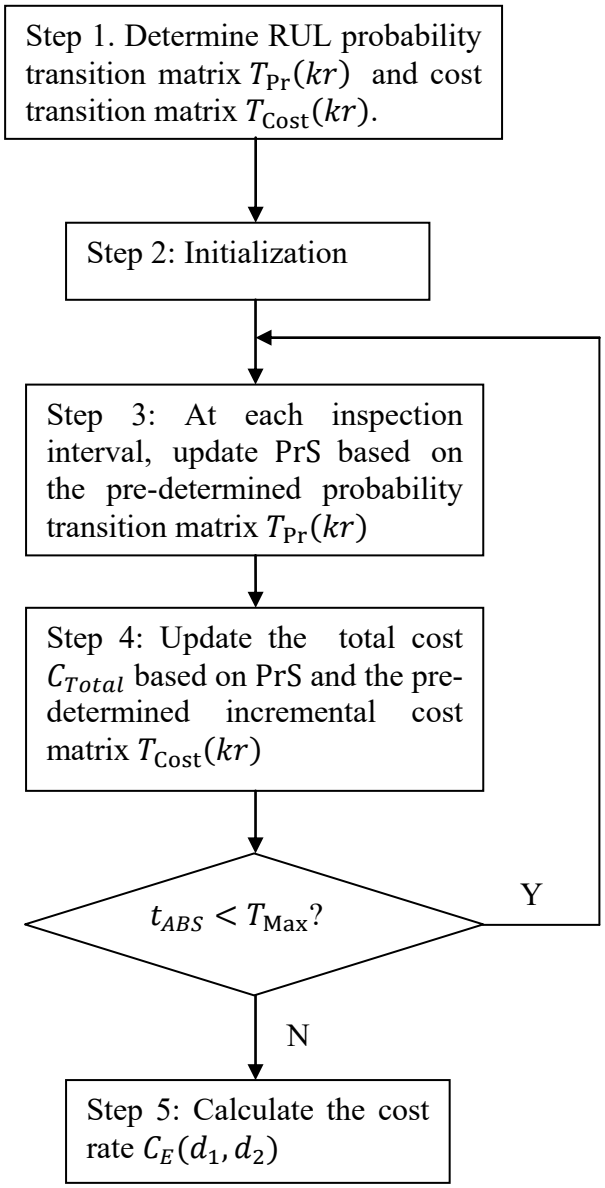

Figure 41. Flowchart of the overall numerical method for cost evaluation

$$kr = \begin{pmatrix} kr_{11} & \cdots & kr_{1M} \\ \vdots & \ddots & \vdots \\ kr_{N1} & \dots & kr_{NM} \end{pmatrix}, \tag{7-2}$$

where kr_{nm} represents the RUL interval value for component m in turbine n, and it can take values from $KV = (1, 2, \dots, K)$. The evaluation of $T_{\mathrm{Pr}}(kr)$ will be presented in the next section.

PrS will be updated at each inspection point, by applying the probability transition matrix $T_{\mathrm{Pr}}(kr)$ to PrS obtained at the previous inspection point. The updated probability distributions matrix $\mathrm{PrS}_{\mathrm{Updated}}$ is

$$\mathrm{PrS}_{\mathrm{Updated}} = T_{\mathrm{Pr}}(kr) \times \mathrm{PrS} \tag{7-3}$$

The "×" is not the product for 2-dimensional matrix, since all the matrices involved in the equation above are multi-dimensional. As another way to put it, for each RUL combination kr, the resulting change in matrix PrS can be obtained by multiplying matrix $T_{\mathrm{Pr}}(kr)$ by the probability of the combination kr, that is

$$\mathrm{PrS}_{\mathrm{Updated}} = \sum_{kr} T_{\mathrm{Pr}}(kr) \cdot P(kr) \tag{7-4}$$

where

$$P(kr) = \prod_{n,m} \mathrm{PrS}(kr(n,m), n, m) \tag{7-5}$$

Step 4. Update the total cost C_{Total} at the current inspection point

The total cost up to the current inspection point, denoted by C_{Total}, will be updated too:

$$C_{Total} = C_{Total} + T_{\mathrm{Cost}}(kr) \times \mathrm{PrS} \tag{7-6}$$

where $T_{\mathrm{Cost}}(kr)$ is the matrix represents the cost generation due to the maintenance actions, including preventive replacements and failure replacements, and the determination of this matrix will be explained in the next section as well.

Step 5. Calculate the cost rate $C_E(d_1, d_2)$

For each set of variable values $d_1$and d_2, eventually, C_{Total}will be updated following the above process until the maximum iteration time T_{Max}. Thus, the cost rate is

$$C_E(d_1, d_2) = \frac{C_{Total}}{T_{\mathrm{Max}}} \tag{7-7}$$

As can be seen above, the probability transition matrix $T_{\mathrm{Pr}}(kr)$ and the cost transition matrix $T_{\mathrm{Cost}}(kr)$ need to be determined first, before being used in the computation described in this section. The algorithm for determining the transition matrixes will be presented in next section.

7.2.2 Determination of transition matrices

As we mention earlier, the proposed cost evaluation algorithm needs to have transition matrices determined first. A flowchart for the procedure of determining matrices $T_{\mathrm{Pr}}(kr)$ and $T_{\mathrm{Cost}}(kr)$ is shown in Figure 42.

The critical parts in the procedure are described in the followings.

As indicated in Section 7.2.1, the matrix PrS will be initialized first, indicating the initial RUL distributions for all the wind turbine components, and it will be updated at each inspection point by applying the transition matrix $T_{\mathrm{Pr}}(kr)$. The probability transition for each kr is determined for the matrix, i.e. the change in $\mathrm{PrS}(k, n, m)$.

$T_{\mathrm{Pr}}(kr)$ is initialized as 0. First probability transitions occur due to the RUL reduction when moving from the previous inspection point to the current inspection point. The RUL for each component will be reduced by 1 unit. The following two cases are considered.

Case 1: Failure replacement when $kr(n, m)$=0, i.e., $RUL_{n,m} = 0$. In this case, the probability of the component in previous RUL state $kr(n, m) - 1$ will be reduced by 1:

$$T_{\mathrm{Pr}}(kr(n,m)-1,n,m)=T_{\mathrm{Pr}}(kr(n,m)-1,n,m)-1 \quad (7\text{-}8)$$

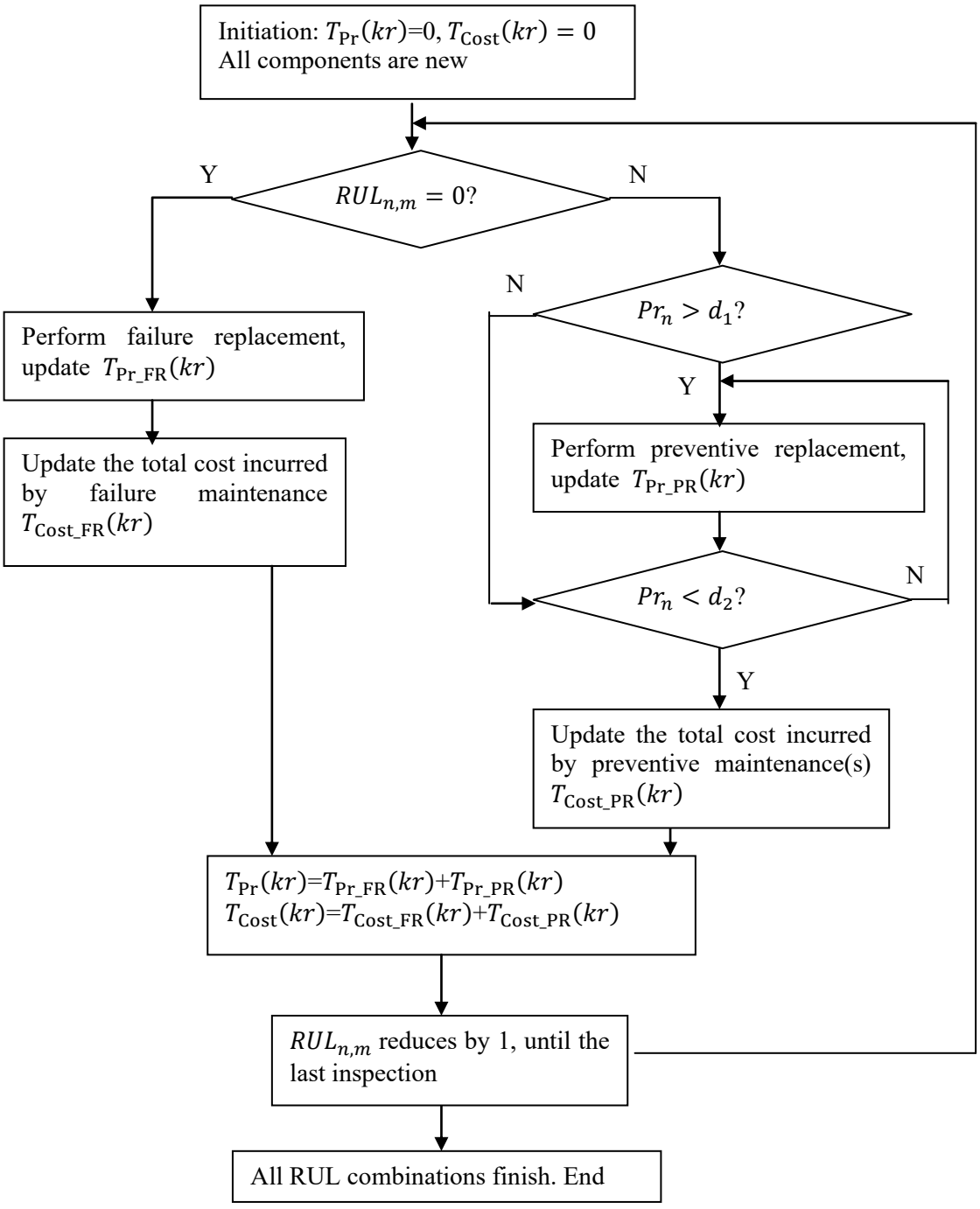

Figure 42. The flow chart of determining transition matrixes

In addition, a new component will be generated:

$$T_{\Pr}(kr(n,m),n,m) = T_{\Pr}(kr(n,m),n,m) + P_{\text{init}}(m), \text{ for each } k \in KV. \quad (7\text{-}9)$$

where $P_{\text{init}}(m)$ is the initial life distribution for component *m*.

Costs will be incurred too, which may include fixed cost to the farm, C_{Farm}, and failure replacement cost for each failed component:

$$T_{Cost}(kr) = T_{Cost}(kr) + C_{Farm} + \sum_{n,m} C_F(n,m) \cdot IF(n,m) \quad (7\text{-}10)$$

$IF(n,m) = 1$ if the component fails, and $IF(n,m) = 0$ otherwise.

Case 2: failure does not occur when $kr(n,m)$>0, i.e., $RUL_{n,m} > 0$. In this case, the probability of the component in previous RUL state $kr(n,m) - 1$ will be reduced by 1, and the probability of the component in current RUL state $kr(n,m)$ will be certainly increased by 1.

$$T_{\Pr}(kr(n,m) - 1,n,m) = T_{\Pr}(kr(n,m) - 1,n,m) - 1 \quad (7\text{-}11)$$

$$T_{\Pr}(kr(n,m),n,m) = T_{\Pr}(kr(n,m),n,m) + 1 \quad (7\text{-}12)$$

Probability transition will occur in the case of preventive replacement for each kr. For a certain kr, for each of the components, the predicted RUL distribution can be obtained based on the prediction accuracy of the prediction tools, such as ANN prediction tool. With this, the failure probability for each component and thus each wind turbine can be obtained. Refer to Tian et al (2011) for more details. Based on the CBM policy defined by (d_1, d_2), for a certain component *m* in turbine *n* that is not failed, if preventive replacement is to be performed on the component according to the CBM policy, the following probability transitions will occur:

$$T_{\Pr}(kr(n,m),n,m) = T_{\Pr}(kr(n,m),n,m) - 1 \quad (7\text{-}13)$$

$$T_{\Pr}(k,n,m) = T_{\Pr}(k,n,m) + P_{\text{init}}(m), \text{ for each } k \in KV \quad (7\text{-}14)$$

Cost will be updated as follows:

$$T_{Cost}(kr) = T_{Cost}(kr) + \sum_{n,m} C_P(n,m) \cdot IP(n,m) + \sum_n C_{Pfix}(n) \cdot IP_{fix}(n) \qquad (7\text{-}15)$$

$IP(n,m) = 1$ if preventive replacement is performed, and $IP(n,m) = 0$ otherwise. $C_{Pfix}(n)$ is the fixed turbine level PR cost, and will be incurred only once for a turbine.

With the algorithm presented above, the probability transition matrix $T_{\mathrm{Pr}}(kr)$ and the cost transition matrix $T_{\mathrm{Cost}}(kr)$ can be determined.

7.3 A numerical example

We consider an example that there are two turbines installed, each turbine has two critical components, i.e. rotor and main bearing. The parameters of failure distribution of each component, the related maintenance cost, and the prediction error standard deviation values for the component using ANN prognosis approach are given in Table 25 [19].

Table 25. Parameter values for major components

Parameters	Rotor	Main bearing
Scale parameter α (days)	3,000	3,750
Shape parameter β	3.0	2.0
Failure replacement cost ($k)	112	60
Variable preventive maintenance cost ($k)	28	15
Fixed preventive maintenance cost ($k)	25	
Fixed cost to the wind farm ($k)	50	
Failure prediction error (standard deviation)	0.12	0.10

Suppose the maintenance lead time for all components is 30 days. The inspection interval is set to be 1.5 years, and there are in total 20 inspections for a component during a typical lifetime of 30 years.

The total maintenance cost can be evaluated using the proposed numerical method described in Section 7.2. The 3D plot of cost vs. failure probability threshold values d_1 and d_2 is shown in Figure 43. d_1 and d_2 values are denoted in the logarithmic scale. It can be seen the average maintenance cost decreases when d_1 and d_2 are selected as certain small values. In the experiments given a range of d_1 and d_2, the lower cost is found to be \$22.7985/day, and the corresponding failure probability threshold values are $d_1 = 0.0251$, $d_2 = 4.642 \times 10^{-10}$. As this partial result, more tests need to be done since there is no optimal point achieved yet given the current range of d_1 and d_2.

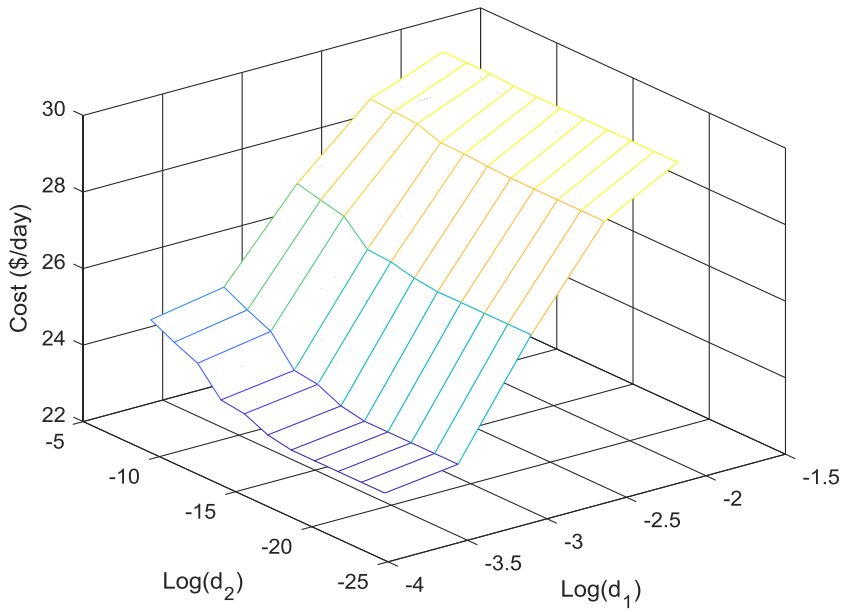

Figure 43. Cost vs. d_1 and d_2 in the log-scale

Figure 44 and Figure 45 show 2D plot when each one of variables is remained at the value corresponding to the lower cost previously, respectively. Figure 46 shows a curve of cost rate vs. number of iterations, it can be observed that the cost rate approaches a steady value after a certain number of iterations. From the results obtained in the example, the threshold values of $d_1$and d_2 are expected to extend the range so that a concave point of the 3D surface shown in Figure 43 may appear.

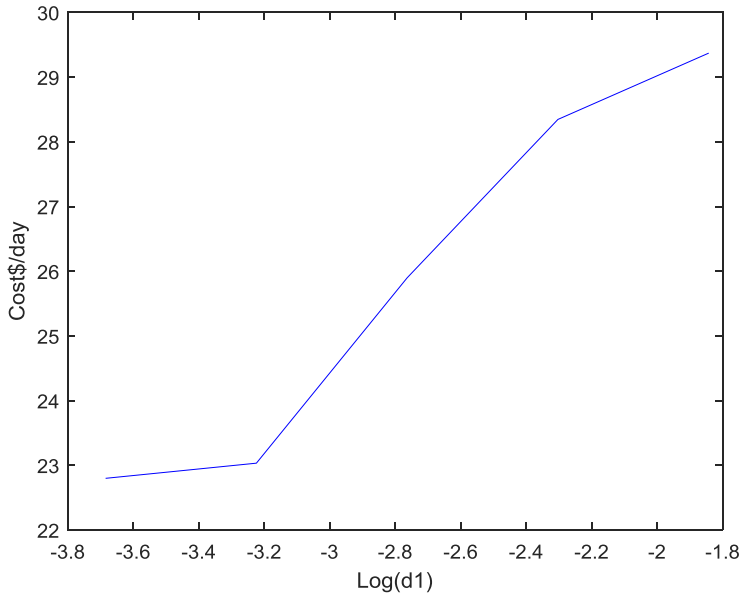

Figure 44. Cost vs. Log(d_1) (d_2 is kept at 4.642×10^{-10})

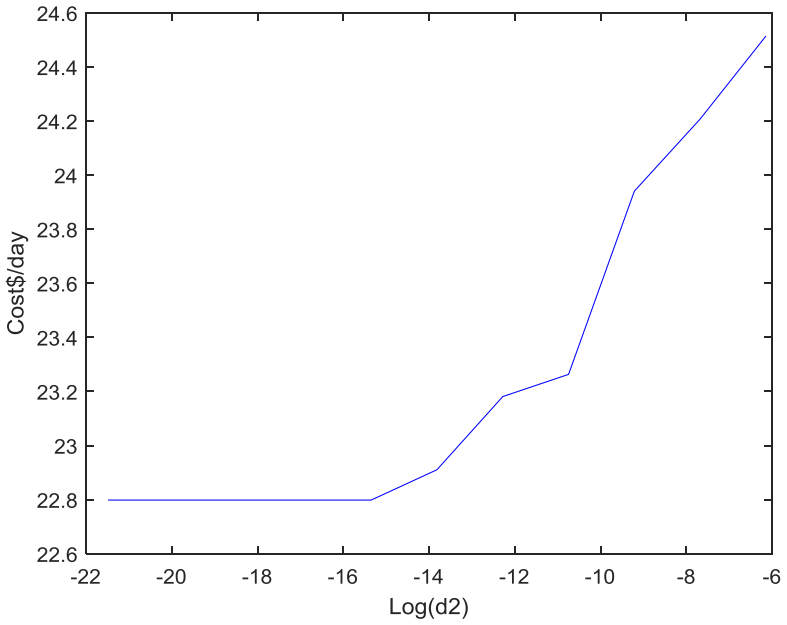

Figure 45. Cost vs. Log(d_2) (d_1 is kept at 0.0251)

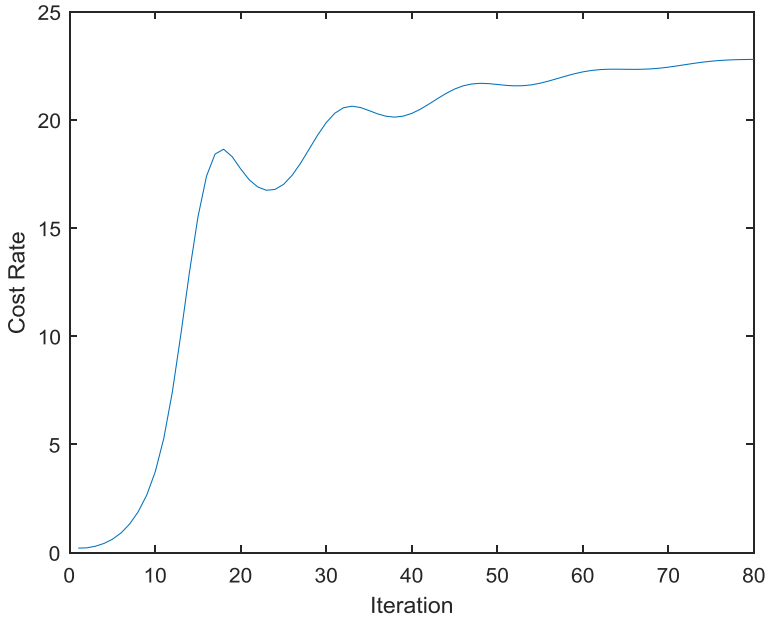

Figure 46. Cost rate vs. number of iterations ($d_1 = 0.0251$, $d_2 = 4.642 \times 10^{-10}$)

7.4 Conclusions

In the existing studies, simulation methods are commonly used to solve the optimization problems for the complex processes. However, the simulation method could lead to variations in estimating the objective values. In particular, for wind power industry the maintenance cost is affected significantly by the selections of decision criterion. A more accurate method is desired regarding the maintenance cost evaluation. In this chapter, a numerical method has been developed to estimate the overall maintenance cost for CBM of wind farms. The CBM policy is defined by two failure probability thresholds, which are low-level threshold d_2 and high-level threshold d_1,$1 > d_1 > d_2 > 0$. A numerical example is given to examining the proposed method and the computation results are presented. It demonstrates the effectiveness of the method by a relatively smooth surface of the cost function. Future research will be focusing on the comparative study with the simulation method given the same example, and the improvement of computing efficiency.

Chapter 8. Conclusions and future work

Nowadays a large size wind turbine can be over 150m hub height, and has about 80m rotor blade length. An unexpected failure may cause catastrophic losses. The O&M of a wind farm is an urgent area to call for research on optimization. There is great value to keep making huge efforts in this area. In this chapter, we conclude the study in the thesis, and suggest several potential works in the future.

8.1 Conclusions

Maintenance management has significant impact on overall cost in wind power industry. Optimizing maintenance strategies is a very vast research area which can benefits the overall cost for wind energy and make it more competitive among the energy resources. Corrective maintenance and time-based preventive maintenance strategies are currently widely adopted in the wind industry due to the worse accessibility of wind turbines, especially for those located remotely or offshore. However, there is a huge demand to reduce wind power cost via maintenance strategy improvement. In this thesis, the objective is to developing cost-effective maintenance strategies for wind farms. Conventional time-based maintenance optimization, and prognostics and CBM optimization within the CBM strategy framework are focused on.

We first improve corrective maintenance and time-based preventive maintenance strategies. Opportunistic maintenance strategies are proposed, which take advantage of economic dependencies existing among the wind turbines, and implement preventive maintenance simultaneously at the instant of performing corrective maintenance. Imperfect preventive maintenance is considered, which deals with the common inspection and maintenance activities

that do not always replace the failed parts in reality. The method can bring immediate benefits of saving the overall maintenance cost for a wind farm.

Prognostics and condition-based maintenance have outstanding advantages of predicting and preventing the failures, which is a relatively new but promising research area to be explored in the wind industry [18]. CBM is the more advanced maintenance strategy, in which the health status of components are continuously monitored and predicted so the unexpected failures can be the most avoided. Prognostics is essential in CBM. Wind turbines work with time-varying wind direction and velocity, which leads to the instantaneously time-varying load applied to the wind turbine load. In this thesis, we focus on gearbox failure due to the gear tooth crack, an integrated prognostics method is developed considering instantaneously time-varying load condition. In a subsequent extended study, uncertainty in gear tooth crack initiation time is further considered for prognostics method development. The numerical examples in both studies demonstrate that the developed methods provide more accurate gear RUL prediction compared to existing methods under constant-load assumption.

A CBM method considering different types and lead times of the installed wind turbines in a farm, as well as the production loss during the shutdown time is also developed. The method is capable of accurately estimate the average maintenance cost for a wind farm with diverse turbines. In addition, we also develop a numerical algorithm for CBM optimization of wind farms that accounts for the inaccuracy in the simulation-based algorithms, which most studies use for solving complex problems. The developed method can avoid the variations in CBM cost evaluation, and the cost rate approaches a steady value after a certain number of iterations in a provided example. The method needs to be studied for higher efficiency in the future work.

From the results in this thesis, we conclude that the research provides several innovative methods for maintenance management in the wind power industry, where some practical issues in the real world are well addressed. The developed methods are able to significantly reduce the overall maintenance cost within either conventional maintenance or condition-based maintenance strategies that the wind farm owners may apply. They are expected to improve the competitiveness of the wind energy among the renewable resources, and contribute to a clean and sustainable energy future.

8.2 Future work

Specifically, with standing on my current research stage, the following works are suggested in the future.

- In prognostics for the wind turbines, the varying rotating speed of the gearbox can be jointly considered with varying load together, which addresses the problem that the variable speed turbines face. The gear crack propagation process under varying speed and varying load condition need to be well modeled.

- In the physical model part of the developed integrated prognostics approach, a mathematical model is used to calculate the contact force on the gear tooth profile when the gear pair are meshing. In the next step, an advanced multi-body simulation tool, SIMPACK, can be employed for studying the complex dynamic behavior of gearboxes. Moreover, taking advantage of complex system dynamics modeling capability within SIMPACK, prognosis for planetary gearboxes in the wind turbine can be studied under time-varying load condition.

- The developed numerical method for evaluating CBM cost in this thesis provides the more accurate result compared to the simulation method. However, the capability of computing the cost for larger size wind farm and more components in a wind turbine is greatly challenged in the current study. The efficiency of the method needs to be improved in the future work.

- Validation of the current developed approaches. More experiments need to be conducted to test the proposed methods, such as the integrated prognostics methods for gearboxes under time-varying external load. Moreover, several proposed optimal maintenance methods in this thesis are expected for applications in the industry projects.

Although prognostic techniques and CBM optimization for wind power industry are very challenging tasks, these suggested future works will be carried out at a positive pace based on the current collected information, and provide the state of the art of wind farm maintenance. In addition, there is also significance to develop the suggested works to achieve robustness.

Bibliography

[1] F. Ding and Z. Tian, "Opportunistic maintenance for wind farms considering multi-level imperfect maintenance thresholds," *Renew. Energy*, vol. 45, pp. 175–182, 2012.

[2] F. Ding, Z. Tian, F. Zhao, and H. Xu, "An integrated approach for wind turbine gearbox fatigue life prediction considering instantaneously varying load conditions," *Renew. Energy*, vol. 129, no. Part A, pp. 260–270, Dec. 2018.

[3] F. Ding, Z. Tian, and A. Amayri, "Condition-based maintenance of wind power generation systems considering different turbine types and lead times," *Int. J. Strateg. Eng. Asset Manag.*, vol. 2, no. 1, pp. 63–79, 2014.

[4] M. H. Firouz and A. Alemi, "Optimal energy and reserve scheduling of wind power producers in electricity market considering demand response," in *2016 IEEE International Conference on Power and Energy (PECon)*, 2016, pp. 652–656.

[5] "A Review and Methodology Development for Remaining Useful Life Prediction of Offshore Fixed and Floating Wind turbine Power Converter with Digital Twin Technology Perspective," *2018 2nd Int. Conf. Green Energy Appl. ICGEA Green Energy Appl. ICGEA 2018 2nd Int. Conf. On*, p. 197, 2018.

[6] J. K. Kaldellis and M. Kapsali, "Shifting towards offshore wind energy—Recent activity and future development," *Energy Policy*, vol. 53, pp. 136–148, 2013.

[7] J. Lee, C. Jin, Z. Liu, and H. D. Ardakani, "Introduction to data-driven methodologies for prognostics and health management," in *Probabilistic prognostics and health management of energy systems*, Springer, 2017, pp. 9–32.

[8] "canada wind farm O&M market_07SEP17_Survey_Results.pdf." .

[9] "Wind Turbine Operations & Maintenance Market - Global Market Size, Trends, and Key Country Analysis to 2025." [Online]. Available: https://www.reportlinker.com/p05001577/Wind-Turbine-Operations-Maintenance-Market-Global-Market-Size-Trends-and-Key-Country-Analysis-to.html. [Accessed: 29-Jun-2018].

[10] Y. Sinha and J. A. Steel, “A progressive study into offshore wind farm maintenance optimisation using risk based failure analysis,” *Renew. Sustain. Energy Rev.*, vol. 42, pp. 735–742, 2015.

[11] G. Haddad, P. A. Sandborn, and M. G. Pecht, “Using maintenance options to maximize the benefits of prognostics for wind farms,” *Wind Energy*, vol. 17, no. 5, pp. 775–791, 2014.

[12] S. Hussain and H. A. Gabbar, “Vibration analysis and time series prediction for wind turbine gearbox prognostics,” *Int. J. Progn. Health Manag.*, pp. 69–79, 2013.

[13] “Wind Turbine Gearbox Prognostic Simulation Research Based on MSET Method--《Journal of System Simulation》2013 年 12 期.” [Online]. Available: http://en.cnki.com.cn/Article_en/CJFDTotal-XTFZ201312035.htm. [Accessed: 10-Jul-2018].

[14] C. E. Plumley, G. Wilson, A. Kenyon, F. Quail, and A. Zitrou, “Diagnostics and prognostics utilising dynamic Bayesian networks applied to a wind turbine gearbox,” in *International Conference on Condition Monitoringand Machine Failure Prevention Technologies, CM & MFPT 2012*, 2012.

[15] J. L. Godwin and P. Matthews, “Prognosis of wind turbine gearbox failures by utilising robust multivariate statistical techniques,” in *Prognostics and Health Management (PHM), 2013 IEEE Conference on*, 2013, pp. 1–8.

[16] B. C. P. Lau, E. W. M. Ma, and M. Pecht, “Review of offshore wind turbine failures and fault prognostic methods,” in *Prognostics and System Health Management (PHM), 2012 IEEE Conference on*, 2012, pp. 1–5.

[17] F. Ding, Z. Tian, and T. Jin, “Maintenance modeling and optimization for wind turbine systems: A review,” in *Quality, Reliability, Risk, Maintenance, and Safety Engineering (QR2MSE), 2013 International Conference on*, 2013, pp. 569–575.

[18] G. de N. P. Leite, A. M. Araújo, and P. A. C. Rosas, “Prognostic techniques applied to maintenance of wind turbines: A concise and specific review,” *Renew. Sustain. Energy Rev.*, 2017.

[19] Z. Tian, T. Jin, B. Wu, and F. Ding, "Condition based maintenance optimization for wind power generation systems under continuous monitoring," *Renew. Energy*, vol. 36, no. 5, pp. 1502–1509, 2011.

[20] A. K. Jardine and A. H. Tsang, *Maintenance, replacement, and reliability: theory and applications*. CRC press, 2013.

[21] F. F. Ding and F. F. Ding, "Comparative Study of Maintenance Strategies for Wind Turbine Systems," masters, Concordia University, 2010.

[22] S. Carlos, A. Sanchez, S. Martorell, and I. Marton, "Onshore wind farms maintenance optimization using a stochastic model," *Math. Comput. Model.*, vol. 57, no. 7–8, pp. 1884–1890, Apr. 2013.

[23] F. Ding and Z. Tian, "Opportunistic maintenance optimization for wind turbine systems considering imperfect maintenance actions," *Int. J. Reliab. Qual. Saf. Eng.*, vol. 18, no. 05, pp. 463–481, 2011.

[24] Y. Lu, L. Sun, J. Kang, H. Sun, and X. Zhang, "Opportunistic maintenance optimization for offshore wind turbine electrical and electronic system based on rolling horizon approach," *J. Renew. Sustain. Energy*, vol. 9, no. 3, p. 033307, May 2017.

[25] Y. M. Ko and E. Byon, "Condition-based joint maintenance optimization for a large-scale system with homogeneous units," *Iise Trans.*, vol. 49, no. 5, pp. 493–504, 2017.

[26] B. R. Sarker and T. Ibn Faiz, "Minimizing maintenance cost for offshore wind turbines following multi-level opportunistic preventive strategy," *Renew. Energy*, vol. 85, pp. 104–113, Jan. 2016.

[27] C. Zhang, W. Gao, S. Guo, Y. Li, and T. Yang, "Opportunistic maintenance for wind turbines considering imperfect, reliability-based maintenance," *Renew. Energy*, vol. 103, pp. 606–612, Apr. 2017.

[28] H. Abdollahzadeh, K. Atashgar, and M. Abbasi, "Multi-objective opportunistic maintenance optimization of a wind farm considering limited number of maintenance groups," *Renew. Energy*, vol. 88, pp. 247–261, Apr. 2016.

[29] A. K. S. Jardine, D. Lin, and D. Banjevic, “A review on machinery diagnostics and prognostics implementing condition-based maintenance,” *Mech. Syst. Signal Process.*, vol. 20, no. 7, pp. 1483–1510, Oct. 2006.

[30] Y. Peng, M. Dong, and M. J. Zuo, “Current status of machine prognostics in condition-based maintenance: a review,” *Int. J. Adv. Manuf. Technol.*, vol. 50, no. 1–4, pp. 297–313, Sep. 2010.

[31] J. Z. Sikorska, M. Hodkiewicz, and L. Ma, “Prognostic modelling options for remaining useful life estimation by industry,” *Mech. Syst. Signal Process.*, vol. 25, no. 5, pp. 1803–1836, Jul. 2011.

[32] I. Alsyouf and I. El-Thalji, “Maintenance practices in wind power systems: A review and analysis,” *Eur. Wind Energy Conf. Exhib. 2008*, vol. 5, pp. 2588–2597, Jan. 2008.

[33] Z. Hameed, Y. S. Hong, Y. M. Cho, S. H. Ahn, and C. K. Song, “Condition monitoring and fault detection of wind turbines and related algorithms: A review,” *Renew. Sustain. Energy Rev.*, vol. 13, no. 1, pp. 1–39, Jan. 2009.

[34] S. Costinas, I. Diaconescu, and I. Fagarasanu, “Wind power plant condition monitoring,” in *Proceedings of the 3rd WSEAS International Conference on Energy Planning, Energy Saving, Environmental Education (EPESE’09), Canary Islands, Spain*, 2009, pp. 1–3.

[35] B. Lu, Y. Li, X. Wu, and Z. Yang, “A review of recent advances in wind turbine condition monitoring and fault diagnosis,” in *Power Electronics and Machines in Wind Applications, 2009. PEMWA 2009. IEEE*, 2009, pp. 1–7.

[36] M. Lucente, “Condition monitoring system in wind turbine gearbox,” *Masters Thesis KTH Coop. NTNU Stockh.*, 2008.

[37] M. C. Garcia, M. A. Sanz-Bobi, and J. del Pico, “SIMAP: Intelligent System for Predictive Maintenance: Application to the health condition monitoring of a windturbine gearbox,” *Comput. Ind.*, vol. 57, no. 6, pp. 552–568, 2006.

[38] M. R. Wilkinson, F. Spinato, and P. J. Tavner, “Condition monitoring of generators & other subassemblies in wind turbine drive trains,” in *Diagnostics for Electric Machines, Power Electronics and Drives, 2007. SDEMPED 2007. IEEE International Symposium on*, 2007, pp. 388–392.

[39] F. Besnard and L. Bertling, “An approach for condition-based maintenance optimization applied to wind turbine blades,” *IEEE Trans. Sustain. Energy*, vol. 1, no. 2, pp. 77–83, 2010.

[40] J. D. Sørensen, “Framework for risk-based planning of operation and maintenance for offshore wind turbines,” *Wind Energy*, vol. 12, no. 5, pp. 493–506, 2009.

[41] J. J. Nielsen and J. D. Sørensen, “Planning of O&M for Offfshore Wind Turbines using Bayesian Graphical Models,” in *European Safety and Reliability Conference: ESREL*, 2010.

[42] E. Byon and Y. Ding, “Season-dependent condition-based maintenance for a wind turbine using a partially observed Markov decision process,” *IEEE Trans. Power Syst.*, vol. 25, no. 4, pp. 1823–1834, 2010.

[43] Y. Wu and H. Zhao, “Optimization maintenance of wind turbines using Markov decision processes,” in *Power System Technology (POWERCON), 2010 International Conference on*, 2010, pp. 1–6.

[44] A. Kusiak and A. Verma, “A data-mining approach to monitoring wind turbines,” *IEEE Trans. Sustain. Energy*, vol. 3, no. 1, pp. 150–157, 2012.

[45] A. Kusiak and A. Verma, “Analyzing bearing faults in wind turbines: A data-mining approach,” *Renew. Energy*, vol. 48, pp. 110–116, 2012.

[46] F. Besnard, K. Fischer, and L. Bertling, “Reliability-Centred Asset Maintenance—A step towards enhanced reliability, availability, and profitability of wind power plants,” in *Innovative Smart Grid Technologies Conference Europe (ISGT Europe), 2010 IEEE PES*, 2010, pp. 1–8.

[47] J. J. Nielsen and J. D. Sørensen, “On risk-based operation and maintenance of offshore wind turbine components,” *Reliab. Eng. Syst. Saf.*, vol. 96, no. 1, pp. 218–229, 2011.

[48] A. Amayri, Z. Tian, and T. Jin, “Condition based maintenance of wind turbine systems considering different turbine types,” in *Quality, Reliability, Risk, Maintenance, and Safety Engineering (ICQR2MSE), 2011 International Conference on*, 2011, pp. 596–600.

[49] A. Amayri, “Condition-Based Maintenance of Wind Turbine Systems Considering Different Turbine Types and Lead Times,” Concordia University, 2011.

[50] E. Pazouki, H. Bahrami, and S. Choi, “Condition Based Maintenance Optimization of Wind Turbine System Using Degradation Prediction,” in *2014 Ieee Pes General Meeting - Conference & Exposition*, 2014.

[51] E. Byon, L. Ntaimo, and Y. Ding, “Optimal maintenance strategies for wind turbine systems under stochastic weather conditions,” *IEEE Trans. Reliab.*, vol. 59, no. 2, pp. 393–404, 2010.

[52] J. Nilsson and L. Bertling, “Maintenance management of wind power systems using condition monitoring systems—life cycle cost analysis for two case studies,” *IEEE Trans. Energy Convers.*, vol. 22, no. 1, pp. 223–229, 2007.

[53] J. A. Andrawus, J. Watson, M. Kishk, and A. Adam, “The selection of a suitable maintenance strategy for wind turbines,” *Wind Eng.*, vol. 30, no. 6, pp. 471–486, 2006.

[54] D. McMillan and G. W. Ault, “Condition monitoring benefit for onshore wind turbines: sensitivity to operational parameters,” *IET Renew. Power Gener.*, vol. 2, no. 1, pp. 60–72, 2008.

[55] G. Haddad, P. A. Sandborn, T. Jazouli, M. G. Pecht, B. Foucher, and V. Rouet, “Guaranteeing high availability of wind turbines,” in *Proceedings of the European Safety and Reliability Conference (ESREL)*, 2011.

[56] “PHM based predictive maintenance option model for offshore wind farm O&M optimization - Google 搜索.” [Online]. Available: https://www-google-com.login.ezproxy.library.ualberta.ca/search?q=PHM+based+predictive+maintenance+option+model+for+offshore+wind+farm+O%26amp%3BM+optimization&ie=utf8&oe=utf8. [Accessed: 10-Jul-2018].

[57] “Prediction of wind turbine gearbox gears fatigue damage under turbulent loading based on spectrum method,” *ResearchGate*. [Online]. Available: https://www.researchgate.net/publication/315028459_Prediction_of_wind_turbine_gearbox_gears_fatigue_damage_under_turbulent_loading_based_on_spectrum_method. [Accessed: 10-Jul-2018].

[58] C. Chen, S. Kunche, and M. Pecht, “Incremental Learning Approach for Improved Prediction,” *2013 Ieee Int. Conf. Progn. Health Manag.*, 2013.

[59] X. Li, J. Cai, H. Zuo, and H. Li, “Optimal Cost-Effective Maintenance Policy for a Helicopter Gearbox Early Fault Detection under Varying Load,” *Math. Probl. Eng.*, vol. 2017, pp. 1–16, 2017.

[60] I. S. Al-Tubi, H. Long, J. Zhang, and B. Shaw, “Experimental and analytical study of gear micropitting initiation and propagation under varying loading conditions,” *Wear*, vol. 328–329, pp. 8–16, Apr. 2015.

[61] M. Gəsperin, P. Bŏskoski, and D. Juricicl, “Model-based prognostics under non-stationary operating conditions,” in *Proceedings of the Annual Conference of the Prognostics and Health Management Society 2011, PHM 2011*, 2014, pp. 368–374.

[62] A. Altamura and D. Straub, “Reliability assessment of high cycle fatigue under variable amplitude loading: Review and solutions,” *Eng. Fract. Mech.*, vol. 121, pp. 40–66, 2014.

[63] P. C. Paris and F. Erdogan, “A critical analysis of crack propagation laws,” 1963.

[64] K. Sobczyk, “Modelling of random fatigue crack growth,” *Eng. Fract. Mech.*, vol. 24, no. 4, pp. 609–623, 1986.

[65] H. Alawi, “Fatigue crack growth prediction under random peaks and sequence loading,” *J Eng Mater TechnolTrans ASME*, vol. 111, no. 4, pp. 338–344, 1989.

[66] H. Alawi and M. Shaban, “Fatigue crack growth under random loading,” *Eng. Fract. Mech.*, vol. 32, no. 5, pp. 845–854, 1989.

[67] S. U. Khan, R. C. Alderliesten, J. Schijve, and R. Benedictus, “On the fatigue crack growth prediction under variable amplitude loading,” *Comput. Exp. Anal. Damaged Mater.*, pp. 77–105, 2007.

[68] W. Q. Zhu, Y. K. Lin, and Y. Lei, “On fatigue crack growth under random loading,” *Eng. Fract. Mech.*, vol. 43, no. 1, pp. 1–12, 1992.

[69] Y. Lei and W. Q. Zhu, “Fatigue crack growth in degrading elastic components of nonlinear structural systems under random loading,” *Int. J. Solids Struct.*, vol. 37, no. 4, pp. 649–667, 2000.

[70] X. Huang and J. W. Hancock, “A reliability analysis of fatigue crack growth under random loading,” *Fatigue Fract. Eng. Mater. Struct.*, vol. 12, no. 3, pp. 247–258, 1989.

[71] H. J. Sutherland and D. P. Burwinkle, “The spectral content of the torque loads on a turbine gear tooth,” *Wind Energy*, vol. 16, no. 1, pp. 91–97, 1995.

[72] Y. Qiu, L. Chen, Y. Feng, and Y. Xu, “An approach of quantifying gear fatigue life for wind turbine gearboxes using supervisory control and data acquisition data,” *Energies*, vol. 10, no. 8, p. 1084, 2017.

[73] “National Instruments Products for Wind Turbine Condition Monitoring - National Instruments.” [Online]. Available: http://www.ni.com/white-paper/7676/en/. [Accessed: 29-Aug-2017].

[74] E. Hau, *Wind turbines: fundamentals, technologies, application, economics*. Springer Science & Business Media, 2013.

[75] “Statistics Show Bearing Problems Cause the Majority of Wind Turbine Gearbox Failures,” *Energy.gov*. [Online]. Available: https://energy.gov/eere/wind/articles/statistics-show-bearing-problems-cause-majority-wind-turbine-gearbox-failures. [Accessed: 11-Jan-2018].

[76] G. Van Kuik and J. Peinke, *Long-term Research Challenges in Wind Energy-A Research Agenda by the European Academy of Wind Energy*, vol. 6. Springer, 2016.

[77] T. L. Anderson, *Fracture Mechanics: Fundamentals and Applications, Fourth Edition*. CRC Press, 2017.

[78] F. Zhao, Z. Tian, and Y. Zeng, “Uncertainty quantification in gear remaining useful life prediction through an integrated prognostics method,” *IEEE Trans. Reliab.*, vol. 62, no. 1, pp. 146–159, 2013.

[79] S. Zouari, M. Maatar, T. Fakhfakh, and M. Haddar, “Following Spur Gear Crack Propagation in the Tooth Foot by Finite Element Method,” *J. Fail. Anal. Prev.*, vol. 10, no. 6, pp. 531–539, Dec. 2010.

[80] Z. Yishu, “A strain energy criterion for mixed mode crack propagation,” *Eng. Fract. Mech.*, vol. 26, no. 4, pp. 533–539, 1987.

[81] M. J. Patricio Dias and R. M. M. Mattheij, “Crack propagation analysis,” 2009.

[82] X. Tian, M. J. Zuo, and K. R. Fyfe, “Analysis of the vibration response of a gearbox with gear tooth faults,” in *ASME 2004 International Mechanical Engineering Congress and Exposition*, 2004, pp. 785–793.

[83] X. Tian, “Dynamic simulation for system response of gearbox including localized gear faults,” PhD Thesis, University of Alberta Edmonton,, Alberta, Canada, 2004.

[84] S. Wu, M. J. Zuo, and A. Parey, “Simulation of spur gear dynamics and estimation of fault growth,” *J. Sound Vib.*, vol. 317, no. 3–5, pp. 608–624, 2008.

[85] H.-H. Lin, R. L. Huston, and J. J. Coy, “On dynamic loads in parallel shaft transmissions: Part I—modelling and analysis,” *J. Mech. Transm. Autom. Des.*, vol. 110, no. 2, pp. 221–225, 1988.

[86] Z. Tian, M. J. Zuo, and S. Wu, “Crack propagation assessment for spur gears using model-based analysis and simulation,” *J. Intell. Manuf.*, vol. 23, no. 2, pp. 239–253, 2012.

[87] V. Sahoo and R. Maiti, “Static load sharing by tooth pairs in contact in internal involute spur gearing with thin rimmed pinion,” *Proc. Inst. Mech. Eng. PART C-J. Mech. Eng. Sci.*, vol. 230, no. 4, pp. 485–499, Mar. 2016.

[88] S. I. Ravindra, “Static and Dynamic Analysis of High Contact Ratio Spur Gear Drive,” PhD Thesis, 2013.

[89] G. K. Sfantos, V. A. Spitas, T. N. Costopoulos, and G. A. Papadopoulos, “Load sharing of spur gears in mesh an analytical and experimental study,” Technical Report, National Tech. Univ. Athens, No. TR-SM-0303, 2003.

[90] R. Laggoune, A. Chateauneuf, and D. Aissani, “Opportunistic policy for optimal preventive maintenance of a multi-component system in continuous operating units,” *Comput. Chem. Eng.*, vol. 33, no. 9, pp. 1499–1510, 2009.

[91] J. Crocker and U. D. Kumar, “Age-related maintenance versus reliability centred maintenance: a case study on aero-engines,” *Reliab. Eng. Syst. Saf.*, vol. 67, no. 2, pp. 113–118, 2000.

[92] O. Mohamed-Salah, A.-K. Daoud, and G. Ali, “A simulation model for opportunistic maintenance strategies,” in *Emerging Technologies and Factory Automation, 1999. Proceedings. ETFA’99. 1999 7th IEEE International Conference on*, 1999, vol. 1, pp. 703–708.

[93] S. A. Haque, A. Z. Kabir, and R. A. Sarker, “Optimization model for opportunistic replacement policy using genetic algorithm with fuzzy logic controller,” in *Evolutionary Computation, 2003. CEC’03. The 2003 Congress on*, 2003, vol. 4, pp. 2837–2843.

[94] F. Besnard, M. Patrikssont, A.-B. Strombergt, A. Wojciechowskit, and L. Bertling, “An optimization framework for opportunistic maintenance of offshore wind power system,” in *PowerTech, 2009 IEEE Bucharest*, 2009, pp. 1–7.

[95] F. Spinato, P. J. Tavner, G. J. W. Van Bussel, and E. Koutoulakos, “Reliability of wind turbine subassemblies,” *IET Renew. Power Gener.*, vol. 3, no. 4, pp. 387–401, 2009.

[96] F. Zhao, Z. Tian, E. Bechhoefer, and Y. Zeng, “An integrated prognostics method under time-varying operating conditions,” *IEEE Trans. Reliab.*, vol. 64, no. 2, pp. 673–686, 2015.

[97] Z. Jiang, Y. Xing, Y. Guo, T. Moan, and Z. Gao, “Long-term contact fatigue analysis of a planetary bearing in a land-based wind turbine drivetrain,” *Wind Energy*, vol. 18, no. 4, pp. 591–611, 2015.

[98] N. Veritas, *Guidelines for design of wind turbines*. Det Norske Veritas: Wind Energy Department, Ris ̧National Laboratory, 2002.

[99] G. L. Johnson and D. Gary, “Wind Turbine Power, Energy, and Torque,” *Wind Energy Syst. Electr. Ed. Ed Prentice-Hall Englewood Cliffs NJ*, pp. 1–4, 2001.

[100] S. M. Muyeen, J. Tamura, and T. Murata, “Wind turbine modeling,” *Stab. Augment. Grid-Connect. Wind Farm*, pp. 23–65, 2009.

[101] K. E. Johnson, “Adaptive torque control of variable speed wind turbines,” National Renewable Energy Lab., Golden, CO (US), 2004.

[102] W. Dong, Y. Xing, T. Moan, and Z. Gao, "Time domain-based gear contact fatigue analysis of a wind turbine drivetrain under dynamic conditions," *Int. J. Fatigue*, vol. 48, pp. 133–146, 2013.

[103] J. M. Jonkman and M. L. Buhl Jr, "FAST User's Guide-Updated August 2005," National Renewable Energy Laboratory (NREL), Golden, CO., 2005.

[104] M. Zhao and J. Ji, "Dynamic analysis of wind turbine gearbox components," *Energies*, vol. 9, no. 2, p. 110, 2016.

[105] D. G. Lewicki, "Gear Crack Propagation Path Studies-Guidelines for Ultra-Safe Design," *J. Am. Helicopter Soc.*, vol. 47, no. 1, pp. 64–72, 2002.

[106] F.-Q. Zhao, M.-J. Xie, Z.-G. Tian, and Y. Zeng, "Integrated Equipment Health Prognosis Considering Crack Initiation Time Uncertainty and Random Shock," *Chin. J. Mech. Eng.*, vol. 30, no. 6, p. 1383, 2017.

[107] D. Banjevic, A. K. S. Jardine, V. Makis, and M. Ennis, "A control-limit policy and software for condition-based maintenance optimization," *INFOR Inf. Syst. Oper. Res.*, vol. 39, no. 1, pp. 32–50, 2001.

[108] P. Caselitz and J. Giebhardt, "Rotor condition monitoring for improved operational safety of offshore wind energy converters," *J. Sol. Energy Eng.*, vol. 127, no. 2, pp. 253–261, 2005.

[109] Z. Hameed, S. H. Ahn, and Y. M. Cho, "Practical aspects of a condition monitoring system for a wind turbine with emphasis on its design, system architecture, testing and installation," *Renew. Energy*, vol. 35, no. 5, pp. 879–894, 2010.

[110] R. Li, "Life distributions from component degradation signals: A Bayesian approach," *Unpubl. Master Thesis Purdue Univ. West Lafayette IN*, 2001.

[111] W. Liu, B. Tang, and Y. Jiang, "Status and problems of wind turbine structural health monitoring techniques in China," *Renew. Energy*, vol. 35, no. 7, pp. 1414–1418, 2010.

[112] Z. Tian, L. Wong, and N. Safaei, "A neural network approach for remaining useful life prediction utilizing both failure and suspension histories," *Mech. Syst. Signal Process.*, vol. 24, no. 5, pp. 1542–1555, 2010.

[113] E. Byon, E. Pérez, Y. Ding, and L. Ntaimo, “Simulation of wind farm operations and maintenance using discrete event system specification,” *Simulation*, vol. 87, no. 12, pp. 1093–1117, 2011.

[114] Z. Tian, “An artificial neural network method for remaining useful life prediction of equipment subject to condition monitoring,” *J. Intell. Manuf.*, vol. 23, no. 2, pp. 227–237, 2012.

[115] B. Stevens, *EXAKT reduces failures at Canadian Kraft Mill*. Retrieved, 2006.

[116] “Windstats Newsletter,” no. 2008–2009.

[117] H. Guo, S. Watson, P. Tavner, and J. Xiang, “Reliability analysis for wind turbines with incomplete failure data collected from after the date of initial installation,” *Reliab. Eng. Syst. Saf.*, vol. 94, no. 6, pp. 1057–1063, 2009.

[118] L. Fingersh, M. Hand, and A. Laxson, “Wind turbine design cost and scaling model,” National Renewable Energy Laboratory (NREL), Golden, CO., 2006.